

Dissertation

**The Role of
Drosophila Apaf-1-related-killer (dark) in Establishing
Synaptic Specificity in the Olfactory System**

Inaugural-Dissertation
zur Erlangung des Doktorgrades
der Naturwissenschaften im Fachbereich Biologie
der Mathematisch-Naturwissenschaftlichen Fakultät
der Westfälischen Wilhelms-Universität Münster

vorgelegt von
Christoph Tobias Scheper
aus Ankum
- 2009 -

Dekan: Prof. Dr. C. Klämbt

Erster Gutachter: PD Dr. T. Hummel

Zweiter Gutachter: Prof. Dr. C. Klämbt

Tag der mündlichen Prüfung: 15.10.2009

Tag der Promotion: 15.10.2009

Table of contents

1	Introduction	1
1.1	Development of neuronal networks	1
1.2	The olfactory system	4
1.2.1	The vertebrate olfactory system	4
1.2.2	The <i>Drosophila</i> olfactory system	6
1.3	Development of the <i>Drosophila</i> olfactory system	9
1.3.1	Early development and specification	10
1.3.2	Targeting and synaptic specificity	10
1.3.3	Zonal organization in-growing ORN axons	12
1.4	Identification of genes involved in olfactory targeting in <i>Drosophila</i>	14
1.5	Aim of this work	15
2	Experimental procedures.....	16
2.1	Materials.....	16
2.1.1	Solutions	16
2.1.2	Antibodies.....	18
2.1.3	Fly Stocks	19
2.2	Methods	27
2.2.1	Cultivation of flies.....	27
2.2.2	Identifications of novel genes involved in ORN targeting	27
2.2.3	Generation of recombinant fly lines / chromosome “cleaning”	27
2.2.4	Clonal analysis	28
2.2.5	Selection of homozygous mutant embryos.....	29
2.2.6	Preparation technique of adult brains	29
2.2.7	Preparation of pupal brains and antennae	30
2.2.8	Cryo sections of adult antenna.....	30
2.2.9	Antibody staining.....	31
2.2.10	Acridin Orange staining	31
2.2.11	Imaging of adult antenna	31
2.2.12	DNA isolation from adult flies	32
2.2.13	DNA isolation from single flies or embryos	32
2.2.14	PCR.....	33
2.2.15	Inverse PCR.....	34

2.2.16	DNA gel electrophoreses.....	34
2.2.17	Sequencing	34
3	Results.....	35
3.1	Mutations in <i>verpeilt</i> cause ectopic mis-targeting of Or47a neurons.....	35
3.2	Identification of the <i>verpeilt</i> locus	37
3.2.1	Complementation analysis	37
3.2.2	P-element mutagenesis.....	38
3.2.3	Generation of <i>verpeilt</i> deletions	39
3.2.4	Sequencing of candidate genes.....	40
3.3	Apoptosis and its effect on Or47a axon targeting	42
3.3.1	The effect of the <i>dark</i> ^{V8} allele on apoptosis	42
3.3.2	Mutations in <i>dark</i> ^{verpeilt} do not affect ORN numbers	45
3.3.3	Suppression of apoptosis does not cause Or47a mis-targeting.....	46
3.3.4	<i>Dark</i> induced ORN mis-targeting is allele specific.....	48
3.3.5	Over-expression of <i>dark</i> does not suppress the OR47a mis-targeting	55
3.3.6	Loss of function of apoptosome components does not cause ORN mis-targeting.....	58
3.4	Projection domains.....	59
3.4.1	Domain organization in the olfactory system of Drosophila.....	60
3.4.2	Projection domain specificity of Or 47a axons.....	62
3.5	Characterization of the ORN targeting phenotype in <i>dark</i> ^{verpeilt}	66
3.5.1	Not all ORN classes are affected in <i>dark</i> ^{verpeilt}	66
3.5.2	The mis-targeting phenotype in <i>dark</i> ^{verpeilt} is Cell autonomous	69
3.5.3	The ectopic glomerulus needs a certain amount of axons to be stabilized	73
3.5.4	Mis-projecting Or47a axons sort out from other classes.....	75
3.5.5	Misprojecting Or47a axons interact with projection neurons	77
3.6	LRR Cell adhesion molecules are predominantly restricted to one projection domain	80
3.6.1	Connectin is mainly expressed in the trichoid sensilla.....	83
3.6.2	Con expression during development	84
3.6.3	The ectopic Or47a glomerulus in <i>dark</i> ^{V8} mutants is Con positive	86
3.6.4	<i>Dark</i> mutant Or47a neurons express Con.....	89
3.6.5	Con mutants do not affect OR47a targeting	89
3.6.6	Knock down in <i>dark</i> mutant ORNs rescues the mis-targeting phenotype.....	90
3.6.7	Con over-expression in 47aORNs does not affect OR47a targeting.....	92
3.6.8	Over expression of Con in PNs leads to changes in ectopic Or47a target specificity ...	93
4	Discussion.....	96

4.1	Mapping of the <i>verpeilt</i> mutations to the <i>dark</i> gene	96
4.2	Phenotypic implications	98
4.3	Projection domains.....	98
4.3.1	In-growing ORN axons sort out in projection domains in <i>Drosophila</i>	98
4.3.2	Domain organization is not sufficient for precise ORN targeting	99
4.4	ORN targeting requires <i>dark</i> function only in some ORN classes	100
4.4.1	The <i>dark</i> ^{<i>verpeilt</i>} induced targeting phenotype is cell autonomous.....	101
4.4.2	<i>Dark</i> ^{<i>verpeilt</i>} affects ORN projection identity.....	102
4.5	Impacts of apoptosis on ORN targeting	103
4.5.1	Lack of apoptosis does not cause ORN mis-targeting	105
4.5.2	The ORN-mis-targeting phenotype is allele specific	106
4.5.3	The <i>dark</i> ^{<i>verpeilt</i>} mutations show dominant negative properties	108
4.6	Connectin is required but not sufficient for lateral OR47a targeting in <i>dark</i> ^{<i>verpeilt</i>} mutants	110
4.6.1	Con is not expressed in all <i>dark</i> ^{<i>verpeilt</i>} mutant Or47a neurons	110
4.6.2	Ectopic Con expression in <i>dark</i> ^{<i>verpeilt</i>} is due to transcriptional up-regulation	112
4.7	Precise regulation of <i>dark</i> is required for olfactory targeting.....	112
5	Abstract.....	116
6	Literature	117
7	Appendix	126
7.1	Abbreviations	126
7.2	Figure Index.....	127

1 Introduction

For every neuronal network the precise connections of the individual neurons are of fundamental importance. How a complex nervous system develops from progenitor cells and how it achieves its extraordinary complexity and specificity in the connections between neurons is one of the most intriguing questions in biology. Every single neuron has to connect to only a small subset of hundreds or thousands of potential target cells to ensure the proper function of the brain. Proper connectivity is required for the precise detection of outer stimuli and the integration of this information to generate an appropriate behavioral response.

Some of the mechanisms that direct the axons of different neuronal subpopulations to their specific targets could be elucidated, for example the involvement of certain diffusible signals that create chemokine gradients allowing axons to orient themselves in a rather rough fashion, or the involvement of some cell adhesion molecules that mediate different axon-axon interactions. Though there has been some advance in understanding how a nervous system develops, the precise mechanisms that lead to the specific connections are still one of the major topics in neurobiology.

1.1 Development of neuronal networks

After initial neurogenesis and early differentiation, the axons face two major challenges. They have to bridge the distance to their target region and, upon arrival, form precise connections with a specific set of target dendrites.

Dependent on the location of the neuron the axons have to grow long distances; this is especially true for neurons of the peripheral nervous system. Several mechanisms have been identified that allow the axon to fulfill this task. The cues that guide the axonal growth cone can be divided in attractants and repellants, and they can work either over long or short distances (Tessier-Lavigne & Goodman 1996; Dickson, 2002). A variety of molecular pathways have been described that guide the axons to the correct position and ensure precise connections of the neurons (Huber et al. 2003).

An example for such a mechanism that directs axonal growth is the Ephrin/Eph-Receptor system, which has been first identified in the chicken eye (Pasquale 1991). Here the two components are expressed in a graded fashion in the ingrowing axons and the dendrites in the target area. Axons with high EphR can detect low amounts of the ligand and therefore react more sensitive, leading to early stopping, while those with a low amount of EphR only react to high Ephrin concentrations, therefore growing to the peak of the gradient. EphR / Ephrin signalling requires cell-cell contacts. This mechanism allows the axons to maintain their position in the retina and project topographically into the optic center of the brain, ensuring a continuous image of the outside world (Brown et al., 2000; Flanagan et al. 1998). The Ephs and Ephrins are subdivided in two subclasses, A and B (Pasquale 2005), that bind subclass specific. Therefore the different classes can account for positioning along different axis, EphA/EphrinA along the anterior-posterior axis and EphB/EphrinB along the dorso-ventral axis.

Another ligand / receptor mechanism is the ROBO / SLIT signaling. It has been shown in vertebrates and invertebrates to have a function in guiding midline crossing of axons (Flanagan & Vanderhaeghen, 1998; Brown et al., 2000). In the *Drosophila* embryonic nervous system the secreted signal Slit is expressed by midline glia cells and repels axons expressing ROBO to cross the midline. By the regulation of expression in a time dependent manner, some commissural axons are allowed to cross when not having turned on *robo* yet, but repressed to cross it again after expressing *robo* (Li et al., 1999; Kidd et al., 1999). With this it can be assured that every neuron only crosses the midline once (if at all). By expressing different forms of the *robo* receptor (1,2,3) also the guidance to one of three longitudinal fascicles can be determined (Simpson et al. 2000a; Simpson et al. 2000b).

A third example for a receptor / ligand based guiding system is the Netrin system that, dependent on the expression of the receptor leads to attraction or repulsion. Netrins can act contact dependent or over longer ranges. Interaction with the receptor *frazzled* leads to attraction (Kolodziej et al. 1996), with UNC5 to repulsion (Keleman & Dickson 2001).

Also proteins of the Semaphorin-family have a function in development of neuronal connections. Semaphorins can be secreted or membrane bound thus acting over long or short distances (Pasterkamp & Kolodkin 2003). Sema6a is described to have a repulsive function in the nervous system; Sema3A leads to misrouting and targeting in inappropriate

positions in the olfactory system of the mouse via interaction with its receptor neuropilin-1. *Sema3A* is expressed in the outer nerve layer and in mitral cells in the olfactory bulb; ingrowing ORNs expressing neuropilin avoid regions of high *Sema* expression. In *Sema3A* mutants many of these neurons are misrouted leading to defects in connectivity and formation of glomeruli in inappropriate positions (Schwartz et al. 2000). In addition, it was shown that a loss of *Sema1a* leads to imprecise targeting of olfactory receptor neurons in the *Drosophila* ORN axons, resulting in a loss of the typical innervation-pattern (Lattemann et al. 2007).

The Cadherin family is a group of transmembrane or membrane anchored cell adhesion proteins that are required for various processes during axonal targeting. The classical Cadherin *Ncad* for example is needed for the proper recognition of target layers in the *Drosophila* eye (Clandinin et al. 2001) or the stabilization of synapses (Prakash et al. 2005). The atypical cadherin *Flamingo* serves several functions in neuronal targeting. It has been described to be involved in the establishment of dendritic fields (Gao et al. 2000) but also in axon guidance (Sweeney, Li & Gao 2002).

In order to start the synapse formation the axonal growth has to be stopped. This process has to be regulated precisely in space and also in time to prevent early stops or overshooting of the axons. The shutdown of the growth machinery and the initiation of synapse formation appear to be regulated on a transcriptional level. The putative transcription factor *Sequoia* has been described to be expressed in a narrow time window in different photoreceptor neurons in the *Drosophila* eye. Loss of function leads to an early stopping, prolonged expression to an overshoot of R8 photoreceptor axons in the medulla (Petrovic & Hummel, 2008).

Though many mechanisms have been identified that are required for the proper pathfinding and targeting of axons, little is known of how different subpopulations interact with each other to discriminate between different potential targets and form specific connections. The olfactory system is an excellent model to study this question because of its easy identifiable classes of different neurons and its discrete connection pattern.

1.2 The olfactory system

The ability to detect different chemosensory cues is crucial for almost every animal. A broad range of odors is used to find proper food sources, mating partners and to detect breeding places, for communication within social groups, as marker for territorial boundaries and, in some cases even for defense purposes.

In order to fulfill all these tasks, the olfactory system has to distinguish between a broad variety of different odors and also to detect the intensity of a given cue. The detection of odors in the olfactory receptor neurons (ORNs) is mediated by a set of G-protein coupled seven trans-membrane receptors (Buck & Axel 1991). This olfactory receptor (OR) family is highly diverse, each member having different substrate specificity. Some receptors are highly sensitive for only a small set of chemical compounds even at very low concentrations; others detect a broader spectrum of odorants, but respond only at somehow slightly higher odorant concentrations.

A hallmark of the olfactory system is the expression of only one receptor-gene per neuron. All neurons expressing the same receptor define a class of ORNs, and every class innervates a specific set of target dendrites, thereby forming distinct synaptic glomeruli in the first processing center of the brain (Ressler et al. 1993; Vassar et al. 1993; Laissue et al. 1999; Couto et al. 2005). Though the basic setup of the olfactory system has been known for years, the mechanisms that guide the ORNs to form these specific connections are rather poorly understood, and the exploration of how the incoming odorant stimuli are connected to a certain behavior is just beginning. Currently there are two models dealing with the question how the incoming information is actually translated to a certain quality. The first model is based on a differential stimulation of subsets of glomeruli which provide information about the incoming odor, like attraction or repulsion (Asahina et al. 2009); other experiments have shown that also stimulation of a single glomerulus can lead to different behavioral responses (DasGupta & Waddell 2008).

1.2.1 The vertebrate olfactory system

In vertebrates, the ORNs are distributed in the olfactory epithelium (OE) in the nasal cavity. From there, they project their axons to the olfactory bulb (OB) which is the first processing unit in the brain. Here they form the olfactory glomeruli. The olfactory epithelium is

subdivided in four major zones. Neurons within one of these zones keep their positional information also when projecting to the olfactory bulb (Mombaerts 2006). Each neuron is thought to express only one type of olfactory receptor, thereby defining the ORN class. In the mouse olfactory system each class can consist of more than a thousand neurons.

The family of the OR-genes is one of the largest known in vertebrate genomes (Mombaerts 2006). In the vertebrate olfactory system the OR-proteins are enriched in the cilia of the ORNs, but it has also been described that during development the ORs are also present in the axon. The choice of the OR expressed by each neuron is controlled by negative feedback regulation to ensure the One Neuron – One Receptor rule (Serizawa, Miyamichi & Sakano 2005). Swapping experiments in which OR-genes were completely or partly replaced showed that they have a crucial role in targeting and convergence (Feinstein & Mombaerts 2004). Since even differences within the trans-membrane domains of the ORs lead to changes in targeting, it appears unlikely that the receptor protein itself is directly involved in the guidance process. It has been shown that the targeting is reliant on cAMP signaling caused by intrinsic OR activity (Imai, Suzuki & Sakano 2006). This activity could be related to the expression of class specific cell adhesion molecules. Further studies revealed a differential expression of certain

signaling molecules that influence convergence in certain parts of the olfactory bulbs. If expressed in only a subset of a given class the ORNs sort out into a second glomerulus. In addition, the expression of Ephrins has been shown to be dependent on the

activity of ORs, suggesting a cAMP dependent mechanism that, reliant on the ORs, influences regulation of guidance molecules (Cutforth et al. 2003; Imai et al. 2006).

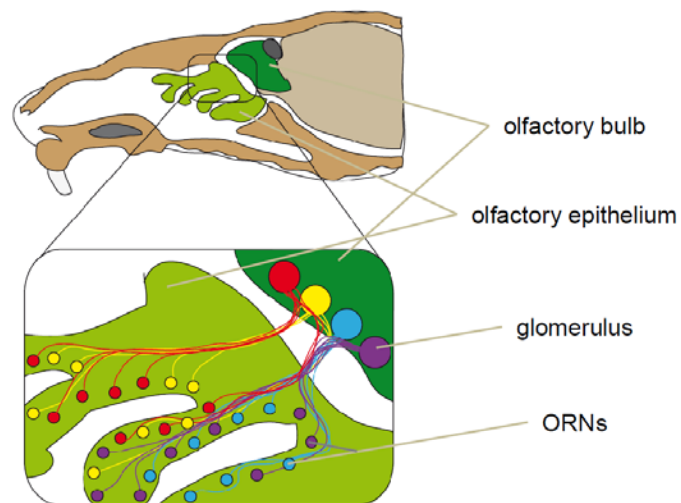


Figure 01 – The vertebrate olfactory system

(A) The olfactory epithelium (light green) is located in the nasal cavity, containing the olfactory receptor neurons (ORNs). ORN axons project to the olfactory bulb (dark green) in the anterior part of the brain. (B) ORNs are subdivided in different OR classes; axons of each class converge onto one glomerulus. OR classes are shown in different colors (adapted from Mombaerts, 2004).

The ORN axons project from the olfactory epithelium to the accessory olfactory bulb in a single unbranched axon (Mombaerts 2006). Neurons of a given class project to a single glomerulus within the lateral and medial hemisphere of each bulb, even if the cells are often distributed widely over the olfactory epithelium (Figure 01). During development ORNs of the same class might project into more than one target, eventually the pattern is refined during the first postnatal days to restrict targeting to one glomerulus. The exact positions of the glomeruli can therefore differ in each individual, though the patterning of given ORN classes to certain regions of the OB is similar in every adult brain. Furthermore the olfactory epithelium can be roughly divided in four zones and this organization is also maintained in the olfactory bulb (Ressler et al. 1993; Mori et al. 2000).

The olfactory system in mammals is one of the few exceptions where adult neurogenesis takes place. Though the main development takes place in the embryo, neuronal stem cells continue to proliferate in the subventricular zone (SVZ), from where they migrate along the rostral migratory stream into the olfactory bulb. Once arrived, they differentiate in three different types of neurons, granule cells, mitral cells and periglomerular cells (Lledo, Merkle & Alvarez-Buylla 2008). Also, there is a constant turnover of ORNs in the olfactory epithelium (Calof et al. 1998). While the neurogenesis in the olfactory epithelium is needed to compensate for a loss of ORNs due to injury or disease, the amount of neurons in the AL is increasing over the whole lifetime; the exact reason remains unknown. Several hypotheses suggest learning and the need for the integration of novel olfactory cue as a explanation, but this could not be proofed by scientific evidence yet.

1.2.2 The *Drosophila* olfactory system

The *Drosophila* olfactory system, though less complex, is basically organized like its vertebrate counterpart. Instead of thousands of ORN classes it only consists of 50 classes, but like in vertebrates every cell just expresses one functional receptor, thereby defining its class. All neurons of the same class project there axons to the same synaptic glomerulus within the antennal lobe, which is the invertebrate homologue of the olfactory bulb (Jefferis & Hummel 2006).

The ORN receptor family in *Drosophila* has roughly sixty members, and, like in the vertebrate system they are seven-transmembrane receptors, but in contrast no associated

G-protein coupled mechanism has been identified. In fact the odor-evoked response of the ORNs appears to be dependent on the activity of the OR itself and a co-receptor, Or83b that serves itself as ion-channel (Sato et al., 2008; Wicher et al. 2008).

Recently an additional type of receptor proteins expressed in the antenna has been found called ionotropic receptors (IRs), which are also expressed in sensory neurons in the antenna and respond to certain odor molecules which do not activate the classical ORs (Benton et al. 2009). In addition, the gustatory receptor Gr21 is expressed in one class of neurons in the antenna (Scott et al. 2001).

The ORNs in the fly are housed in two peripheral organs, the maxillary palps and the third antennal segment. The surface of these organs is covered with small hair-like sensilla that contain defined sets of ORNs. The sensilla can be subdivided in three major types, basiconic, coeloconic and trichoid and contain up to four ORNs. Trichoid sensilla are found predominantly in the distal part of the antenna, basiconic in the basal part and coeloconic in between these two types. The borders between the different types are not very distinct and form a mixed pattern with more trichoids at the bottom and more basiconics towards the junction of the third and second antennal segment. The maxillary palps only have basiconic sensilla. The different ORN types distribute in the sensilla in stereotyped combinations, and can therefore be grouped not only according to the receptor expressed but also to the type of sensillum in which they are housed. ORs are expressed by neurons housed in trichoid and basiconic sensilla, IRs in coeloconic, and Gr21 is only found in the basiconic sensilla type ab1 (Couto, Alenius & Dickson 2005).

About 40 OR genes can be attributed to distinct ORNs, and in general the one receptor one neuron rule applies to most of the ORN classes. Some OR genes appear to be expressed equally in the same neurons, for example the Or65a, b and c. These receptors containing a high degree of redundancy seem to have developed from duplications.

Another exception to this rule is the receptor Or83b. It is expressed in almost all ORNs and forms heterodimers with the individual ORs of every class. The dimerization is described to be required for the proper distribution of the ORs to the dendrites and enhance the ability to detect odors (Larsson et al. 2004); Neuhaus et al. 2005).

The only “real” exceptions are the co-expression of OR33c and OR85e in a pb2 neuron and OR49a and 85f in an ab10 neuron. For the pb2 neuron it was shown that its response profile to odorant stimuli only depends on OR85e, suggesting that the function only depends on one type of receptor. Something similar might be true for the Or49a/Or85f class (Couto, Alenius & Dickson 2005).

ORNs of the same class project their axons and form synaptic glomeruli in the antennal lobe (AL), the insect equivalent of the OB (Figure 02). Interestingly, the projection appears to be not correlated to the other ORN class in the same sensillum, and the target glomeruli

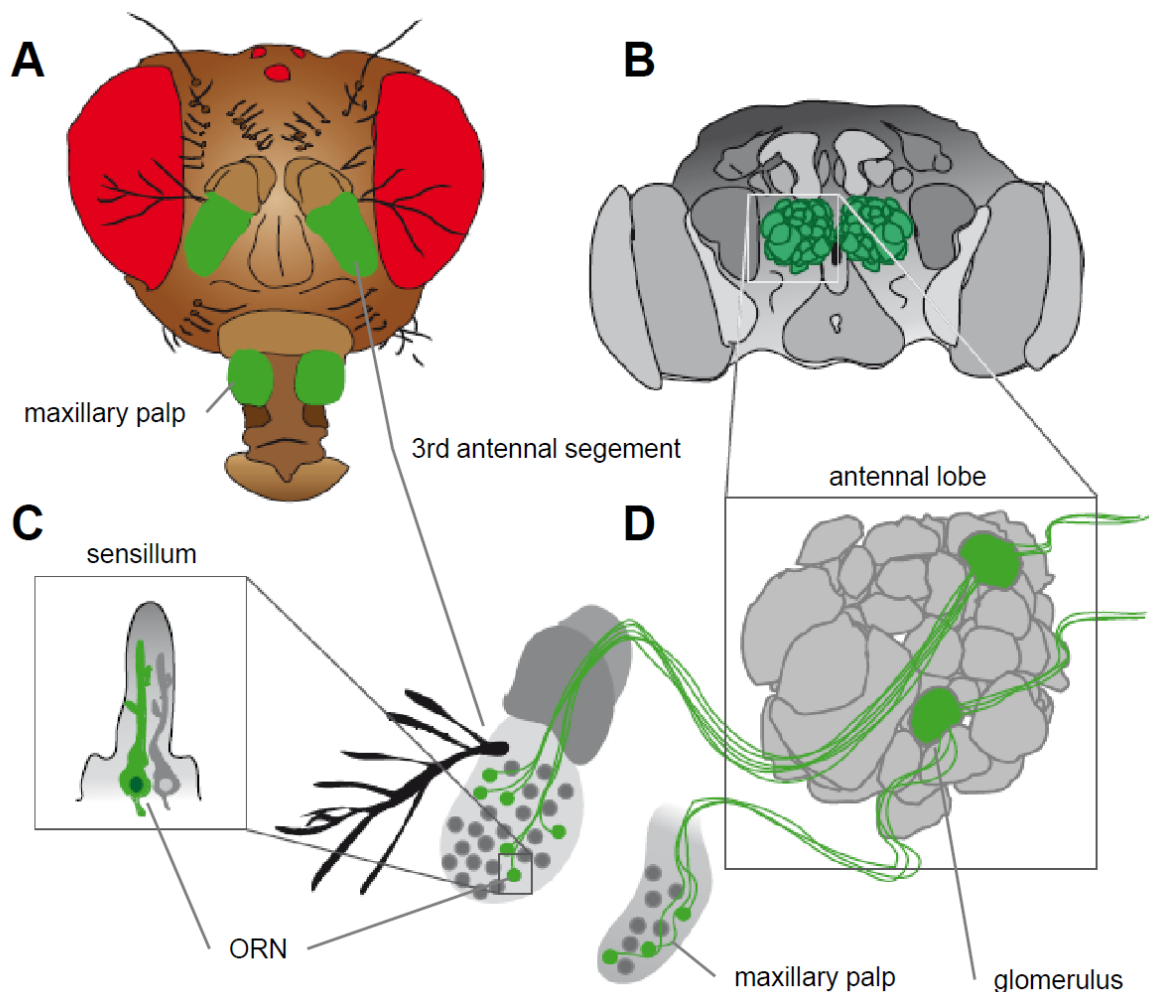


Figure 02 – The *Drosophila* olfactory system

(A) The peripheral olfactory organs, the third antennal segment and the maxillary palps (green) are located on the anterior part of the fly head. (B) The ORNs project their axons to the antennal lobe on the anterior surface of the brain (green). (C) ORNs are housed in peripheral sensilla, ORNs of a given class are distributed over the antenna or the maxillary palps respectively. (D) The axons of every class converge onto a single glomerulus in the ipsi-lateral hemisphere of the AL, most classes also extend a commissural branch to the equivalent glomerulus on the contra-lateral side.

can be on the opposite sides of the AL. In contrast to the vertebrate system, the projection pattern in the *Drosophila* olfactory system is extremely stereotypic. Each glomerulus can be attributed to the respective ORN class by position and shape. The in-growing ORNs project to their specific target glomerulus on the ipsi-lateral side of the AL; most of the classes also form an additional branch that crosses the midline forming a commissure and innervates the equivalent glomerulus in the contra-lateral hemisphere of the AL.

The ORNs form synapses within the glomeruli and innervate the dendrites of the so called projection neurons (PNs). These neurons project their axons to the higher olfactory centers in the *Drosophila* brain, the mushroom bodies and the lateral horn (Jefferis et al. 2001). On average, each glomerulus receives input from about 30 ORN axons on three to five PN dendrites per glomerulus. The cell bodies of the PNs are arranged in three clusters around the AL, dorsal, lateral and ventral. The position of the PN soma is not related to the glomerulus it sends its dendrites to, some PNs from the dorsal cluster form glomeruli which are rather ventral in the AL (Spletter et al. 2007). The olfactory glomeruli are also interconnected by several classes of interneurons (Stocker, Heimbeck & Belle 1997), some of which only get innervated by few, others which appear to send dendrites to almost all glomeruli. The interneurons are thought to pre-process the olfactory information before it is relayed to the higher olfactory centers. The exact processes and mechanisms enabling the comparison and integration of different odor qualities and concentrations are yet unknown.

In contrast to the vertebrate system, the olfactory system in *Drosophila* shows no adult neurogenesis and cannot compensate for a loss of ORNs or PNs. Berdnik et al. could show that after loss of ORNs or PNs the morphological structure of the equivalent counterpart does not change, glomerular structures of PN dendrites remain after loss of the ORNs and vice versa. Neighboring neurons do not extend in the adjacent space. Only if an ipsi-lateral lesion of one antenna was performed, an increase of contra-lateral innervations was observed (Berdnik et al. 2006).

1.3 Development of the *Drosophila* olfactory system

The main development of adult the olfactory system in *Drosophila* takes place during the pupal stage which lasts about 100 hours. During this period the sensilla containing the

ORNs form, the fate of the neurons is determined, axons and dendrites grow out and form the AL and finally the Ors are expressed.

1.3.1 Early development and specification

The primordial tissue of which the later ORNs derive, the eye-antennal imaginal disc is formed during larval stages. Progenitor cells create cell lineages that later form the sensilla in early pupal stage (Lienhard & Stocker 1991). The different sensilla types are pre-specified mainly by two basic helix-loop-helix (bHLH) transcription factors, *atonal*, which determines coelocoinc sensilla, and *amos*, which leads to basiconic and trichoid sensilla (Gupta & Rodrigues 1997). Differentiation of trichoid and basiconic sensilla is regulated by the expression levels of the transcription factor *lozenge*, high levels lead to basiconic, low to trichoid sensilla (Reddy et al. 1997).

The determination of the neurons within one sensillum is mediated by Notch signaling to ensure that the different cells do not express the same OR (Endo et al. 2007). In contrast to the vertebrate system, the actual expression of the receptors starts at a very late stage in pupal development, arguing against an instructive role of these genes in establishing synaptic specificity (Jefferis et al. 2004). Further evidence for this was shown by Dobritsa et al., 2003, who could show that in swapping experiments in *Drosophila*, deletion or replacement of OR genes had no effect on the targeting on the affected ORNs. The projection neurons develop from neuroblasts in the CNS in a precise order which already determines target specificity. The first PNs for example always connect with the DL1 glomerulus (Jefferis et al. 2001). The morphology of the PN dendrites is dependent on a precise regulation involving miRNAs regulated via Dicer1 and pasha, though the microRNAs involved are yet unknown (Berdnik et al. 2008).

1.3.2 Targeting and synaptic specificity

The developing ORNs start to send out the first axons along three large fascicles around 15 - 20 hours after puparium formation (APF), forming the antennal nerve. Roughly at the same time the PNs start to extend their dendrites towards the forming AL. The ORN axons enter the forming AL at a slightly ventral shifted lateral position and start to sort out from

each other and begin to form proto-glomeruli in the AL region, also sending axon branches across the commissure. Axons of the maxillary ORN classes arrive later and reach reach the AL about 30h APF from a more ventral position.

The formation of the proto-glomeruli is dependent on the cell adhesion molecule N-Cadherin (Ncad) in both PN dendrites and axons. Loss of Ncad in ORNs does not affect the general targeting to the AL, but affect the sorting of the different ORN classes and the convergence to a condensed glomerulus. Instead of growing inside the AL the axons stay on the surface and fail to establish contacts with the PNs (Hummel & Zipursky 2004). The loss of function in PNs has a similar effect, the dendrites still invade the AL, but fail to sort out into distinct glomeruli and partially overlap with neighboring dendrites (Zhu et al. 2006). The loss in either the ORNs or the PNS does not affect the targeting of the corresponding neuron type.

The loss of the Ig-receptor molecule Dscam results has an opposite effect to the phenotype observed in *ncad* mutants in ORN targeting (Hummel et al. 2003). Instead of converging in a single glomerulus some axons form little ectopic glomeruli all over the AL and sometimes even outside of the target area, while others manage to reach their desired position. The sorting is not affected, as some maxillary classes, which converge to early in the suboesophageal ganglion (SOG), still form a couple of glomeruli according to the Or expressed. The *dscam* gene can, due to alternative splicing, give rise to more than 39000 different isoforms (Schmucker et al. 2000). This high degree of diversity appears to be important, since over-expression of *dscam* in a whole ORN class prevents early stopping, but lead to a failure of convergence in the target area. The same experiment in single neurons has no effect, suggesting a repellent function of *dscam* depending on the diverse isoforms (Zierau et al. in preparation). Furthermore, *dscam* interacts with the SH2/SH3 adaptor Dock, which in turn has been shown to interact with the serin / threonin kinase Pak. Pak can bind to GTPases of the Rho-family and regulates the actin cytoskeleton. Mutations in both Dock and Pak lead to ectopic targeting in the olfactory system (Ang 2003), a phenotype that looks somewhat similar to the defects in *dscam* loss of function alleles.

The above described mechanisms are thought to be required in all ORN classes. Analysis focusing on the POU domain transcription factor Abnormal chemosensory jump 6 (Acj6)

could show that here only some ORN classes are affected. The null phenotype of *acj6* leads to a loss of convergence, affected ORNs terminate not only in the desired glomerulus, but also in the surrounding area. Other classes show no defects. It could be shown that Acj6 is required in some ORNs cell-autonomously, in others non-cell-autonomously, and in others not at all. Even mis-targeting ORNs, when projecting to a false position formed convergent termini, indicating a strong inter-axonal communication. Loss of Acj6 in PNs also shows projection defects (Kuranaga et al. 2006; Kuranaga & Miura 2007). Similar results were found for another POU domain protein, *pdm3* (Tichy, Ray & Carlson 2008), suggesting a transcriptional code in different ORN classes that mediate intrinsic targeting specificity and inter axonal interactions leading to proto-glomeruli formation.

Glomerular convergence is also regulated by the transmembrane molecule Sema1a, which is expressed differentially in neighboring glomeruli. Loss of Sema1a leads to innervations in adjacent glomeruli. The proto-glomeruli formation during earlier development appears to be not affected in Sema1a mutants, supporting the hypothesis that its expression levels are used later to control intra-class convergence (Lattemann et al. 2007).

OR expression starts in the first classes, this process lasts until around 80h to 90h APF. The restriction of receptor expression to one OR in each ORN requires the putative transcription factor *sequoia* (*seq*), loss of *seq* leads to co-expression of sensillum-related ORNs in one neuron (Brochtrup, personal communication).

1.3.3 Zonal organization in-growing ORN axons

The first processing center in the olfactory system, the AL or the olfactory bulb, includes a rather great variety of potential glomerular targets to in-growing ORN axons. The arriving fibers possess some intrinsic targeting competence to avoid unspecific synapsing by sorting out into more or less distinct projection domains that guide them toward the correct region of the target area.

The mouse olfactory system has been described to be divided in four major zones in both the olfactory epithelium and the olfactory bulb (Figure 03). ORNs of a given class usually project their axons to the according region of the OB. Each of the zones contains a specific set of ORNs. More homologous ORs tend to be expressed by neurons housed in the same

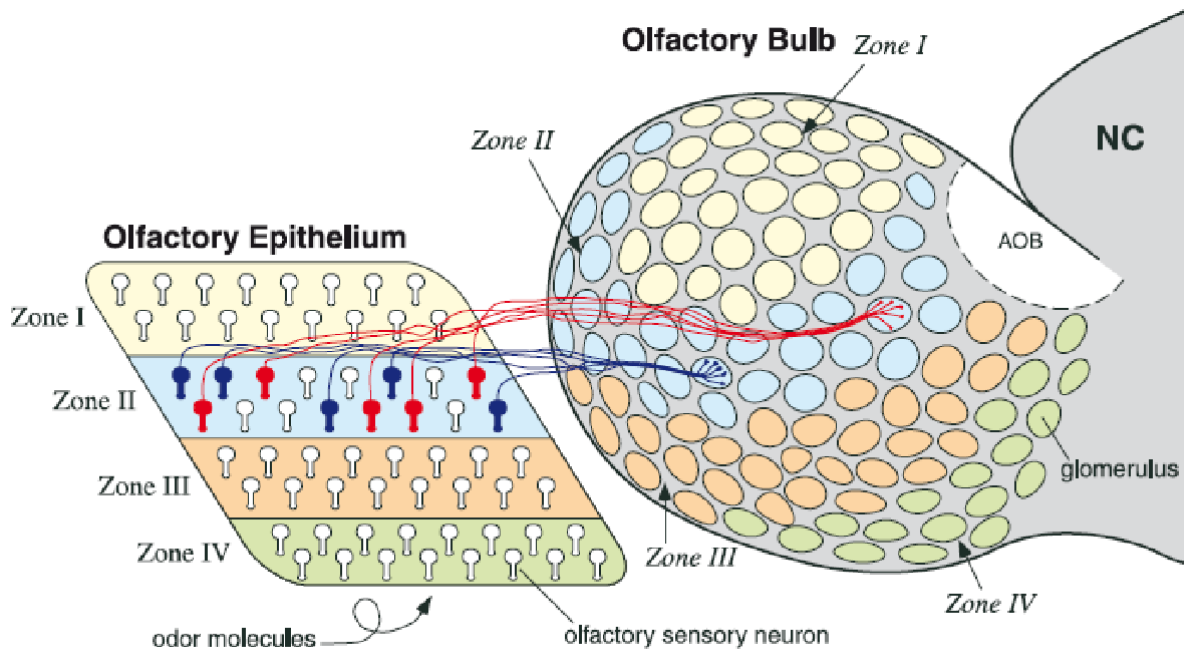


Figure 03 – Zonal organization in the mouse olfactory system

The mouse olfactory epithelium is subdivided in four major zones, ORNs within these zones project to equivalent zones in the olfactory bulb. ORNs of different classes, sort out within their zone to form class specific glomeruli (adapted from Mori et al. 2000).

zone. This zonal organization is also maintained in the olfactory bulb (Mori 1999). Recent studies could show that there indeed is a pre-sorting in mouse ORN axons, as shown by Imai et al by knocking out the *Sema3A* gene. According to their model, the axons sort out along a gradient of *Sema3a* which acts in concert with the receptor *Neuropilin*. Loss of *Sema3a* leads to a non typical mixing of ORNs resulting in mis-targeting (Imai et al. 2009).

Neuropilin is also involved in ORN targeting in *Xenopus laevis*, where the ORNs sort out according to the expression strength, again suggesting a gradient. Here it appears to counteract a high level of *Plexin* which guides the axons in the opposite direction (Satoda et al. 1995).

A domain organization has also been shown in the moth *Manduca sexta*. Here, the sorting process is dependent on the distribution of glia cells that guide axons into certain routes that lead to their specific glomeruli (Tolbert et al. 2004). The organization of ORN axons in projection domains appears to be a common feature in many organisms. Also, most of the molecules described above to be involved in this organization have also been reported to have a function in axonal targeting in *Drosophila*. Therefore, one of the aims of this work

was answer the question if there is a similar organization in *Drosophila*. The projection behavior of *Drosophila* provides some evidence for that, so also the question arises whether domain organization is of functional relevance, and if so, how it is established.

1.4 Identification of genes involved in olfactory targeting in *Drosophila*

To identify novel components required for proper development and function of the olfactory system in *Drosophila*, a major histological screen was performed previous to this work. An unbiased EMS approach was chosen to uncover so far unknown genes that are involved in targeting and synaptic convergence. The principle of the screen was based on the FRT/FLP system to induce mitotic clones in the developing eye-antennal imaginal disc. To visualize potential changes in the patterning of the glomeruli, a Gal4 dependent marker chromosome containing several Or-Gal4 elements with a synaptic GFP labeled reporter was induced. The mutant chromosomes were examined in this background for alterations in the innervations pattern of the labeled Or-classes. In total, about 5000 mutant lines were screened, of which about 5% showed a defect. Several complementation groups could be identified, indicating a high degree of saturation of the screen. Chosen mutants were then used for further analysis (Zierau, 2007; Steffes, 2007). In this work, the role of the pro-apoptotic gene *Drosophila apaf-1 related killer (dark)* in olfactory system development was analyzed.

1.5 Aim of this work

The aim of this work is to gain further insights in the mechanisms that guide axons to their target cells. During a large scale forward genetic screen several mutations were identified leading to specific defects in the projection pattern in the olfactory system of *Drosophila*.

In a large scale forward genetic screen the complementation group *verpeilt* was identified to cause specific mis-targeting in the olfactory system. One part of this thesis was the identification of the gene affected in these mutants. In a second part the ectopic innervations formed in this complementation group were characterized in detail.

The main focus of this thesis is the characterization of mutations in the pro-apoptotic factor *dark* that causes a specific mis-targeting of some ORN classes. Different genetic and molecular approaches are used to determine the mechanisms responsible for this phenotype and if this process is dependent on apoptosis or on an apoptosis unrelated mechanism.

2 Experimental procedures

2.1 Materials

2.1.1 Solutions

All reagents and chemicals were purchased from following companies at quality level pro-analysis:

Aldrich (Steinheim)	Baker (Groß-Gerau)	Biomol (Hamburg)
Biozym (HamelN)	Fluka (Neu Ulm)	Roche (Mannheim)
GIBCO/BRL (Eggenstein)	Merck (Darmstadt)	Pharmacia/LKB (Freiburg)
Roth (Karlsruhe)	Serva (Heidelberg)	Sigma (Deisenhofen)

Drosophila standard medium (per liter): 77g corn flour
8,5g of agar
18g dry yeast
10g soy flour
82g malt extract
41g of sugar beet syrup
4,5 ml propionic acid
15 ml Nipagin solution

Water, Corn flour and Agar and are cooked while stirring. Soy flour and dry yeast are dissolved in water until no clots remain then added together with malt and syrup to the boiling food. When the temperature has cooled down to 60°C propionic acid and Nipagin solution are added.

Nipagin solution: 100g Nipagin (methyl 4-hydroxybenzoate) ad 1000ml 70% EtOH

PBS: 130 mM NaCl
7 mM Na₂HPO₄
3 mM KH₂PO₄
2,7 mM KCl, pH 7,6

PBT :	0,1% Triton X-100 in PBS
Paraformaldehyd-stock (PFA, 8%):	dilute 0,8 g Paraformaldehyd in 10 ml aqua dest., add 70 µl of 1M NaOH, incubate for 30 min at 37°C. steril filtration with 0,2 µm filter. For fixation of brains and antenna dilute the stock with PBS up to 2% concentration.
Squishing buffer (SQUIB)	10 mM Tris pH 8,2 1 mM EDTA 25 mM NaCl 200 µg/ml Proteinkinase K (final concentration)
TBE:	50 mM Tris/HCl, pH 8,2 50 M boracic acid 5 mM EDTA
DNA Loading Buffer (10x):	4 M urea 50 mM EDTA spatula tip of bromophenol blue spatula tip of xylene cyanol
Ethidium Bromide:	10 mg/ml Stocksolution, use 1 µl/50 µl agarosegel
RNAse-H ₂ O:	0,2 µg RNAse per ml autoclaved ddH ₂ O
Neomycin-stock solution (G418):	25 mg G418/ml PBS spatula tip of food dye

2.1.2 Antibodies

2.1.2.1 Primary antibodies

Name	Origin	Dilution	Source
Anti GFP	rabbit	1:1000	Invitrogen
Anti n-cadherin	rat	1:20	Hybridoma Bank
nc82	mouse	1:20	Stortkuhl et al., 1994
Anti CD2	Mouse	1:1000	Invitrogen
Anti CD8	rat	1:1000	Caltech
Anti Connectin	mouse	1:50	Meadows et al., 1994
22C10	mouse	1:50	Hybridoma Bank
anti c-Myc	mouse	1:5	Hybridoma Bank
Anti β Galactosidase	rabbit	1:1000	Cappel, MP Biomedcals
Anti elav	rat	1:10	Hybridoma Bank

2.1.2.2 Secondary antibodies / intercalating dyes

Name/ specificity	Conjugation	Dilution	source
Goat anti mouse	Alexa 488	1:500	Molecular Probes
Goat anti rabbit	Alexa 488	1:300	Molecular Probes
Goat anti mouse	Alexa 568	1:300	Molecular Probes
Goat anti mouse	Alexa 568	1:300	Molecular Probes
Highly cross absorbed			
Goat anti rat	Alexa 568	1:300	Molecular Probes
Goat anti mouse	Alexa 568	1:300	Molecular Probes
Goat anti rat	Alexa 647	1:300	Molecular Probes
Goat anti HRP	Cy3	1:300	Molecular Probes
Goat anti HRP	Cy5	1:200	Invitrogen
toto		1:5000	

2.1.3 Fly Stocks

2.1.3.1 General stocks

Stock	Source/reference
OregonR	Lindsley & Zimm, 1992
W ¹¹¹⁸	Lindsley & Zimm, 1992
eyFLP; Gla Bc hs-hid/ CyO	Thomas Hummel, unpublished
eyFLP UAS-CD8; Tft/CyO	Georg Steffes, 2007
eyFLP UAS-CD2; Tft/CyO	Georg Steffes, 2007
eyFLP UAS-syt; Tft/CyO	Georg Steffes, 2007
eyFLP UAS>CD2>CD8; Tft/CyO	Georg Steffes, 2007
eyFLP UAS>CD2>CD8 UAS-dsred; Tft/CyO	Georg Steffes, 2007
hsFLP; Tft/CyO	Golic & Lindquist, 1989
hsFLP UAS-CD2; Tft/CyO	Georg Steffes, 2007
N a323/FM7 bb; Tft/CyO bb?	Edenfeld, 2004
Tft/CyO	Thomas Hummel, unpublished
Gla/CyO <i>twiG4</i> UAS-GFP	Tobias Storck
Sp/CyO; MKRS/TM2	Thomas Hummel, unpublished
Bl/CyO; TM2/TM6	Thomas Hummel, unpublished
Bl/CyO <i>twiG4</i> UAS-GFP; TM2/TM6 GFP?	Thomas Hummel, unpublished
TM3/TM6	Thomas Hummel, unpublished
CyO delta 2-3/Bc EGFR E1	Mareike Strunk, 2005
Sp/CyO; sb delta 2-3/TM2	Georg Steffes, 2007
<i>w-;; π Δ 2-3, Ki, pp/π Δ 2-3, Ki, pp</i>	Robertson et al., 1988
UAS-CD8-tomato/TM3	Frank Schnorrer
Sp/CyO; UAS-act5cCherry/TM2	Raiko Stephan
eyFLP; FRT42 ubi-GFP nls/CyO	Bloomington Stock Center
Sp/CyO; UAS-CD2/TM2	Thomas Hummel, unpublished
FRT42 Gal80	Lee & Luo, 1999
FRT42 PCNA	Thomas Hummel, unpublished
FRT42 PCNA/CyO; "Multimarker 1"/TM3 ser, actGFP	Ariane Zierau

Stock	Source/reference
UAS-laminGFP/CyO	Christina Gohl
UAS-CD8/CyO	Lee and Luo, 1999)
eyFLP;FRT42 GMR-GFP Or22a:syt/CyO	Georg Steffes
FRT42/CyO; TM2/TM6	Thomas Hummel, unpublished
UAS-laminGFP/TM2	Robert Fricke
UAS-CD8-cherry	Frank Schnorrer
Sp/CyO ^{twiGal4} UAS-GFP; UAS-laminGFP/TM2	Thomas Hummel, unpublished
eyFLP gr-lacZ; FRT82 GMR-hid/TM6	Thomas Hummel, unpublished

2.1.3.2 Gal4 driver

Stock	Source/reference
lzGal4 UAS-syt; FRT42 Gal80/CyO	Georg Steffes, 2007
dllGal4 UAS-CD8/CyO	Christian Heringer, 2007
dllGal4/CyO; Or46a:syt, Or47a:syt/TM2	Christian Heringer, 2007
eyFLP elavGal4; FRT42 Or47a:syt/CyO	Christian Heringer, 2007
eyFLP elavGal4; FRT42 Gal80/CyO	Thomas Hummel, unpublished
GH146Gal4	Stocker et al., 1997
E132Gal4	Halder et al., 1995
capsGal4	Hayashi et al., 2002
elavGal4	Lin and Goodman, 1994
FRT42 Gal80/CyO; elavGal4 UAS-CD8/TM6	Thomas Hummel, unpublished
FRT42 Gal80/CyO; conGal4 UAS-CD2/TM6	Zierau, 2007
FRT42 PCNA/CyO; conGal4 UAS-CD2/TM6	Zierau, 2007

2.1.3.3 OR Marker

The Or-markers were recombined with UAS-sytGFP, UAS-CD8GFP and UAS-CD2GFP and established with an FRT42 either PCNA or Gal80 to perform single class analysis.

Stock	Source/reference
Or19aGal4	Couto et al. 2005
Or22aGal4	Vosshall et al., 2000
Or23aGal4	Vosshall et al., 2000
Or42aGal4	Couto et al. 2005
Or42bGal4	Couto et al. 2005
Or43aGal4	Couto et al. 2005
Or43bGal4	Couto et al. 2005
Or46aGal4	Vosshall et al., 2000
Or47aGal4	Vosshall et al., 2000
Or47bGal4	Vosshall et al., 2000
Or49aGal4	Fishilevich and Vosshall, 2005
Or49bGal4	Couto et al. 2005
Or59cGal4	Hummel et al. 2003
Or65aGal4	Fishilevich and Vosshall 2005
Or67aGal4	Couto et al. 2005
Or67bGal4	Couto et al. 2005
Or67cGal4	Couto et al. 2005
Or69aGal4	Couto et al. 2005
Or71aGal4	Hummel et al. 2003
Or82aGal4	Couto et al. 2005
Or83cGal4	Couto et al. 2005
Or88aGal4	Komiyama et al., 2004
Or92aGal4	Komiyama et al., 2004
Or98aGal4	Couto et al. 2005
Gr21dGal4	Scott et al. 2001

Stock	Source/reference
Or83bGal4	Larrson et al. 2004
Or47a::sytGFP	Vosshall et al., 2000
Or47a::CD8GFP	Couto et al. 2005
Or23a::CD8GFP	Couto et al. 2005

2.1.3.4 Deficiencies & lethal P-insertions

Stock	Source/reference
Df(2R)nap9/Dp(2;2)BG, In(2LR)Gla, wg[Gla-1]	Bloomington Stock Center / Barry Ganetzky
Df(2R)ST1, Adh[n5] pr[1] cn[*]/CyO	Bloomington Stock Center / Jose Bonner
Df(2R)cn9/CyO, amos[Roi-1] sp[*] <P>	Bloomington Stock Center / C. Nusslein-Volhard
w[118]; Df(2R)H3C1/CyO	Bloomington Stock Center / Ken Howard
w[118]; Df(2R)H3E1/CyO	Bloomington Stock Center / Ken Howard
w[1]; Df(2R)w45-30n, cn[1]/CyO	Bloomington Stock Center / Berkeley Drosophila Genome Proj.
Df(2R)BSC29, cn[1] bw[1] sp[1]/CyO	Bloomington Stock Center / Kevin Cook
w[1118]; Df(2R)B5, px[1] sp[1]/CyO, Adh[nB]	Bloomington Stock Center / Martha O'Brien
Df(2R)X1, Mef2[X1]/CyO, Adh[nB]	Bloomington Stock Center / Martha O'Brien
Df(2R)stan1, P{ry[+t7.2]=neoFRT}42D cn[1] sp[1]/CyO	Bloomington Stock Center / Michael Ashburner
Df(2R)en-A/CyO	Bloomington Stock Center / MaryAnn Martin
Df(2R)en30/SM5; Dp(1;Y)B[S]	Bloomington Stock Center / Caltech Stock Center
Df(2R)BSC39, cn[1] bw[1]/SM6a, bw[k1]	Bloomington Stock Center / Kevin Cook

Stock	Source/reference
Df(2R)CB21/CyO; ry[506]	Bloomington Stock Center / Kate Beckingham
Df(2R)BSC40/SM6a	Bloomington Stock Center / Kevin Cook
Df(2R)BSC3, w[+mC] unch[k15501] cn[1] bw[1] sp[1]/SM6a, bw[k1]	Bloomington Stock Center / Kevin Cook
Df(2R)vg-C/CyO, P{ry[+t7.2]=sevRas1.V12}FK1	Bloomington Stock Center / Caltech Stock Center
Df(2R)CX1, wg[12] b[1] pr[1]/SM1	Bloomington Stock Center / Nick Baker
Df(2R)BSC18/SM6a	Bloomington Stock Center / Kevin Cook
Df(2R)BSC11/SM6a	Bloomington Stock Center / Kevin Cook
w[a] N[fa-g]; Df(2R)Jp1/CyO	Bloomington Stock Center / Bill Saxton
w[a] N[fa-g]; Df(2R)Jp8, w[+]/CyO	Bloomington Stock Center / Bill Saxton
Df(2R)BSC49/SM6a	Bloomington Stock Center / Kevin Cook
y[1]; Df(2R)P803-Delta15, cn[1]/SM1; sv[spapoll]	Bloomington Stock Center / John Tomkiel
w[1118]; Df(2R)ED1, P{w[+mW.Scer\FRT.hs3]=3'.RS5+3.3'}ED1/SM6a	Bloomington Stock Center / DrosDel Project
Df(2R)BSC44/SM6a	Bloomington Stock Center / Kevin Cook
Df(2R)robl-c/CyO, y[+]	Bloomington Stock Center / Aaron Bowman
y[1] w[67c23]; Df(2R)k10408, P{w[+mC]=lacW}mthl3[k10408]/CyO	Bloomington Stock Center / Berkeley Drosophila Genome Proj. / Istvan Kiss
Df(2R)BSC45/SM6a	Bloomington Stock Center / Kevin Cook
y[1] w[67c23]; Df(2R)14H10Y-53/SM6a	Bloomington Stock Center / Bill Gelbart
y[1] w[67c23]; Df(2R)14H10W-35/SM6a	Bloomington Stock Center / Bill Gelbart
Df(2R)PC4/CyO	Bloomington Stock Center / Jose Bonner / Trudi Schupbach
y[1] w[*]/Dp(1;Y)y[+]; Df(2R)P34/CyO	Bloomington Stock Center / Winifred Doane
Df(2R)BSC26/CyO	Bloomington Stock Center / Kevin Cook

Stock	Source/reference
Df(2R)BSC22/SM6a	Bloomington Stock Center / Kevin Cook
Df(2R)017/SM1	Bloomington Stock Center / D. Henderson
Df(2R)AA21, c[1] px[1] sp[1]/SM1	Bloomington Stock Center / Kim Fetchel
Df(2R)BSC19, cn[1] bw[1]/SM6a	Bloomington Stock Center / Kevin Cook
Df(2R)Egfr5, b[1] pr[1] cn[1] sca[1]/CyO, P{ry[+t7.2]=sevRas1.V12}FK1	Bloomington Stock Center / Jim Price
P{EPgy2}Vha44 ^{EY02202}	Gene Disruption Project members, 2001-
PBac{WH}CG33960 ^{f02042}	Gene Disruption Project members, 2001-
PBac{RB}CG4927 ^{e03031}	Gene Disruption Project members, 2001-
P{SUPor-P} ^{KG01703}	Gene Disruption Project members, 2001-
P{EPgy2}CG5522 ^{EY01316}	Gene Disruption Project members, 2001-
P{EPgy2}Ef1beta ^{EY05513}	Gene Disruption Project members, 2001-
PBac{WH}Cbp53E ^{f00876}	Gene Disruption Project members, 2001-
P{EPgy2}RhoGEF2 ^{EY08391}	Gene Disruption Project members, 2001-
PBac{WH}CG6967 ^{f07741}	Gene Disruption Project members, 2001-
P{EPgy2}GstS1 ^{EY07338}	Gene Disruption Project members, 2001-
P{EPgy2} ^{EY06179}	Gene Disruption Project members, 2001-
P{EPgy2} ^{EY01972}	Gene Disruption Project members, 2001-
Df(2R)Exel7145	Ryder, 2004
Df(2R)Exel6065	Ryder, 2004
Df(2R)ED2847	DrosDel Project
Df(2R)ED2751	DrosDel Project
Df(2R)ED1	DrosDel Project
Df(2R)Exel6066	Ryder, 2004
P[lacW]CG6426 ^{K04810}	Spradling et al., 1999
Df(2R)vpt#1	This work
Df(2R)vpt#2	This work
Df(2R)vpt#3	This work

2.1.3.5 Dark alleles

Stock	Source/reference
dark82/CyO actGFP; UAS-dark wt H4/TM3 sb	Akdemir/Abrams, 2002
dark82/CyO actGFP; UAS-dark wt e5.1/TM3 sb	Akdemir/Abrams, 2002
dark82/CyO actGFP; UAS-dark v C8/TM3 sb	Akdemir/Abrams, 2002
dark82/CyO actGFP; UAS-dark v G6/TM3 sb	Akdemir/Abrams, 2002
FRT42 dark H16/CyO	Srivastava/Bergmann, 2006
FRT42 dark S7/CyO	Srivastava/Bergmann, 2006
FRT42 dark V5/CyO	Steffes, 2007
FRT42 dark C1/CyO	Srivastava/Bergmann, 2006
FRT42 dark M20/CyO	Srivastava/Bergmann, 2006
FRT42 dark G8/CyO	Srivastava/Bergmann, 2006
FRT42 dark N10/CyO	Srivastava/Bergmann, 2006
FRT42 dark P56/CyO	Srivastava/Bergmann, 2006
FRT42 dark D3/CyO	Srivastava/Bergmann, 2006
FRT42 dark B2/CyO	Srivastava/Bergmann, 2006
FRT42 dark G29/CyO	Srivastava/Bergmann, 2006
FRT42 dark G15/CyO	Srivastava/Bergmann, 2006
FRT42 dark N5/CyO	Srivastava/Bergmann, 2006
FRT42 dark V10/CyO	Scheper, 2005
FRT42 dark E4/CyO	Srivastava/Bergmann, 2006
FRT42 dark B5/CyO	Srivastava/Bergmann, 2006
FRT42 dark V8/CyO	Scheper, 2005
FRT42 dark J7/CyO	Srivastava/Bergmann, 2006
FRT42 dark V14/CyO	Seidl, 2006
P[lacW] Ark ^{k11502} /CyO	Kanuka et al., 1999
P[lacW] vpt ⁶²⁸ /CyO	This Work
P[lacW] vpt ⁶⁹⁷ /CyO	This Work
P[lacW] vpt ²⁰⁵⁷ /CyO	This Work

2.1.3.6 Connectin stocks

Stock	Source/reference
Con ^{fvex238}	Nose et al., 1994
FRT42 UAS-conRNAi/CyO	VDRC, Dietzl et al. 2007
FRT42 dark v8 Or47a:syt UAS-conRNAi/CyO	This work
UAS-conRNAi/CyO; con ^{fvex238} /TM6	This work
FRT42 Gal80/CyO; conGal4 UAS-CD2/TM6	Ariane Zierau, 2007
FRT42 PCNA/CyO; conGal4 UAS-CD2/TM6	Ariane Zierau, 2007
FRT42 dark V8 Or47a:syt/CyO; con ^{fvex238} /TM6	This work
FRT42/CyO; con ^{fvex238} /TM2	This work

2.1.3.7 Apoptosis effectors

Stock	Source/reference
UAS-DIAP-1/TM2	obtained from Liane Bolke/ Arno Müller
UAS-DRONC DN/CyO	obtained from Liane Bolke/ Arno Müller
UAS-p35/CyO	Hay et al, 1994
UAS-darkRNAi	VDRC
UAS-DroncRNAi	VDRC
UAS-DriceRNAi	nigFly
DIAP1th4	Goyal et al., 2000
P{w[+mC]=EP}Dredd[EP1412] w[1118]	Elrod-ERricson et al., 2000

2.2 Methods

All stocks are kept at 25°C on *Drosophila* standard medium. For crossings virgin females were collected 0-4h after eclosion and crossed to males of various ages.

2.2.1 Cultivation of flies

All stocks are kept at 25°C on *Drosophila* standard medium. For crossings virgin females were collected 0-4h after eclosion and crossed to males of various ages.

2.2.2 Identifications of novel genes involved in ORN targeting

To identify novel genes a large scale EMS mutagenesis screen was performed (Steffes, 2007). Male flies carrying a FRT42 and a white⁺-labeled Or22a:sytGFP insertion were mutagenized using ethyl methyl sulfonate (EMS) to induce point mutations and lethal stocks were established. The flies were crossed to a “Multimarker”-chromosome, containing four OrGal4 insertions combined with a UAS-sytGFP (Zierau, 2007), and the phenotype was observed in *eyFLP* induced mitotic clones. The offspring of this cross were analyzed for defects in the innervations pattern of the ORNs.

2.2.3 Generation of recombinant fly lines / chromosome “cleaning”

Lethal alleles showing an ORN targeting defect had to be “cleaned” in order to separate the mutation of interest from putative background hits induced during the mutagenesis and to remove the Or22a:sytGFP insertion. The mutant alleles were crossed to a wild type chromosome with a FRT42 insertion. Virgins carrying the mutant chromosome in trans to the wild type chromosome were crossed against a balancer stock. White⁻ males from this cross were re-crossed against the balancer to establish stocks. Absence of the white⁺ insertion served as a readout that recombination had occurred. The stocks were examined for lethality by crossing to a deletion or independent allele of the same complementation group to confirm that the mutation was still present. Adult brains were dissected to validate the phenotype.

2.2.4 Clonal analysis

To circumvent the lethality of the alleles and allow the examination of ORN targeting defects in the adult olfactory system the FRT/FLP system was used that allows the tissue specific induction of mitotic clones (Xu & Rubin 1993).

For most experiments in this thesis the Flipase was expressed under the control of the *eyeless* promoter (*eyFLP*) (Newsome, Asling & Dickson 2000). Several experiments required specific labeling of only few cells, in this case a flipase under the control of the *hsp70* promoter was used (*hsFLP*) (Golic & Lindquist 1989).

During mitosis FLP induced recombination leads to different outcomes. Either the cells remain heterozygous or one homozygous mutant cell and one homozygous wildtype cell is generated. If these cells divide, they form homozygous patches in the adult animal. To increase the size of the homozygous mutant clones a cell lethal mutation can be introduced on the counter-chromosome leading to cell autonomous cell death thus favoring the homozygous mutant cells (Shipman-Appasamy et al., 1991) (Figure 04 A).

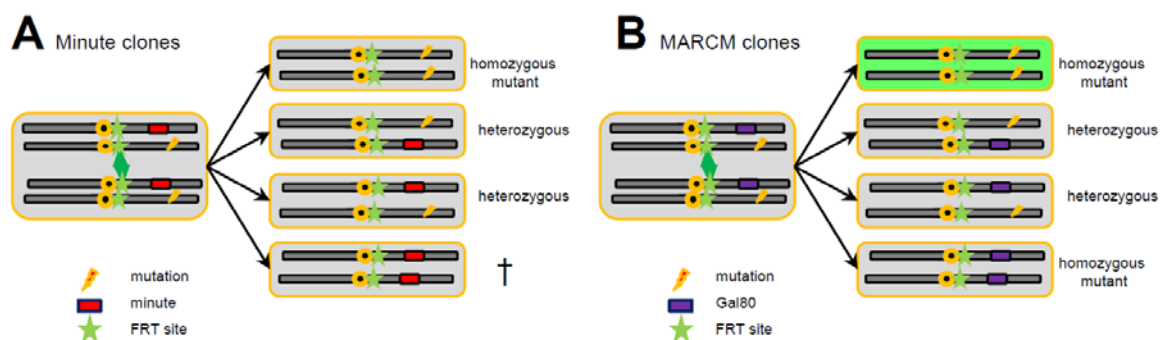


Figure 04 – Scheme of mitotic recombination techniques

(A) The induction of mitotic recombination combined with a *Minute* mutation leads to an increased mutant to wild type clone size ratio. Homozygous *minute* cells die. (B) Induction of mitotic clones combined with a *Gal80* element allows labeling of homozygous mutant cells (green cell), but leaves homozygous wild type cells in the background.

The FRT/FLP system can also be combined with the heterologous UAS/*Gal4* expression system (Brand & Perrimon, 1993). In addition, introducing a *Gal80* element that suppresses *Gal4*, it allows visualizing homozygous mutant cells in a heterozygous or homozygous wild type background. This method is called “mosaic analysis with a repressible cell marker” (MARCM, Lee & Luo, 1999) (Figure 04 B).

2.2.5 Selection of homozygous mutant embryos

To select for homozygous embryos the allele are established over a balancer marked with a GFP (e.g. $CyO_{twiGal\ 4-UASGFP}$). The stocks are put in little bins on apple agar plates that have been prepared with yeast before. The plates are changed every twelve hours. After having collected enough embryos, they are washed off the plates with PBT and bleached in 5% NaOCl to remove the chorion. After that they are washed at least five times with H_2O . The embryos are transferred to a fresh agar-plate an examined for GFP fluorescence under a UV-microscope. GFP negative embryos are selected for further analysis.

2.2.6 Preparation technique of adult brains

Flies of the desired phenotype are anesthetized with CO_2 and immediately killed in 70% EtOH. The dead flies are washed with PBS three times. The flies are transferred to a silicon plate and covered with a drop of PBS to prevent drying out. The dissection process is schematically shown in Figure 05. To dissect the brain, first the proboscis is removed by grabbing it (I) with one pair of tweezers and holding the head down with the other (II). This leaves a hole (III) which is used to grab both sides of the head exoskeleton (IV). By carefully pulling to one side the first half is removed (V), subsequently the other (VI). The brain is now freely accessible (VI) and can be detached from the body. Optionally remaining tracheae can be removed.

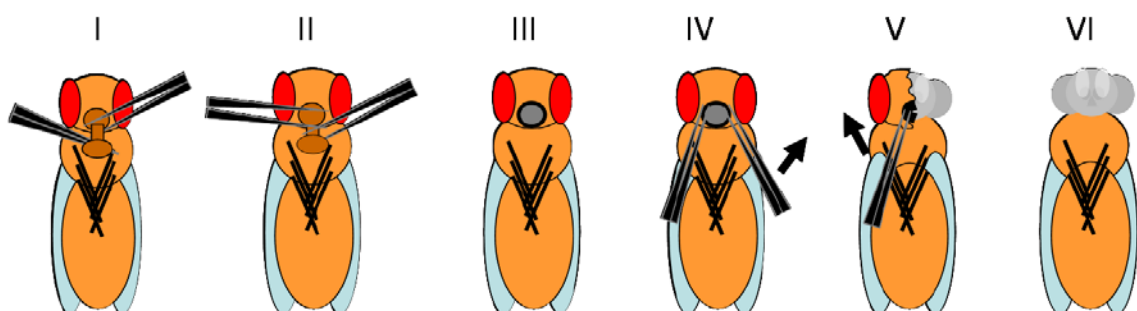


Figure 05 –Dissection method for adult brains

For details see text (2.2.6).

2.2.7 Preparation of pupal brains and antennae

To determine the age pupae have to be staged. The desired developmental stadium is selected. The pupae are carefully removed from the vial and transferred to a stripe of double sided adhesive tape. Next the operculum gets removed and the puparium gets cut longitudinally and carefully opened. The pupa is transferred carefully to a second stripe of tape and covered with PBT. Then a little whole is pinched in the anterior part of the pupae and slowly enlarged. The brain or antenna are picked out of the body and transferred to a fixation solution.

2.2.8 Cryo sections of adult antenna

- Decapitate flies of the desired genotype
- Arrange heads in a drop of OCT™ Cryostat medium (TissueTek, Netherlands) on a object slide
- Freeze heads at -20°C for at least 20 minutes
- Remove droplet with heads from object slide and fixate on the object holder of the Cryostat with OCT™ Cryostat medium, freeze the object holder to ensure proper attachment
- Collect 14µm slices of the antenna on SuperFrost®Plus microscope slides (Menzel-Gläser, Braunschweig)
- Fix for seven minutes in 4% PFA at room temperature
- Wash 2x in PBS for ten minutes
- Wash 30 min in PBT to permeabilize
- Block 30 min in 10% goat serum
- Incubate in first antibody (in 10% goat serum) over night at 4°C
- Wash 3x for 15 minutes in PBS
- Incubation in second antibody for 2 hours at room temperature
- Wash 3x for 15 minutes in PBT
- Add a drop of VectaShield™ mounting medium (Linaris, Wertheim), put on a cover slip, seal with nail polish
- Store at 4°C

2.2.9 Antibody staining

- Fixate brains in 2% PFA for 90 minutes on a shaker
- Remove fixation solution, add PBT
- Wash 3x in PBT for 15 minutes
- Block in 10% goat serum for 60 min at room temperature
- Incubate in first antibody at 4°C over night
- Wash 3x in PBT for 15 minutes
- Incubate in second antibody 3 hours at room temperature
- Wash 3x in PBT for 15 minutes
- Place specimen on a object slide, cover with a drop of VectaShield™ mounting medium
- Put on cover slip with little rubber feet to prevent mechanical stress on the specimen
- Store at 4°C

2.2.10 Acridin Orange staining

- Dissect tissue of interest
- 5 min 2µM Acridin-Orange solution
- 5 min washing in 1xPBS
- Mount samples (use rubber-feet for cover slip)
- Analyze directly under a fluorescence microscope (FITC/GFP filter)

2.2.11 Imaging of adult antenna

Whole antenna of adult flies carrying a GFP labeled OR marker are removed from the fly head and washed two times for ten minutes in PBT. The antennae are transferred to an objective slide in a drop of PBT. The liquid is removed with a piece of tissue paper, then the antenna are arranged on the slide. A drop of VectaShield™ mounting mediums added and a cover slip with little rubber feet put on to prevent squeezing of the antenna. The antennae are examined directly under a confocal microscope.

2.2.12 DNA isolation from adult flies

DNA from adult flies was extracted using the DNEasy™ blood & tissue kit from Quiagen according to the following protocol:

- Anesthetize 30 flies of the desired genotype and freeze them for 30min at -20°C in an 1,5 ml Eppendorf tube
- Add 160 µl PBS and 20 µl RNase A solution
- Homogenize flies using a grinder
- Add 25 µl Proteinase K
- Add 200 µl Buffer AL and vortex immediately
- Incubate at 56°C for 10 minutes
- Centrifuge for 2 minutes at 13000rpm with a tabletop centrifuge
- Transfer supernatant to a fresh Eppendorf tube
- Add 200µl 100% EtOH and vortex
- Transfer to a column and centrifuge for 1 minute at 8000rpm
- Discard flow-through
- Add 500µl Buffer AW1 and centrifuge for 1 minute at 8000rpm
- Discard flow-through
- Add 500µl Buffer AW1 and centrifuge for 3 minute at 13000rpm
- Transfer column to a fresh Eppendorf tube
- Add 200µl of ddH₂O to the column
- Centrifuge for 1 minute at 13000rpm
- Store at -20°C

2.2.13 DNA isolation from single flies or embryos

- Place one fly or 30 embryos in a 0,5 ml tube and mash the fly for 5 to 10 seconds with a pipette containing 50µl of SQUIB, without expelling any liquid (sufficient liquid escapes from the tip) Then expel the remaining Buffer.
- Incubate at 25-37°C (or room temperature) for 20- 30 min
- Inactivate the Protein Kinase C by heating to 85°C for 1-2min

This preparation can be stored at 4°C for months. Typically use 1µl of the DNA preparation is used in 10-15µl reaction volume. It does not matter if fly parts (wings, bristles, legs) are inadvertently added to the PCR.

2.2.14 PCR

The following reaction is performed for a final reaction volume of 20 µl.

Template DNA	ca. 100 ng/µl of the final volume
10x Polymerase Buffer	2µl
dNTPs(10mM)	0,2µl
MgCl ₂ (25mM)	0,8µl
5' primer (10µM)	3µl
3' primer (10µM)	3µl
<i>Taq</i> DNA polymerase	0,5µl
sterile H ₂ O	ad 20µl

This protocol is an example for a standard PCR. Concentrations of components can vary because of different primers, template DNAs or DNA-Polymerases.

Standard temperature profile:

1. Initial denaturation 95°C 3:00 min
 2. De-naturation 95°C 1:00 min
 3. Annealing 60°C 0:25 min (variable)
 4. Extension 72°C 1 min/kb
- Iterations of step 2-4 35x
5. Final extension 72°C 8:00 min
 6. Cooling 4°C as needed

Temperature and length of the steps may vary according to the efficiency of the polymerase, the sequence of the template or the annealing properties of the primer.

2.2.15 Inverse PCR

Inverse PCR was used to determine the location of P-insertions. This method allows analyzing unknown sequences flanking a known DNA sequence, in this case the P insertion.

Initially genomic DNA of flies carrying the P-insertion of interest is isolated (1.2.12). This DNA is restricted with a set of statistically frequent cutting enzymes. The obtained fragments are re-ligated at a low DNA concentration and temperature to promote the formation of circular fragments. These fragments are used as a template for a PCR. Primers are chosen that bind within the known sequence of the P-insertion but point outwards. The PCR product can directly get sequenced and analyzed.

2.2.16 DNA gel elektroforeses

The DNA fragments originating from the PCR were analyzed in agarose gels (0,8 – 2 % agarose in TBE) with ethidium bromide (1 μ l/100ml gel) using a horizontal gel electrophoresis at 100-150 V. 5 μ l per gel HyperLadderTM from Bioline was used as a quantitative DNA standard. Samples were prepared with 10x DNA loading buffer.

2.2.17 Sequencing

Sequencing reactions were performed using the sequencing kit DYEnamic ET (Dye Terminator Cycle Sequencing Kit for MegaBACE (DNA Analysis Systems, GE Healthcare) according to the manufacturers advice.

The sequences were analyzed using different applications from the Lasergene7 software bundle (DNA-Star).

3 Results

The scope of this work was to identify regulatory mechanisms underlying the precise formation of the olfactory map in the antennal lobe of *Drosophila*. The *verpeilt* complementation group shows stereotypic mis-targeting in the olfactory system. Different genetic and histological experiments were performed to determine the gene affected in the *verpeilt* mutations and to determine the underlying control mechanism of synaptic specificity.

3.1 Mutations in *verpeilt* cause ectopic mis-targeting of Or47a neurons

In a forward genetic mosaic screen a complementation group containing four independent alleles, called *verpeilt* (*vpt*, German for uncoordinated, woozy) based on a stereotypic innervation defect of sensory receptor neurons (ORNs) was identified. All *verpeilt* mutations are homozygous lethal at late pupal stages.

In the mosaic screen five different ORN classes were analyzed in the background of the mitotic clones to identify alterations in the connectivity pattern in sensory neuron innervation (Scheper, 2005, see 2.2.2). *Vpt* mutants are characterized by an additional innervation at a stereotyped position in the dorso-lateral area of the antennal lobe (AL) (hence referred to as ectopic glomerulus). Single ORN class analysis reveals that the ectopic glomerulus was exclusively caused by Or47a-axons (Figure 06).

All *verpeilt* alleles found in the screen exhibited a similar, stereotypic mis-innervation of Or47a axons in the dorso-lateral side of the AL, in close proximity to the DA3 glomerulus (Figure 06 A, 06 B). A closer inspection of the neuropil organization (e.g. anti-N-Cadherin pattern) in this area showed that the mis-projecting axons target to an area which in the wild type provides a small empty “pit” directly adjacent ventro-lateral to the DA3 glomerulus. (Figure 06 A', 06 B'). Interestingly, the Or-class 23a that innervates the DA3 glomerulus is not affected by *vpt*, (Figure 06 C, 06 D). In addition, the axonal projections towards their target glomerulus are disturbed.

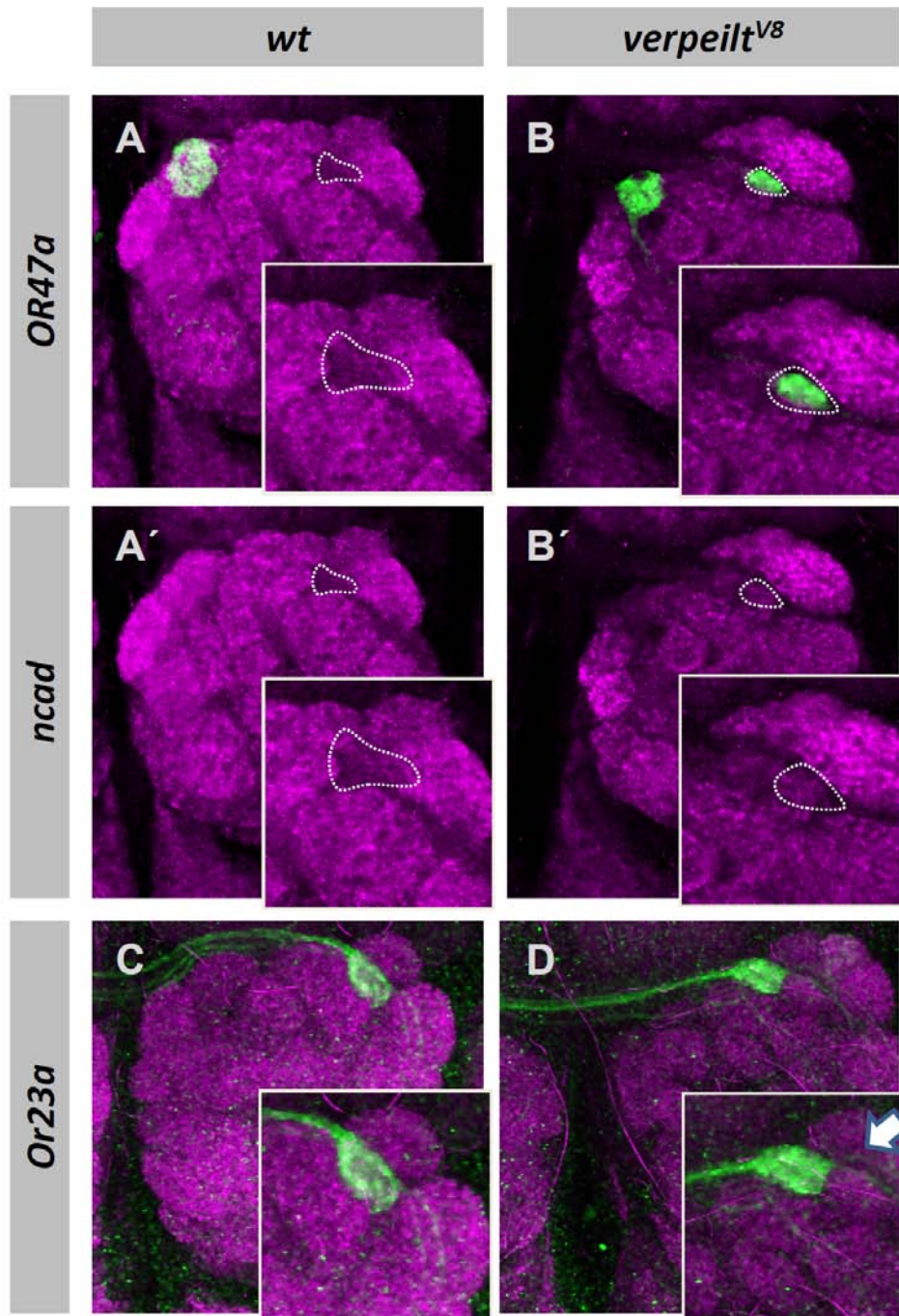


Figure 06 – *verpeilt* causes a stereotype ORN innervation in the dorso-lateral antennal lobe

A-B' Innervation of Or47a in wildtype and *verpeilt* mutants. (A) In the wildtype Or47a neurons converge to a single glomerulus. (B) In *verpeilt* mutants Or47a neurons innervate a second glomerulus in the dorso-lateral AL next to the DA3 glomerulus. (A',B') The area next to the DA3 glomerulus is not innervated in wildtype (dotted line), in *verpeilt* mutants this space is occupied by neuropil. (C,D) The targeting of Or23a is not affected, though in *verpeilt* the neighboring area is filled with neuropil (arrow in (D)). Genotypes: (A), *eyFLP; FRT42/FRT42 PCNA; Or47aGal4 UAS-sytGFP*, (B) *eyFLP; FRT42dark^{V8}/FRT42 PCNA; Or47aGal4 UAS-sytGFP*, (C) *eyFLP; FRT42/FRT42 PCNA; Or23aGal4 UAS-sytGFP*, (D) *eyFLP; FRT42dark^{V8}/FRT42 PCNA; Or23aGal4 UAS-sytGFP*. Or47a expression is labeled with α -GFP (green), neuropil with α -ncad (magenta).

The mis-targeting of OR47a axons in *vpt* mutant clones is mostly ventro-lateral of the DA3 glomerulus, but in very rare cases also on more lateral positions. Also remarkable for an axon connectivity mutant is the full penetrance of this defect. The four *verpeilt* alleles found in the screen, *vpt*^{V5}, *vpt*^{V8}, *vpt*^{V10} and *vpt*^{V14} show very little variance in the ectopic glomerulus regarding the position or diameter/size (data not shown).

3.2 Identification of the *verpeilt* locus

One of the main topics of this thesis was the identification of the *verpeilt* loci in the different alleles. Different approaches were used to identify the affected gene.

3.2.1 Complementation analysis

In a first approach the *verpeilt* mutations were crossed against a set of deficiencies covering most parts of the right arm of the 2nd chromosome. With this it was possible to locate the lethality of the *verpeilt* mutation to cytological region 53D14 - 53F8, which contains about 244kb with 44 predicted genes. All available lethal P-element insertions within this region complement the *verpeilt* lethality (Figure 07).

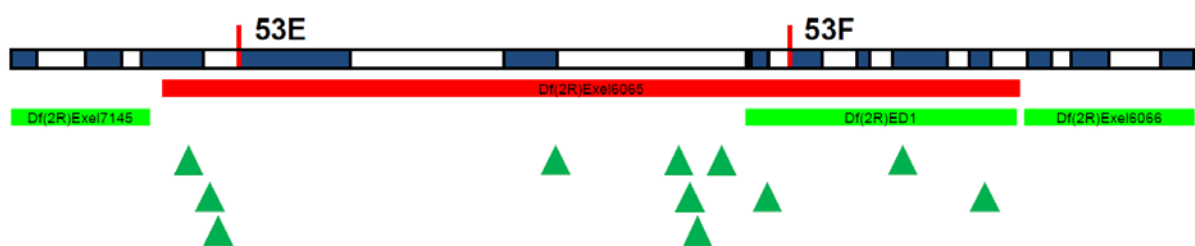


Figure 07 –Genomic region containing the *verpeilt* locus

Green bars resemble deficiencies that complement, red bars the deficiency that does not complement the *verpeilt* lethality. Locations of P-elements tested against *verpeilt* are indicated by green triangles. The upper white and blue bar represents the cytologic bands in the region 53D10 - 53F13.

3.2.2 P-element mutagenesis

Another attempt was to obtain a P-element insertion into the *verpeilt* locus using a “local hop” strategy (Tower et al. 1993). Three homozygous lethal P-insertions could be isolated, $P[lacW]vpt^{628}$, $P[lacW]vpt^{697}$ and $P[lacW]vpt^{2057}$, upon remobilization of the homozygous viable $P[lacW]CG6426^{K04810}$. Mapping of the insertion loci via inverse PCR revealed different positions for each of the P-elements. $P[lacW]vpt^{628}$ maps to the cytologic region 53F8 in the 5' UTR of a gene called *GstS1*, $P[lacW]vpt^{687}$ is inserted in the cytologic region 54A2, close to a small nucleolar RNA (snoRNA), $P[lacW]vpt^{2057}$ in the region 53D12, with no annotated gene in the adjacent 2kb or so. Interestingly, $P[lacW]vpt^{687}$ and $P[lacW]vpt^{2057}$ do not even map within the designated 53D14 -53F8 interval (Figure 08). In addition, excision of the P-elements could not reverse the *verpeilt* lethality. From these results it was suggested that the non-complementing of the *verpeilt* lethality might be caused by an imprecise excision of initial $P[lacW]CG6426^{K04810}$, causing a damage of neighboring genes. Analysis of the genomic region adjacent to the former $P[lacW]CG6426^{K04810}$ insertion site in $P[lacW]vpt^{628}$, $P[lacW]vpt^{697}$ and $P[lacW]vpt^{2057}$ could not detect changes in the DNA sequence.

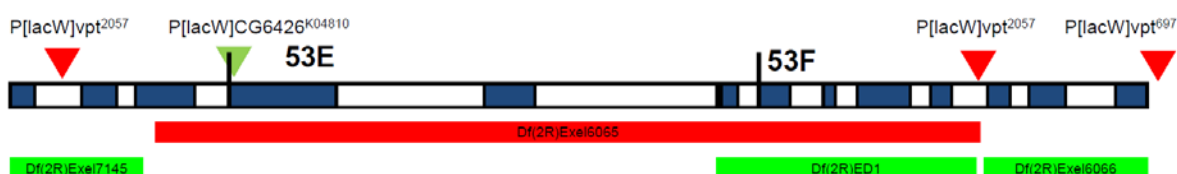


Figure 08 – Locations of the *verpeilt* P-element insertions

The green triangle shows the P-element that was mobilized, red triangles the created insertions.

As these results did not provide valuable information on the *verpeilt* locus a meiotic mapping approach was performed. By comparing the recombination frequency between the *verpeilt* lethality and a defined set of twelve insertions carrying a white mini-gene it is possible to measure relative distances. . The insertions used are shown in Table 01. The lowest recombination frequency was observed for the insertion $PBac\{WH\}Cbp53E^{f00876}$ with 0,002 cM. This equals a distance of roughly 10kb.

Table 01 – Insertions used for meiotic mapping and relative distances

Insertion	Cytologic location	cM
<i>P{EPgy2}Vha44^{EY02202}</i>	53C1	1,8
<i>PBac{WH}CG33960^{f02042}</i>	53C4	1,03
<i>PBac{RB}CG4927^{e03031}</i>	53C8	1,11
<i>P{SUPor-P}^{KG01703}</i>	53D2	0,61
<i>P{EPgy2}CG5522^{EY01316}</i>	53D8	0,58
<i>P{EPgy2}Ef1beta^{EY05513}</i>	53D14	0,35
<i>PBac{WH}Cbp53E^{f00876}</i>	53E4	0,002
<i>P{EPgy2}RhoGEF2^{EY08391}</i>	53E10	0,24
<i>PBac{WH}CG6967^{f07741}</i>	53F4	0,09
<i>P{EPgy2}GstS1^{EY07338}</i>	53F8	0,18
<i>P{EPgy2}^{EY06179}</i>	54A2	0,49
<i>P{EPgy2}^{EY01972}</i>	54B1	0,67

3.2.3 Generation of *verpeilt* deletions

Since within this radius no other gene is annotated (except *Cbp53E* in which the *PBac{WH}Cbp53E^{f00876}* is inserted), smaller deficiencies to define a small group of candidate genes were created. Using a set of transposable elements called “piggyBac” that contain FRT sites it is possible to delete defined parts of the chromosome. When two of these piggyBacs are combined in trans recombination can be induced with a flipase under the control of a heat shock promoter (hsFLP), thus leading to the deletion of the genomic region between the two piggyBac insertions (Figure 09A, Parks et al., 2004).

Three deletions were created, *Df(2R)vpt#1*, *Df(2R)vpt#2* and *Df(2R)vpt#3*, covering overlapping areas of the chromosome ranging from 53D13 to 53F8 (Figure 09B). Combinatorial complementation analysis including the previous used deficiencies localized the *verpeilt* locus to the cytological region 53E3 to 53E10. This region is 42,6 kb long and contains eleven genes.

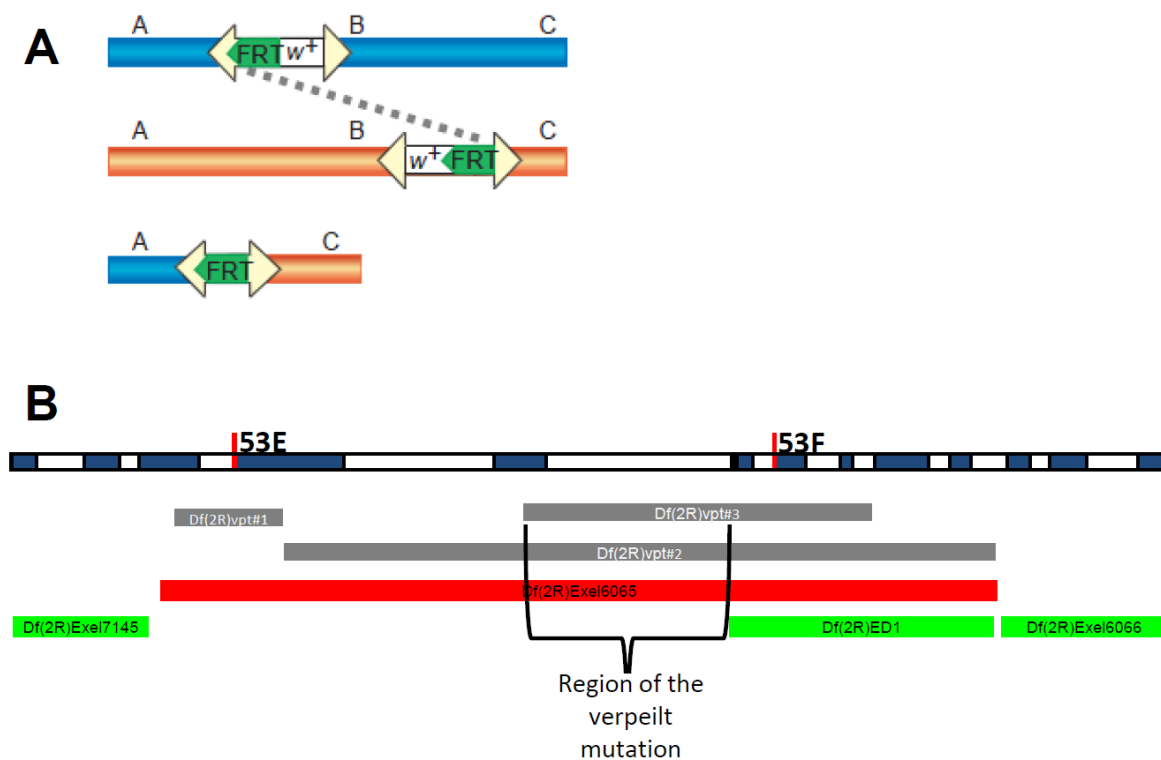


Figure 09 – Creation of deficiencies by FRT containing piggyback insertions

(A) Two PBac insertions are brought in trans. hsFLP induced recombination leads to deletion of the sequence between the two insertions (taken from Parks et al. 2004). (B) Locations of the deficiencies created in this work (grey bars) in comparison to the previous available deficiencies (green and red bars).

3.2.4 Sequencing of candidate genes

The remaining eleven candidate genes were then analyzed for sequence changes. The coding regions of the genes were amplified via PCR and then sequenced (Niehues, 2008). All four alleles of *verpeilt* showed point mutations in CG6829, the *Drosophila ark* gene (Rodriguez et al. 1999). The locations and the nature of the mutations are shown in Figure 10.

The *dark* gene spans over 6660bp and encodes for two predicted isoforms (Figure 11A) (Rodriguez et al. 1999; Zhou et al. 1999; Kanuka et al. 1999). The shorter isoform has not been described functionally yet; most studies only deal with the larger isoform. The large Dark protein is 1440 amino acids long and has a molecular weight of 165,8 kDa. It contains five domains, a N-terminal caspase recruitment domain (CARD) that is required for the interaction with DRONC and other caspases (Godzik 2003), followed by a CED4/NOD

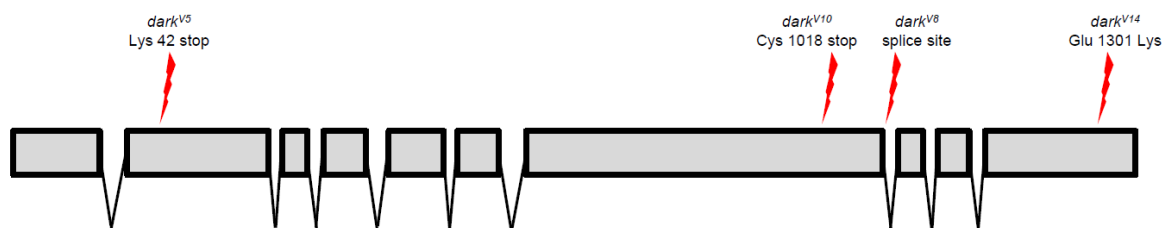


Figure 10 – Locations of the *dark*^{verpeilt} mutations

domain, a conserved helical domain (HD2), about 16 WD40 repeats, presumably involved in the oligomerization of *dark* and a regulatory C-terminal domain (Figure 11B, Yu et al., 2006; Srivastava et al., 2006). The mutations in the alleles found in the screen lead to a premature stop in two cases (*vpt*^{V5}, *vpt*^{V10}) in the CED4/Nod domain and the WD40 repeats respectively, one allele has a defective splice site after exon 8 (*vpt*^{V8}) and one mutation causes an amino acid exchange in the C-terminal domain (*vpt*^{V14}). Because of the allele-specific phenotypes (see below) the *verpeilt* mutations were named *dark*^{verpeilt}.

Dark has been described to encode for a pro-apoptotic factor, functioning as activator of the initiator caspase DRONC (Snipas et al. 2008). The Dark protein forms an octamer called the apoptosome that recruits DRONC, promoting its homo-dimerization and auto cleavage,

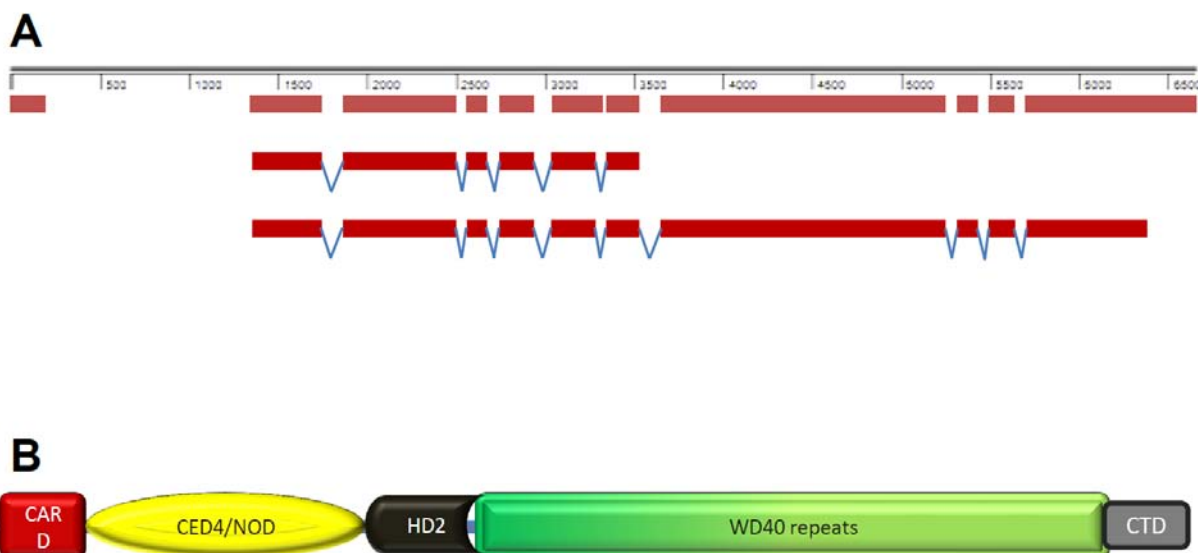


Figure 10 – Locations of the *dark*^{verpeilt} mutations

(A) Gene structure (upper red bars) and coding sequence (lower red bars). (B) Protein structure

thus leading to its activation. The activated DRONC dimer can activate the effector caspase DrICE which in turn leads to the initiation of programmed cell death. *Dark* and *DRONC* are expressed constantly in *Drosophila*. To prevent unspecific apoptosis the *Drosophila* inhibitor of apoptosis protein 1 (DIAP1) binds to the apoptosome after the *dark* mediated auto-activation of DRONC. This leads to a cleavage of the c-terminus of *dark* at the amino acid residue 1292 by DRONC, followed by a disassembly of the apoptosome-complex and finally leading to a degradation of the active DRONC dimer by the ubiquitin ligase domain of DIAP1. Only when an apoptotic stimulus is given a set of three genes, *grim*, *reaper* and *hid*, is expressed that inhibit DIAP1 function and leading to an accumulation of active DRONC and subsequent activation of DrICE.

3.3 Apoptosis and its effect on Or47a axon targeting

Apoptosis would serve a valuable explanation for the phenotype observed in the olfactory system. Loss of apoptosis could lead to additional neurons that then form an ectopic glomerulus. To analyze this, first the effect on apoptosis in the *dark*^{verpeilt} alleles found in the screen had to be determined.

3.3.1 The effect of the *dark*^{V8} allele on apoptosis

To check this, the central nervous system of L3 larvae was dissected and stained with Acridine orange, a dye which incorporates in the DNA of dying cells. It has been shown by Mills et al. that mutations in *dark* have the property to reduce apoptosis (Mills et al. 2006). In these experiments a clear decrease of apoptosis can be observed in *dark*^{V8} homozygous mutant L3 CNS compared with the wild type, though the decrease in the observed allele is not as strong as shown by Mills et al (Figure 12).

A different approach to analyze the effect on apoptosis is the GMR-*hid-eyFLP* (GheF) assay (Xu et al. 2005). By expressing the DAIP1 suppressor *hid* under the control of the eye specific GMR promoter apoptosis can be induced. Homozygous clones of mutations in downstream pro-apoptotic genes in the eye disc can attenuate this effect because the apoptosis cannot be initiated properly.

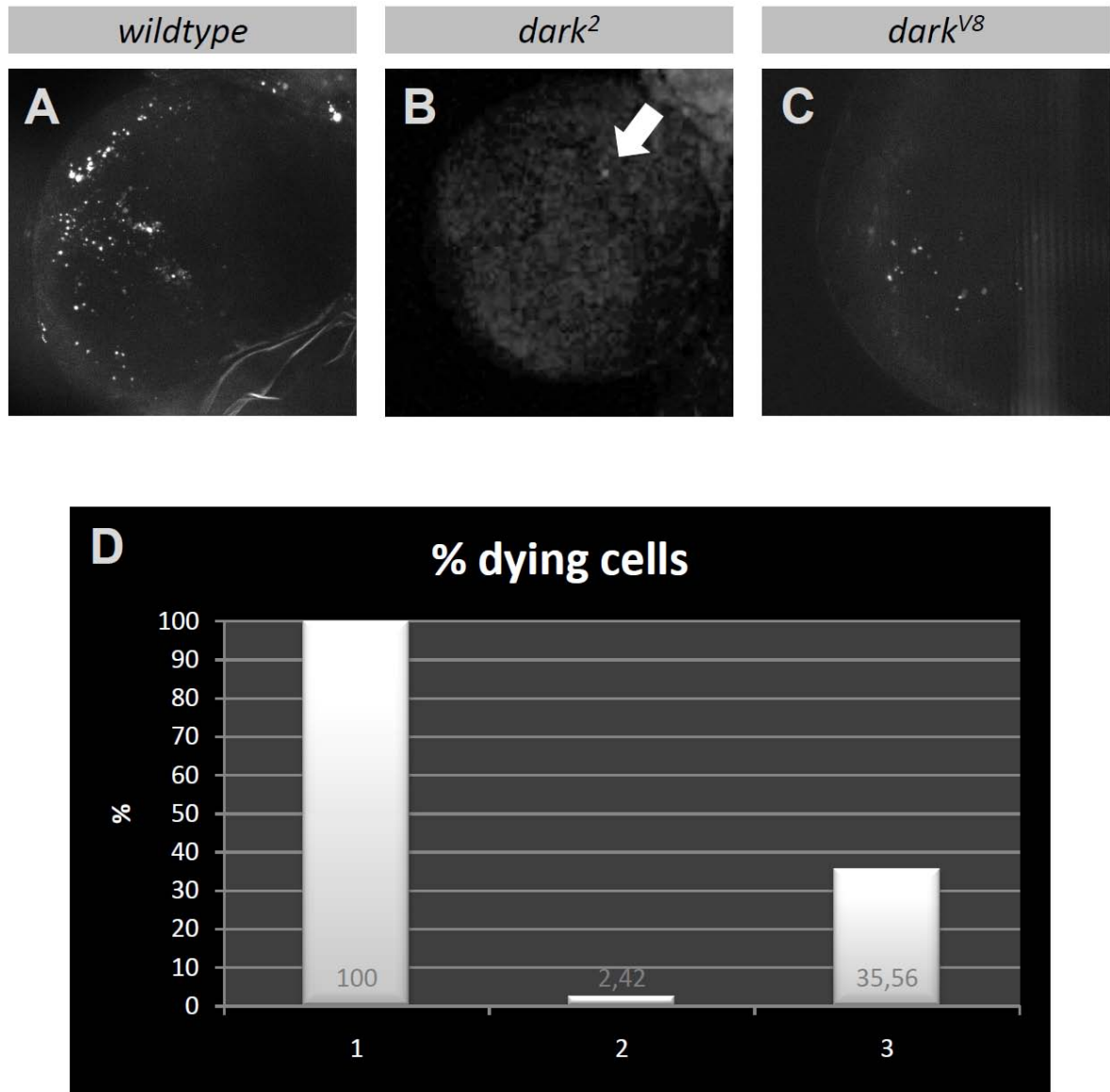


Figure 12 – *Dark*^{verpeilt} mutants show reduced cell death

(A-C) Acridin-Orange staining of wildtype (A) and mutant L3 larval optic lobes. The amount of dying cells is reduced in *dark* mutants. (B) In *dark*² only one cell is labeled with Acridin-Orange (arrow) (taken from Mills et al 2006). (D) The percentage of dying cells is shown graphically. Genotypes: (A) wild type, (B) *dark*² / -, (C) *dark*^{V8} / -.

In this experiment all tested *dark* alleles lead to a strong suppression of *hid* induced apoptosis. Expression of *hid* in the eye leads to a dramatic reduction of ommatidia (Figure 13 A, B). The defined null allele *dark*⁸² almost completely blocks the effect of *hid* and restores the size of the eye almost to its full extend. In addition, the structure of the eye is somehow rough, indicating a slight mis-regulation of apoptosis of inter-ommatidial cells (Figure 13 C). Two other EMS alleles, *dark*^{H16} and *dark*^{V8} had a similar ability to affect *hid*

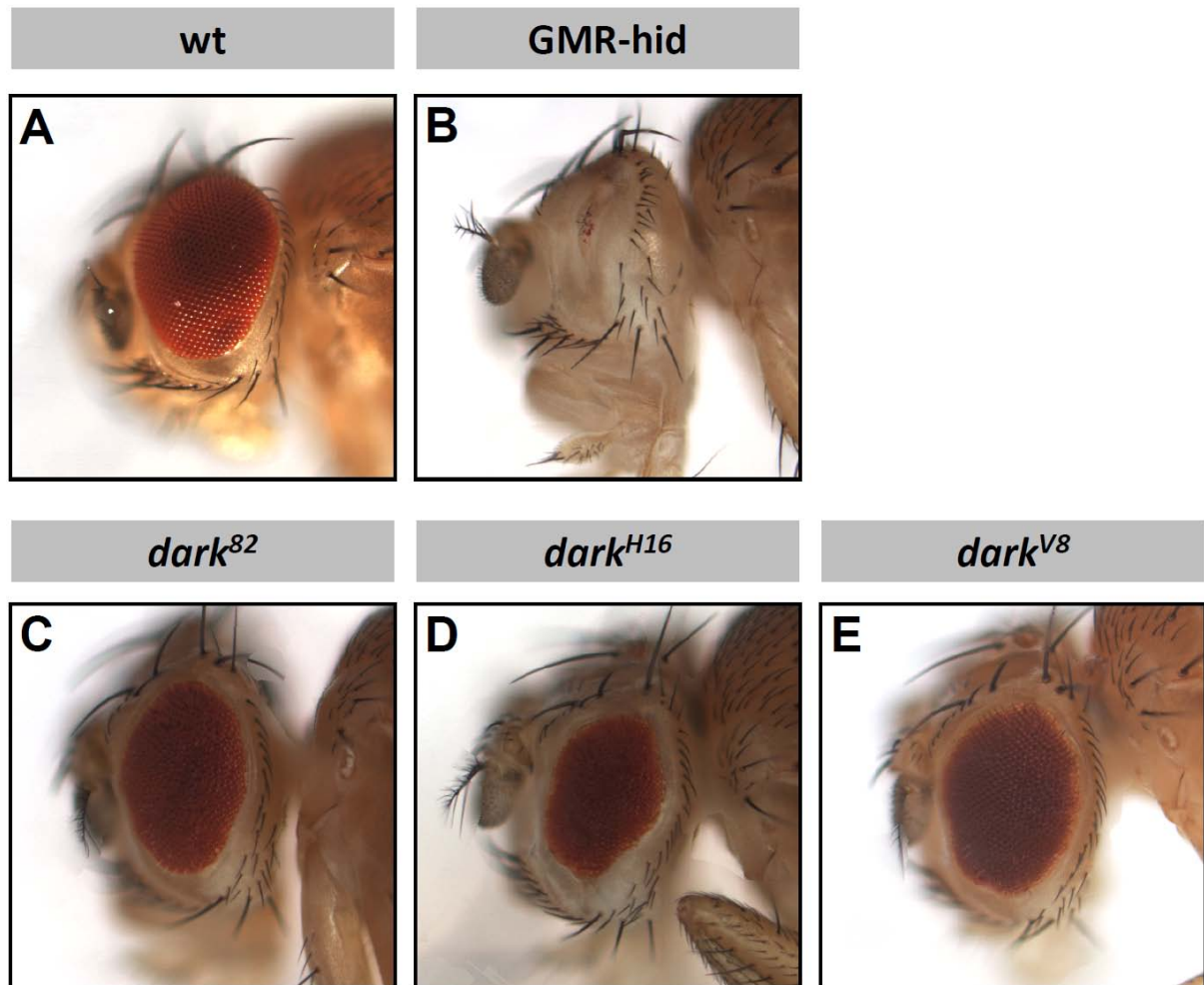


Figure 13 – *Dark*^{vpt} alleles suppress hid-induced apoptosis

(A) Wild type eye. (B) GMR-hid induces strong reduction of the size of the eye. (C) *dark*⁸² can suppress hid induced apoptosis, restoring the eye almost to its full size. (D) The allele *dark*^{H16} shows a similar reduction of the eye phenotype in a GMR-hid background. (E) The *dark*^{V8} rescues the size of the eye and also the ommatidial pattern. Genotypes: (A) wt, (B) eyFLP;;GMR-hid, (C) eyFLP; FRT42*dark*⁸²/FRT42;GMR-hid;GMR-hid, (D) eyFLP; FRT42*dark*^{H16}/FRT42;GMR-hid, (E) eyFLP; FRT42*dark*^{V8}/FRT42;GMR-hid;GMR-hid

induced apoptosis. The *dark*^{H16} allele contains a premature stop codon in the Card domain. In the Ghf assay, *dark*^{H16} also strongly suppresses Hid induced apoptosis, though it does restore the complete size of the eye (Figure 13 D). The eye in *dark*^{V8} is rescued to a similar extent as in the *dark*⁸² allele. The pattern of the ommatidia is even more regular than in *dark*⁸². This points to a slightly altered effect on apoptosis in this allele (Figure 13 E).

Taken together, these results confirm the involvement of the *dark*^{vpt} alleles found in the screen and suggests a function of the apoptosome complex in regulating ORN targeting.

3.3.2 Mutations in *dark*^{verpeit} do not affect ORN numbers

The ectopic targeting of Or47a axons in *dark*^{verpeit} mutants could be explained by additional Or47a neurons caused by a decrease in apoptosis which than project to an additional target. To test this possibility, the number of Or47a neurons in wild type and *dark*^{V8} mutant antenna was quantified.

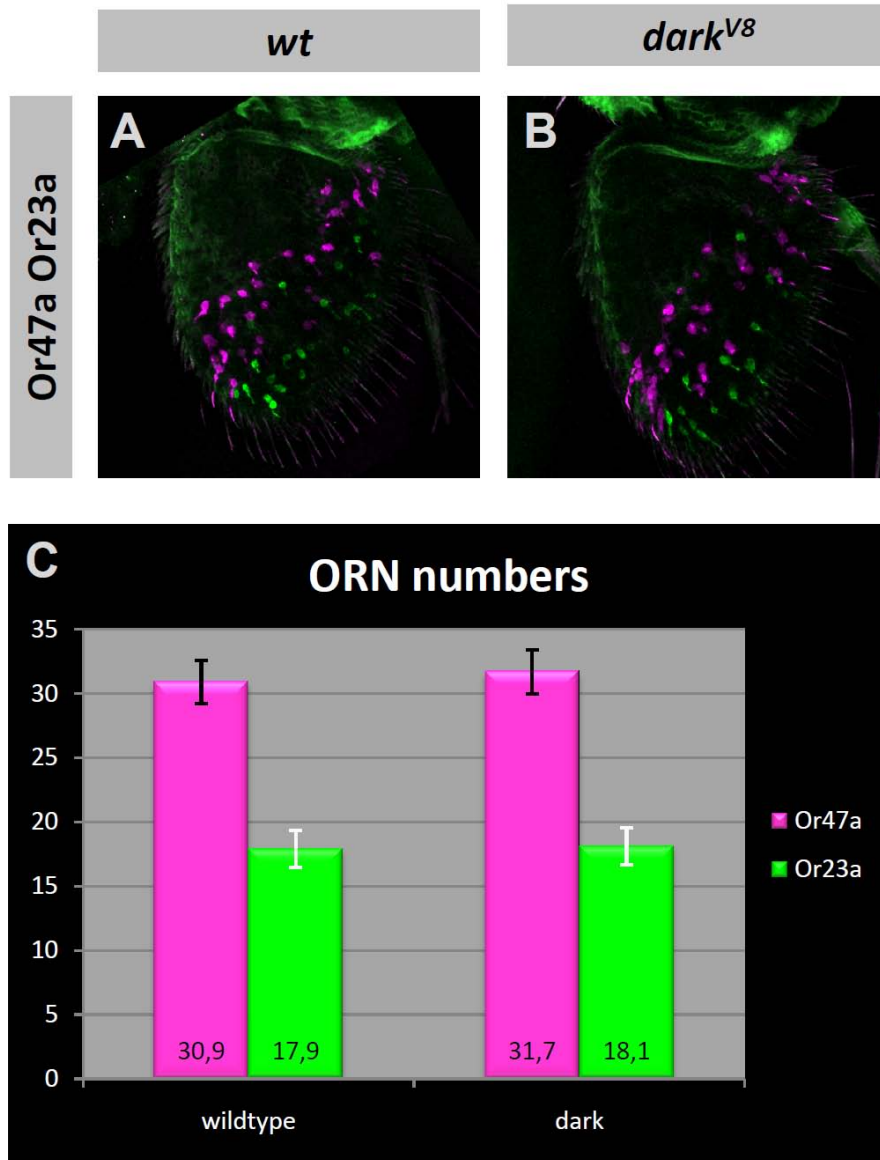


Figure 14 – *Dark*^{V8} does not affect ORN numbers

(A) OR47a and Or23a neurons labeled in a wild type antenna or (B) *dark*^{V8} mutant antenna. No changes in the number or spatial patterning in these two ORN classes have occurred. (C) Quantification of the ORN numbers in wild type and *dark*^{V8}. Genotypes: (A) eyFLP; FRT42 Or23a:CD8/FRT42 Or23a:CD8; Or47aGal4 UAS-CD8 cherry, (B) eyFLP; FRT42 Or23a:CD8 *dark*^{V8}/FRT42 Or23a:CD8; Or47aGal4 UAS-CD8 cherry. Or23a innervations labeled with GFP (green), Or47a neurons with cherry CD8 (magenta).

The ORNs were labeled by the expression of an OrGal4 driven GFP. A comparison of the ORN numbers in wild type and *dark*-mutant antenna revealed no differences in the amount of Or47a expressing neurons; the average number does not change significantly (Figure 14). On average in wild type antenna 30.9 Or47a neurons are found (antennae analyzed: $n=31$), in *dark*^{V8} mutant antenna the mean number of Or47a neurons is 31.7 ($n=39$). In addition the number of Or23a neurons was counted. The target of this class, the DA3 glomerulus is located directly adjacent to the ectopic glomerulus formed by Or47a neurons; therefore an increase of Or23a could affect the projection behavior. Also the numbers of Or23a neurons is not changed significantly, in the wild type on average 17.9 cells of this class are found ($n=14$), in *dark*^{V8} 18.1 ($n=14$). This suggests that the mis-targeting found in *dark*^{V8} mutants is not due to an increase of the number of ORNs.

3.3.3 Suppression of apoptosis does not cause Or47a mis-targeting

Although the number of Or47a neurons is not altered in *dark*^{V8} mutants, involvement of apoptosis in the formation of the ectopic structure cannot be excluded. To test this,

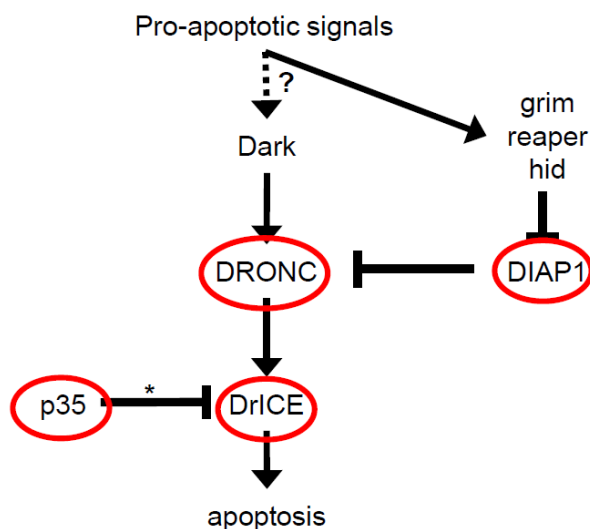


Figure 15 – The *Drosophila* apoptosis pathway

Red circles indicate the components that were manipulated to suppress apoptosis. The p35 (indicated with an asterisk) is a bacterial protein that specifically inhibits DrICE. It is not involved in the endogenous apoptosis pathway of *Drosophila*.

apoptosis was suppressed in the nervous system and the antennal progenitor tissue and examined the effects on ORN targeting were examined. Two different Gal4 lines were used in this experiment, the pan-neural driver *elavGal4* and *dllGal4*, which is expressed in the developing eye-antennal imaginal disc. These lines were crossed to several UAS constructs encoding factors that are described to block apoptosis. The stages at which the apoptosis pathway was disturbed are shown in Figure 15.

A dominant negative form of DRONC was tested that can bind to the Dark

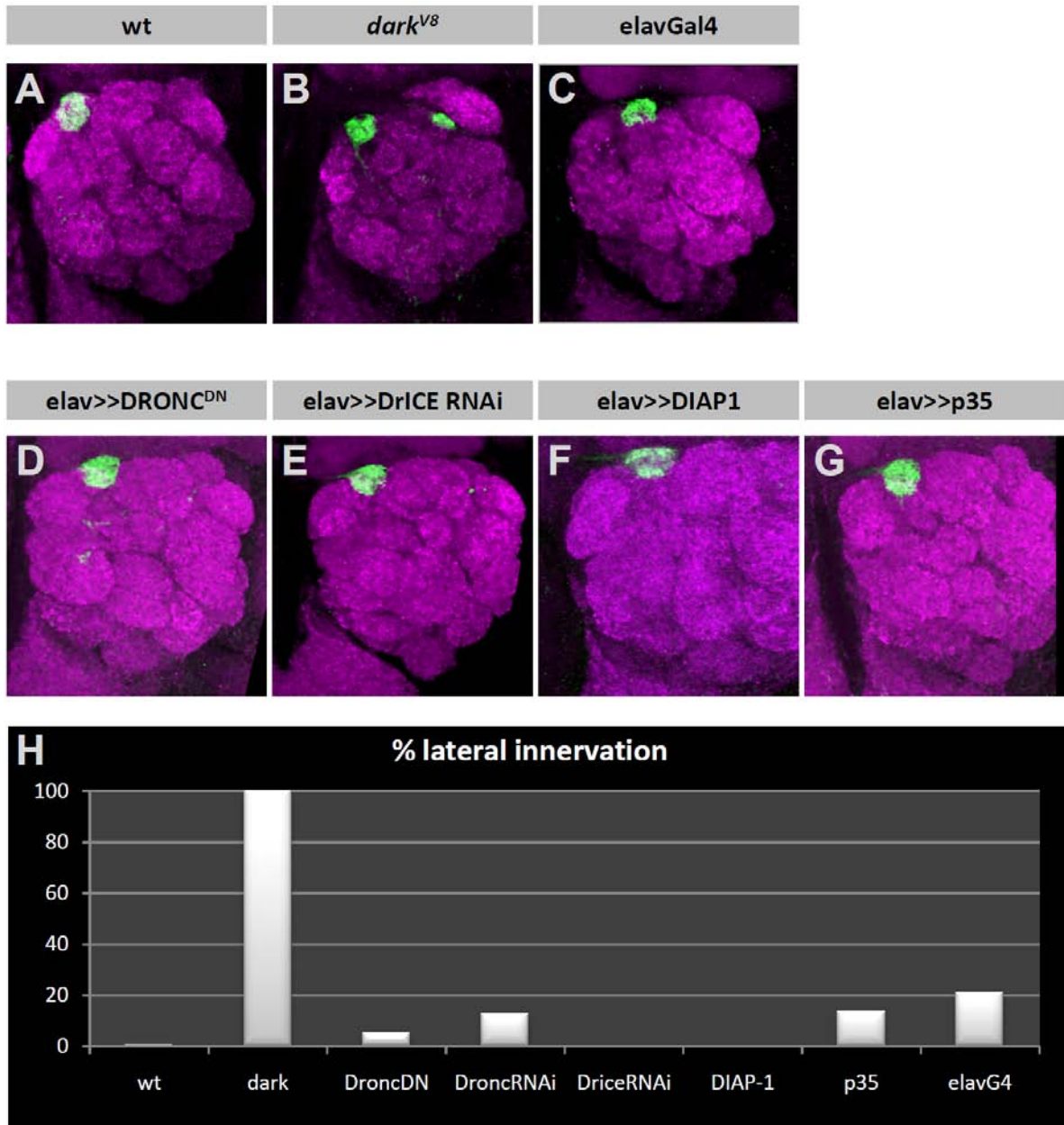


Figure 16 – Suppression of apoptosis does not affect Or47a targeting

(A-C) Controls with either wild type (A), *dark*^{V8} (B) or elavGal4 (C). In wild type and elavGal4 no mistargeting of Or47a neurons can be observed. (D-G) Expression of suppressors of apoptosis. None of the tested candidates affects Or47a targeting. Neither DRONC^{DN} (D), DrICE RNAi (E), DIAP1 (F) or p35 (G) induce the formation of an ectopic glomerulus comparable to *dark*^{V8}. The results are quantified in (H). Genotypes: (A) wt, (B) eyFLP; FRT42 *dark*^{V8} 47a::syGFP/FRT42 (C) elavGal4;; (D)elavGal4; UAS-DRONC^{DN}, (E) elavGal4 UAS-DriceRNAi, (F) elavGal4; UAS-DIAP1, (G) elavGal4; UAS-p35. Or47a expression is labeled with α -GFP (green), neuropil with α -ncad (magenta).

apoptosome, but cannot activate DrICE, therefore it is not able to induce programmed cell death (Meier et al. 2000; Hawkins et al. 2000). The over-expression of DRONC^{DN} with either

elavGal4 in the nervous system or DllGAL4 in the antennal disc has no effect on Or47a targeting; the innervation is restricted to the wild type target, the DM3 glomerulus (Figure 16 D). Expression of a DRONC RNAi construct has a similar phenotype, again the Or47a innervations was not affected (data not shown). Also, knock down of DrICE via RNAi does not lead to any changes in the Or47a axon targeting (Figure 16E).

Over-expression of DIAP1, a general Inhibitor of dark/DRONC induced apoptosis (Muro 2005) does not lead to a comparable mis-targeting defect as in *dark*^{V8} mutants (Figure 16F). UAS-p35, which encodes a baculoviral protein that inhibits effector caspase function and prevents cell death in Drosophila (Hay, Wolff & Rubin 1994) had no effect on ORN targeting. Also in this over-expression background the Or47a axons project only to the DM3 glomerulus (Figure 16G).

These results point to an apoptosis-independent mechanism of *dark* in ORN targeting.

3.3.4 *Dark* induced ORN mis-targeting is allele specific

The *dark* alleles found in the screen were all identified according to their mis-targeting phenotype in the olfactory system. To test whether other *dark* alleles also cause a similar ectopic glomerulus several other *dark* alleles from different sources were examined.

In total 22 alleles were tested for defects in olfactory targeting. First a defined null allele *dark*⁸² in which the complete open reading frame was removed by imprecise P-element insertion (Akdemir et al. 2006) was tested. Surprisingly, the phenotypic characterization of the *dark*⁸² allele reveals no alteration in the Or47a axon projection pattern in eyFLP clones (Figure 17C). Next the homozygous viable P-insertion P[lacW]Ark^{k11502} was tested. It localizes in the 5'UTR of *dark* and significantly reduces *dark* expression levels (Zhou et al. 1999). However, this allele also does not cause ectopic targeting of Or47a neurons (data not shown).

In an EMS screen for suppressors of hid induced apoptosis 33 other *dark* alleles have been identified using the GheF method (Srivastava et al. 2006). 15 of these alleles were included into this study, one of which (*dark*^{S7}) has exactly the same base exchange leading to a premature stop as the *dark*^{V5} allele that was found in the screen that identified the *verpeilt* complementation group.

In total 18 EMS-induced *dark* alleles were analyzed. All EMS induced *dark* alleles have been characterized for the nature of their mutation; one half contains a premature stop codon, the other half an amino acid exchange. The changes in the DNA sequence are found all over the coding sequence, and every domain is at least affected by one mutation.

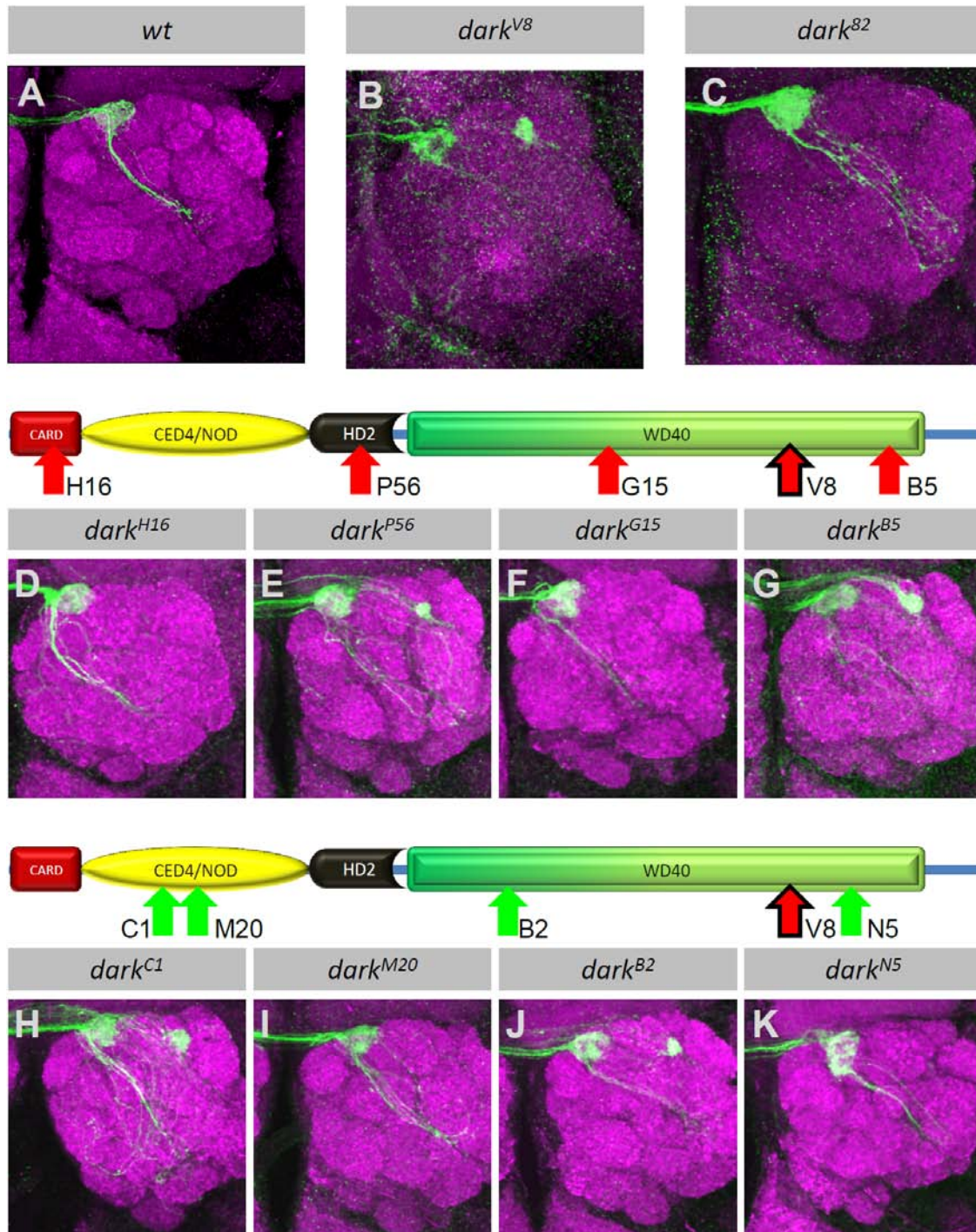


Figure 17 – Allele-specific effects of *dark* on ORN targeting

See Figure legend on next page.

Figure 17 – Allele-specific effects of *dark* on ORN targeting

Several mutations affecting different domains of the *Dark* Protein were tested for a phenotype in the olfactory system. In the wild type only the DM3 glomerulus gets innervated (A). The *dark*^{V8} mutation causes the formation of an ectopic glomerulus in addition to DM3 in the dorso-lateral AL. (C) The defined null-allele *dark*⁸² does not cause ectopic targeting. (D-G) *Dark* alleles containing a premature stop at different positions do not always lead to ectopic glomerulus formation. The red arrows in the protein scheme above indicate the position of the truncations. The black framed red arrow shows the position of the *dark*^{V8} mutation. The alleles *dark*^{H16} (D) and *dark*^{G15} do not affect *Or47a* targeting, while the alleles *dark*^{P56} and *dark*^{B5} show an ectopic glomerulus similar to the phenotype observed in *dark*^{V8}. (H-K) Mis-sense mutations in the *dark* gene do not always induce ectopic glomerulus formation. The green arrows in the protein scheme above indicate the position of the truncations the black framed red arrow again the position of the *dark*^{V8} mutation. Mutations in the CED4/NOD domain show an ectopic glomerulus in the *dark*^{C1} (H), but not in *dark*^{M20} (I). In the allele *dark*^{B2} (J) an ectopic glomerulus appears, while *dark*^{N5} does not affect ORN targeting. Genotypes: (A) eyFLP UAS-mCD8GFP; FRT42/FRT42 Gal80; Or47aGal4 UAS-mCD8GFP, (B-K) eyFLP UAS-mCD8GFP; FRT42*dark*^(alleleXX)/FRT42 Gal80; Or47aGal4 mUAS-CD8GFP. Or47a expression is labeled with α -GFP (green), neuropil with α -ncad (magenta).

Eleven *dark* alleles displayed an ectopic Or47a glomerulus, similar to the *verpeilt* complementation group (Figure 17 E, G, H, J, data not shown). The additional innervation shows little variations according to its size or position. Only in the allele *dark*^{E4} the ectopic glomerulus sometimes appears slightly smaller than in the other alleles. In the remaining seven alleles Or47a neurons all exclusively innervate the wild type glomerulus, no change in ORN targeting can be observed (Figure 17 D, F, I, K, data not shown).

It was also tested whether the targeting of the Or23a class is affected, since the target glomerulus of this class, DA3, is located directly adjacent to the ectopic Or47a glomerulus found in *dark*^{verpeilt} alleles. The innervation of the DA3 glomerulus of Or23a axons is indistinguishable from the pattern found in wild type brains (data not shown).

The mis-targeting defect is not dependent on the kind of mutation in *dark* and is found both truncated and mis-sense alleles. Vice versa, also truncations or mis-sense mutations not necessarily cause ectopic targeting.

Furthermore, no obvious correlation between the domains affected and the ability to induce ORN mis-targeting. For example, of the five mutations located in the CED4 domain only three cause an ectopic Or47a glomerulus. In addition, the length of the putative remaining sequence in the truncated alleles is not directly linked with the induction of the mis-innervation of Or47a neurons. Some alleles containing early stops do not induce the

phenotype, while others, only a few amino acid longer alleles do and even longer alleles again are not able to cause mis-targeting.

The influence on *hid* induced apoptosis shows a slight bias according to the allele strength. Alleles that only cause weak or medium suppression in the GheF assay mostly also do not cause the formation of the ectopic glomerulus, with the exception of the allele *dark*^{B2} that exhibits a strong mis-targeting phenotype in the olfactory system while only moderately affecting *hid*-induced apoptosis. In contrast, strong rescue of the eye phenotype in the GheF assay is not correlated with the strength of the ectopic projections in the olfactory system. Four alleles are able to rescue the eye to almost its full extend, but do not affect targeting of Or47a axons at all.

A summary of the results of the phenotypic characterization of the different alleles is shown in Table 02. The *dark* alleles causing ectopic targeting of Or47a neurons are hence referred to as *dark*^{verpeilt}.

Table 02 – Summary of phenotypes in the observed *dark* alleles.

Allele	Type	change	AS position	ORN axon targeting	Loss of apoptosis	Domain affected
<i>dark</i> ⁸²	deletion	1277 upstream of start to 19 downstream of stop	-	wt	strong	all
<i>P[lacW]</i> <i>Ark</i> ^{k11502}	P- Element	Insertion in 5'UTR	-	wt	medium	-
<i>H16</i>	stop	Lys > stop	42	wt	strong	Card
<i>S7/V5</i>	stop	Trp > stop	207	strong	strong	CED4/NOD
<i>C1</i>	missense	Asp > Gln	333	strong	strong	CED4/NOD
<i>M20</i>	missense	Ala > Thr	336	wt	weak	CED4/NOD
<i>G8</i>	missense	Cys > Trp	346	strong	strong	CED4/NOD
<i>N10</i>	missense	Leu > Asn	349	wt	medium	CED4/NOD
<i>P56</i>	stop	Gln > stop	499	strong	strong	HD2
<i>D3</i>	missense	Asp > Asn	607	wt	strong	WD40
<i>B2</i>	missense	Ser > Asn	627	strong	medium	WD40
<i>G29</i>	stop	Tyr > Stop	779	strong	strong	WD40
<i>G15</i>	stop	Trp > stop	837	wt	strong	WD40
<i>N5</i>	missense	Asp > Glu	977	wt	medium	WD40
<i>V10</i>	stop	Cys > stop	1018	strong	n.d.	WD40
<i>E4</i>	missense	Ser > Phe	1024	medium	strong	WD40
<i>B5</i>	stop	Gln > stop	1030	strong	strong	WD40
<i>V8</i>	stop	splice site	1124	strong	strong	WD40
<i>J7</i>	stop	Gln > stop	1282	wt	medium	C-terminal domain
<i>V14</i>	missense	Glu > Lys	1301	strong	strong	C-terminal domain
<i>P[lacW]</i> <i>vpt</i> ⁶²⁸	n.d.	n.d.	n.d.	wt	n.d.	n.d.
<i>P[lacW]</i> <i>vpt</i> ⁶⁹⁷	n.d.	n.d.	n.d.	wt	n.d.	n.d.
<i>P[lacW]</i> <i>vpt</i> ²⁰⁵⁷	n.d.	n.d.	n.d.	wt	n.d.	n.d.

All alleles tested are homozygous lethal except $P[lacW]Ark^{k11502}$. In three of the mutant stocks, $dark^{M20}$, $dark^{N10}$ and $dark^{N5}$ occasional homozygous escapers are found.

To check whether different *dark* mutations can complement each other a series of dark trans-combinations with all EMS alleles and the $dark^{82}$ null allele was generated. While most of the combinations do not complement the lethality the alleles $dark^{M20}$ and $dark^{N10}$ are able to rescue almost all other alleles to viability. $Dark^{N5}$ complements about 2/3 of the other alleles, including $dark^{M20}$ and $dark^{N10}$. These three alleles also display only weak suppression of apoptosis and cause no phenotype in the olfactory system and can therefore be characterized as weak hypomorphs (data not shown).

Occasional escapers found in these trans-combinations often displayed bristle phenotypes affecting the number or polarity, indicating an additional role of *dark* in non-apoptotic caspase functions in SOP development, also described by Kuranaga & Miura, 2007 (data not shown).

3.3.4.1 Or47a mis-targeting in viable *dark* trans-combinations

The rescue to viability in the trans-situations described above raises the question whether it is also sufficient to suppress the formation of the ectopic glomerulus in the olfactory system. Therefore exemplarily $dark^{V8}$ in combination with the alleles $dark^{M20}$, $dark^{N10}$ and $dark^{N5}$, and additionally with $P[lacW]Ark^{k11502}$ was tested. Neither the $dark^{V8}/dark^{N5}$ nor the $dark^{V8}/P[lacW]Ark^{k11502}$ combinations showed an ectopic innervation in the dorso-lateral AL (Figure 18 C,F). In contrast, $dark^{V8}/dark^{M20}$ and the $dark^{V8}/dark^{N10}$ lead to Or47a axon mis-targeting, though the ectopic structure appears somewhat smaller than in *eyFLP* clones of $dark^{V8}$ (Figure 18 D, E). $Dark^{M20}$ and $dark^{N10}$ both affect the CED4/NOD domain of *dark*, suggesting a putative requirement for this domain in directing Or47a axons to their proper target.

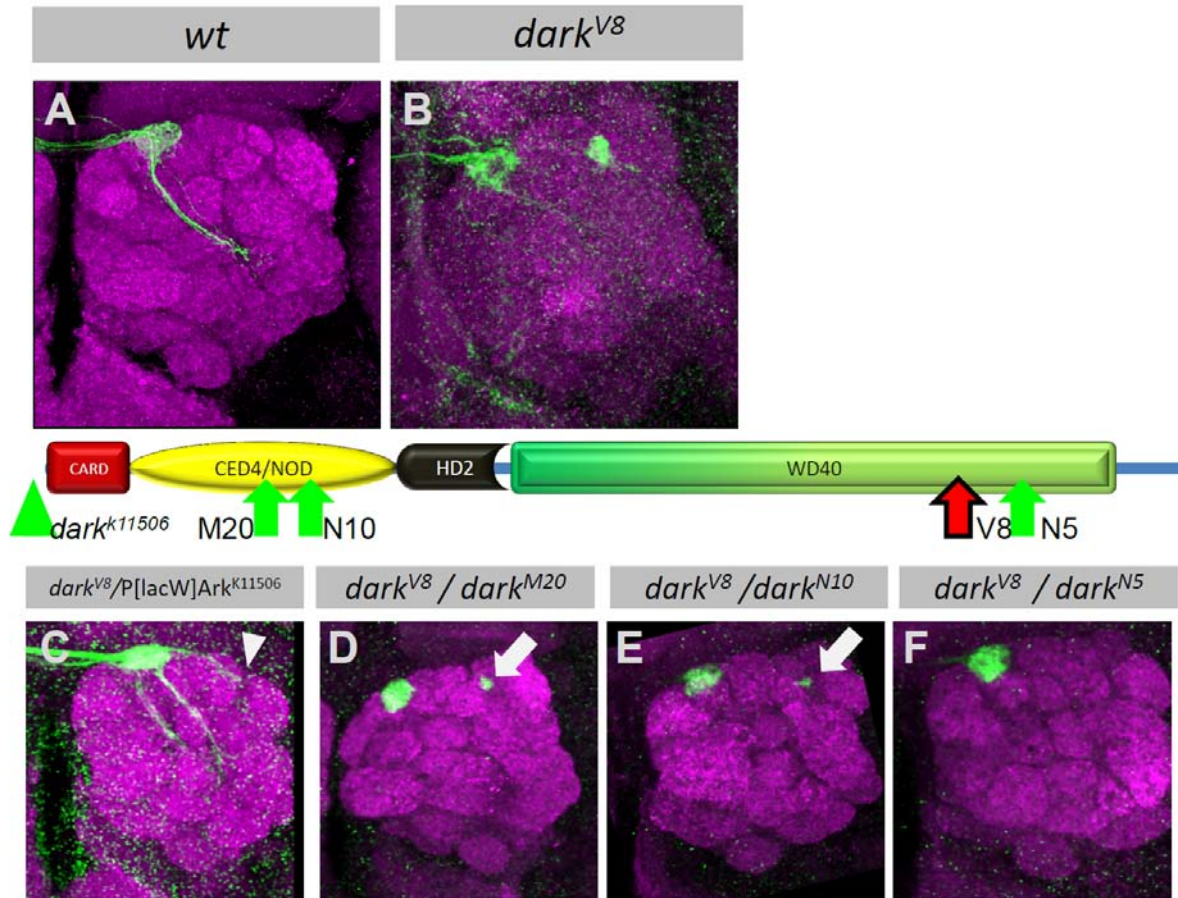


Figure 18– Or47a mis-targeting in viable dark trans-combinations

(A-B) Controls with either wild type (A) or *dark^{V8}* (B). (C-F) Trans-combinations of different *dark* alleles. Green arrows in the scheme above indicate the location of the mutations, the green arrowhead shows the location of the P[lacW]Ark^{K11506}, the black framed red arrow the location of the *dark^{V8}* mutation. (C) the combination of *dark^{V8}* and P[lacW]Ark^{K11506} does not show ectopic targeting, though some axons travel along the dorso-lateral AL (arrowheads). (D-E) Transcombinations of *dark^{V8}* with *dark^{M20}* or *dark^{N10}*, both affecting the CED4/NOD domain, show little ectopic targeting in the dorso-lateral AL (arrows). (F) A trans-combination of *dark^{V8}* and *dark^{N5}* displays only innervation of DM3. Genotypes: (A) eyFLP UAS-mCD8GFP; FRT42/FRT42 Gal80; Or47aGal4 UAS-mCD8GFP, (B) eyFLP UAS-mCD8GFP; FRT42 *dark^{V8}*/FRT42 Gal80; Or47aGal4 UAS-mCD8GFP; (C) eyFLP UAS-mCD8GFP; FRT42 *dark^{V8}*/FRT42 P[lacW]Ark^{K11506}; (D-F) *dark^{V8}* 47a:sytGFP/*dark^{alleleXX}*. Or47a expression is labeled with α -GFP (green), neuropil with α -ncad (magenta).

3.3.5 Over-expression of *dark* does not suppress the OR47a mis-targeting

The decrease in apoptosis in *dark*⁸² can be rescued by re-expression of wild type *dark*. In the next experiment it was tested whether the expression of wild type *dark* is also able to rescue the *dark*^{verpeilt} alleles. When UAS-*dark* is expressed in a *dark*^{V8} mutant background this is not sufficient to restore viability. Neither expression with the ubiquitous driver daughterlessGal4 nor with the pan neural driver elavGal4 nor DllGal4 can circumvent the lethality in *dark*^{V8} homozygous animals. Also, a *dark*^{V8}/*dark*⁸² trans-combination cannot be rescued in this experiment (Table 03).

Table 03 – Expression of wild type *dark* in *dark*^{V8} mutant background

	<i>dark</i> ^{V8} / <i>dark</i> ^{V8}	<i>dark</i> ^{V8} / <i>dark</i> ⁸²
dllGal4	†	†
daGal4	†	†
elavGal4	†	†

Over-expression of wild type *dark* in MARCM clones with elavGal4 is not sufficient to suppress the formation of the ectopic glomerulus in *dark*^{V8} mutants (Figure 19). Dependent on the temperature, effects on the morphology of the additional glomerulus can be observed. At 25°C the lateral glomerulus appears somehow smaller (Figure 19 C); however, a subsequent quantification of the glomerular volumes shows no significant decrease (Figure 19 G). Similarly, at 29°C the volume of the ectopic glomerulus is unaffected. In contrast to the situation at 25°C the morphology of the lateral structure is affected. About 70% of the brains show several alterations in the form and/or the position of the ectopic glomerulus, it often appears elongated, sometimes almost reaching to the DM3 glomerulus or loses its stereotypic position ventro-lateral from the DA3 glomerulus and is shifted to the dorsal border of DA3. In some cases the mis-projecting ORNs form two small glomeruli instead of one (Figure 19 D, E, F).

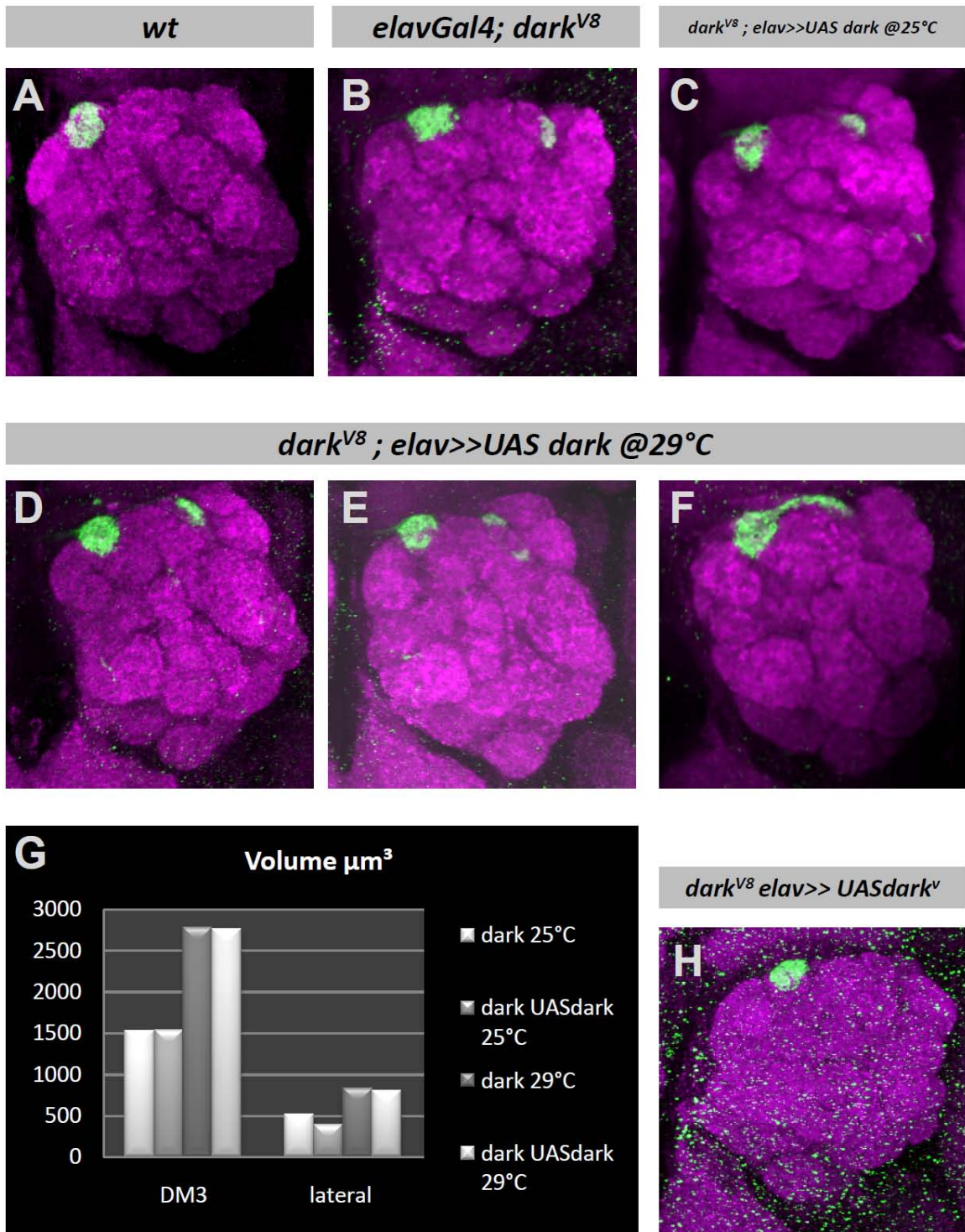


Figure 19 – Over-expression of wild type dark in *dark^{V8}* ORNs
 See figure legend on next page.

Figure 19 – Over-expression of wild type dark in *dark*^{V8} ORNs

(A-B) Controls with either wild type (A) or *elavGal4; dark*^{V8} (B). (C) Over-expression of UAS-*dark*^{wt} with *elavGal4* in *dark*^{V8} MARCM clones at 25°C does not suppress the formation of the lateral glomerulus. (D-E) Also at 29°C, over-expression of UAS-*dark*^{wt} with *elavGal4* in *dark*^{V8} MARCM clones does not prevent ectopic targeting, but has an effect on the morphology on the lateral OR47a glomerulus. In some cases no change can be observed (D), in others the ectopic glomerulus is split (E, arrows), or elongated towards the DM3 glomerulus (F, arrowheads). No decrease in the volume of the ectopic structure can be observed (G). (H) Over-expression of UAS-*dark*^V with rescues the ectopic targeting phenotype of *dark*^{V8}. Genotypes: (A) *eyFLP; FRT42 47::syGFP/FRT42 Gal80*, (B) *eyFLP elavGal4; FRT42 dark*^{V8} *47a::syGFP/FRT42 Gal80*, (C-F) *eyFLP elavGal4; FRT42 47a::syGFP/FRT42 Gal80; UAS-dark*^{wt}, (H) *eyFLP elavGal4; FRT42 47a::syGFP/FRT42 Gal80, UAS-dark*^V. Or47a expression is labeled with α -GFP (green), neuropil with α -ncad (magenta).

In addition, a second over-expression construct, UAS*dark*^V, in which an amino acid exchange from Aspartate to Alanine at position 1292 is introduced, was tested. This alteration inhibits the cleavage of Dark at its C-terminal domain by DRONC, therefore preventing the disassembly of the dark octamer. Leaky expression of *dark*^V alone without a driver is sufficient to rescue the lethality of *dark*⁸², therefore this construct is described to encode a hypermorphic variant of *dark* (Akdemir et al. 2006).

The UAS- *dark*^V expression without a Gal4 driver is also sufficient to rescue the lethality of the *dark*^{V8} allele. When expressed under the control of *elavGal4* in MARCM clones, no ORN mis-targeting can be observed (Figure 19H), indicating a full rescue of the *dark*^{V8} allele.

These result support the evidence for an apoptosis independent mechanism of *dark* in ORN targeting. Though the fact that the *dark*⁸² null allele does not cause a phenotype is puzzling, it clearly demonstrates that apoptosis is not involved in ORN targeting. The ability to induce ORN mis-targeting appears also not to be related to defects in a specific domain of the *dark* protein. Since wild type *dark* forms an octamer, it could be that diverse changes in *dark* could influence this oligomerization, resulting in a defective apoptosome with a somehow dominant negative influence on ORN target choice.

3.3.6 Loss of function of apoptosome components does not cause ORN mis-targeting

One possible explanation would be that a defective apoptosome bind to one of the components of the apoptosome machinery, but fails to process and/or release it, therefore preventing it from executing its function in ORN targeting.

Loss of any of these components should have a similar effect and therefore also lead to ORN mis-targeting. DRONC appears not to be a likely candidate since over-expressing a dominant negative form or RNAi has no effect on ORN targeting (see 1.3.3). Therefore loss of function of the apoptosis inhibitor DIAP-1 were analyzed for their influence on Or47a targeting. Using eyFLP clones in the eye-antennal imaginal disc were induced and the effect of the amorph DIAP-1 allele *th4* examined. Similar to the over-expression of DIAP1 no *vpt* like phenotype can be observed in the loss-of-function situation (Figure 20C). It was also tested whether LOF alleles of the atypical caspase DREDD, which has been described to interact with the Dark apoptosome. DREDD is not directly involved in apoptosis but has been described to play a role in bacterial defense (Cooper, Granville & Lowenberger 2009). None of the tested alleles show lateral innervation of Or47a neurons, but frequently ectopic innervations in the ventro-medial AL are observed (Figure 20 D).

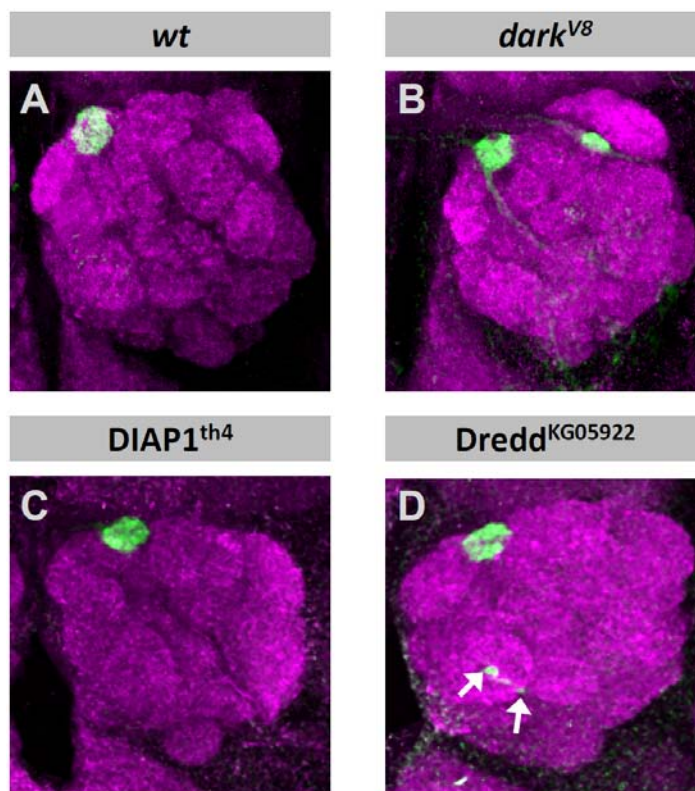


Figure 20 – Loss of function of apoptosome components does not cause ORN mis-targeting

(A-B) Controls with either wild type (A) or *dark^{V8}* (B). In eyFLP induced mitotic clones the amorph DAIP1 allele *th4* does not affect Or47a targeting (C). In homozygous flies carrying the hypomorph *Dredd^{KG05922}* frequently ectopic termini are found in the ventro-medial area of the AL (arrows), but not in the dorso-lateral area (D). Genotypes: (A) eyFLP; FRT42 47a::sytGFP/FRT42 Gal80, (B) eyFLP; FRT42 *dark^{V8}* 47a::sytGFP/FRT42 Gal80, (C) eyFLP GMR::lacZ; FRT42 47a::sytGFP/+; DIAP1^{th4} FRT80/FRT80, (D) *Dredd^{KG05922}/Dredd^{KG05922}*; FRT42 47a::sytGFP/+. Or47a expression is labeled with α -GFP (green), neuropil with α -ncad (magenta).

However, since $DIAP1^{th4}$ is not described to be a null mutant, the remaining function could be sufficient to prevent Or47a axons from mis-targeting. If in $dark^{verpeilt}$ mutants $DIAP1$ is titrated out by a defective apoptosome, over-expression of $DIAP1$ should compensate for this hence preventing the ORNs from innervating ectopic targets. To test this hypothesis $DIAP1$ was expressed in eyFLP induced MARCM clones in $dark^{V8}$ mutants. In this situation Or47a axons still target to two glomeruli, also no change in the position or morphology as in over-expression of wild type $dark$ can be detected (Figure 21). These results suggest that $DIAP1$ has no effect on $dark$ mediated control of ORN targeting.

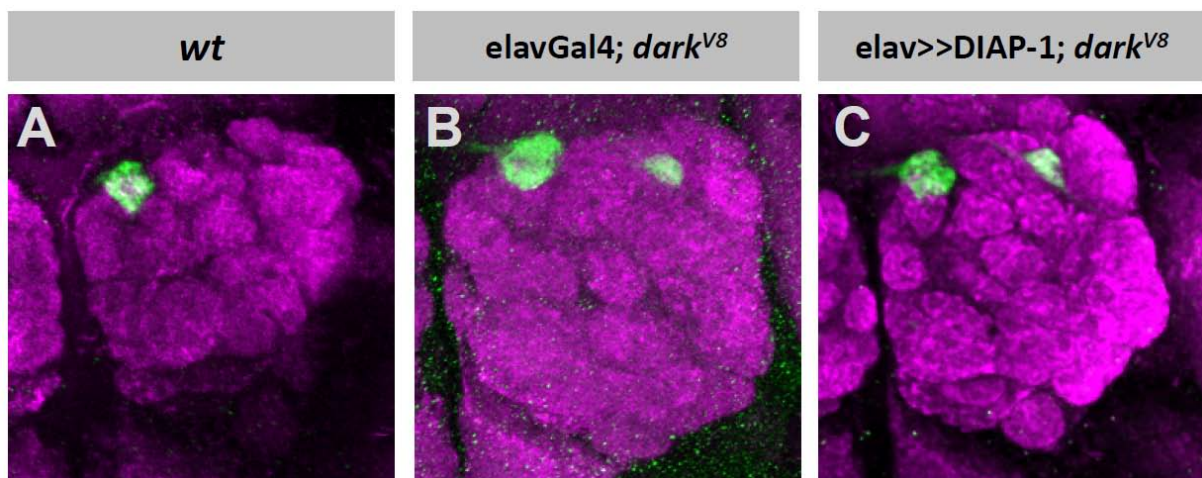


Figure 21 – Over-expression of DAIP-1 does not affect Or47a-targeting in $dark^{V8}$

(A-B) Controls with either wild type (A) or $elavGal4; dark^{V8}$ (B). Over-expression of $DIAP1$ in $dark^{V8}$ mutant clones shows no effect on lateral targeting of Or47a axons (C). Genotypes: (A) eyFLP; FRT42 47a::sytGFP/FRT42 Gal80, (B) eyFLP; FRT42 $dark^{V8}$ 47a::sytGFP/FRT42 Gal80, (C-F) eyFLP $elavGal4; FRT42$ 47a::sytGFP/FRT42 Gal80; UAS- $DIAP1$. Or47a expression is labeled with α -GFP (green), neuropil with α -ncad (magenta).

3.4 Projection domains

To investigate the mechanisms that lead to the formation of the ectopic glomerulus in $dark^{verpeilt}$ mutants the projection pathways of the axons on their way to their target were closely analyzed. In the wild type the axons grow across the surface of the AL in a loose fascicle, finally innervating the DM3 glomerulus. In $dark^{V8}$ this pattern is often lost, the axons grow in a broad band across the AL (Figure 22). The axons that form the lateral glomerulus grow more dorsally, eventually ending up in the wrong place. This disturbed projection behavior leads to the question whether an organized ingrowth is required for proper target selection.

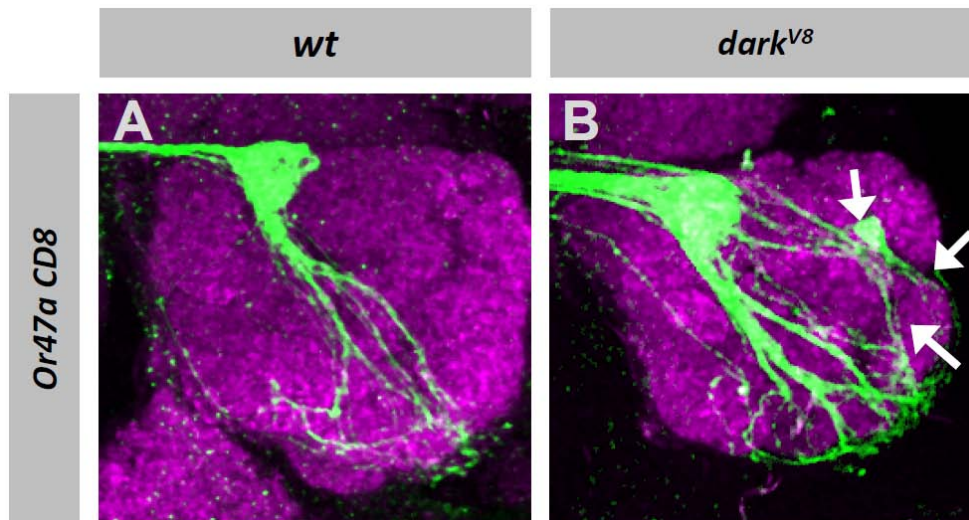


Figure 22 – Or47a-axons project on alternative routes in *dark*^{V8}

(A) In wild type flies the axons of Or47a neurons grow relatively straight from the entry point of the AN across the anterior surface of the AL to the DM3 glomeruli. (B) In *dark* mutant clones the axons look less ordered, some grow more lateral and innervate a dorso-lateral glomerulus (arrows). Genotypes: (A) eyFLP UAS-mCD8GFP; FRT42/FRT42 Gal80; Or47aGal4 UAS-mCD8GFP, (B) eyFLP UAS-mCD8GFP; FRT42 *dark*^{V8}/FRT42 Gal80; Or47aGal4 UAS-mCD8GFP. Or47a expression is labeled with α -GFP (green), neuropil with α -ncad (magenta).

3.4.1 Domain organization in the olfactory system of *Drosophila*

A zonal organization of in-growing ORNs in the olfactory system has been described in several organisms including mouse, *Xenopus* and the moth *Manduca*. An equivalent organization in the *Drosophila* olfactory system has not been shown so far.

During the investigation it was found that ORNs in *Drosophila* show an ordered projection pattern. When the majority of ORN axons is labeled with a Or83bGal4 driven CD2 reporter, four major projection domains can be identified, three on the anterior side of the AL, a dorso-lateral, a central and a ventro-medial one (Figure 23A-A''). The fourth domain runs along the posterior side of the AL (data not shown). During a single class analysis it was found that ORNs of a given class mainly project along one of the domains, usually the one that passes closest to their class specific target glomerulus (Figure 23C-E; Figure 26, Table 04). The antennal classes use all projection domains, the maxillary classes are only found in the ventro-medial class.

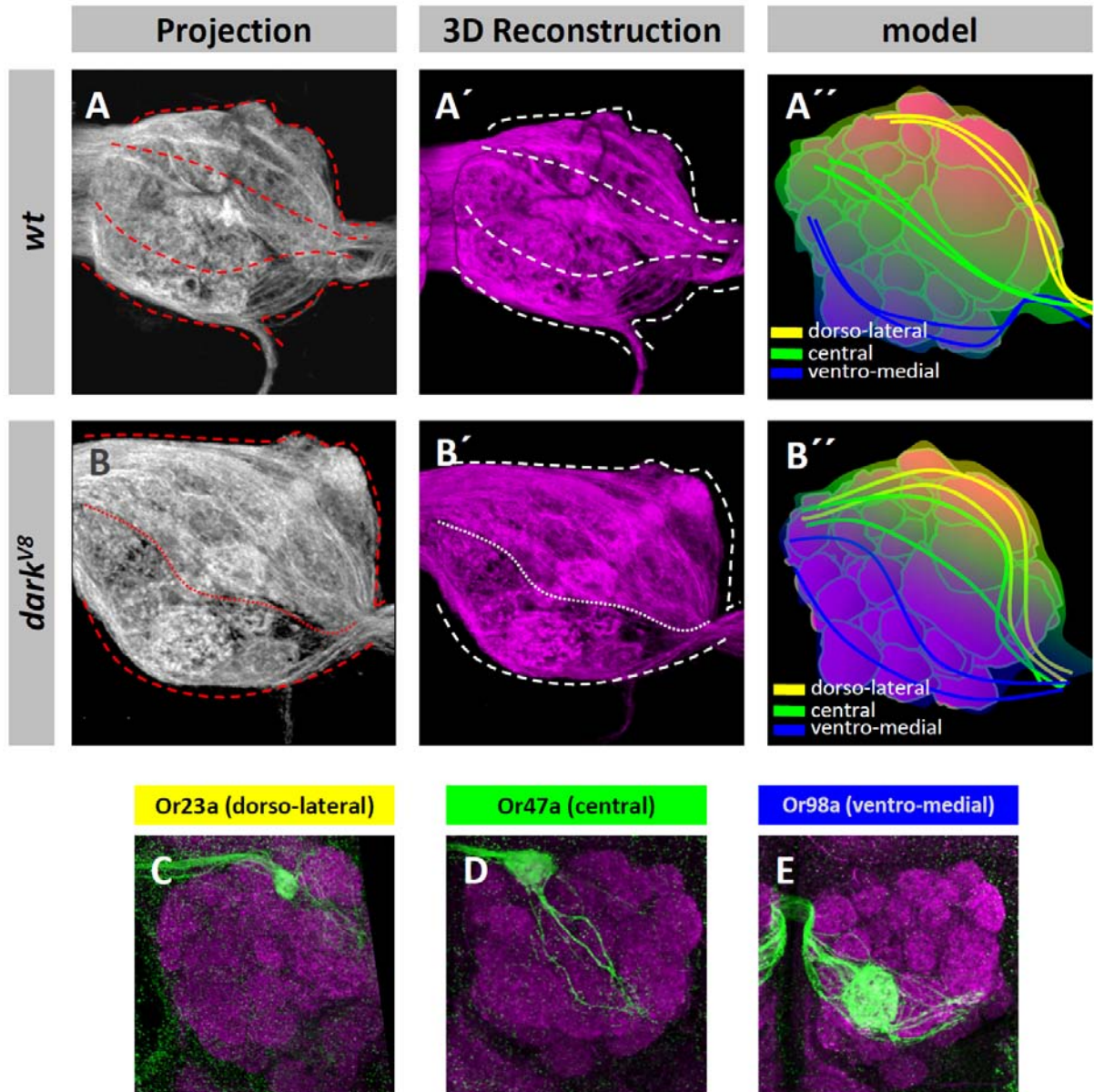


Figure 23 – Domain organization of ORN axons in *Drosophila*

Ingrowing ORN axons in the *Drosophila* olfactory system sort out into projection domains. (A) Labeling of all ORNs reveals a segregation of ORN axons in three projection domains on the anterior surface of the AL, visible in full projections and 3D reconstructions of confocal image stacks (dotted lines in A, A') (A'') scheme of the anterior projection domains. (B) In *dark^{V8}* this organization is lost, especially the dorso-lateral and the central domain are fused with each other (B, B'), a scheme is shown in (B''). (C-E) ORNs of the same class preferentially project within one domain. (C) Or23a class axons project along the dorso-ventral domain, (D) Or47a axons along the central domain and (E) Or98a axons in the ventro-medial domain. Genotypes: (A) +,+; Or83bGal4 UAS-CD2; (B) eyFLP; FRT42 *dark^{V8}*/FRT42; Or83bGal4 UAS-CD2, (C) eyFLP UAS-mCD8; FRT42/FRT42; Or23aGAL4 UASmCD8, (D) eyFLP UAS-mCD8; FRT42/FRT42; Or47aGAL4 UASmCD8, (E) eyFLP UAS-mCD8; FRT42/FRT42; Or98aGAL4 UASmCD8. (A,B) Or83b expression is labeled with α -CD2 (gray or magenta) (C-E) OR expression is labeled with α -GFP (green), neuropil with α -ncad (magenta).

In *dark* mutants, the different projection domains are hardly visible; especially the dorso-lateral and the central domain appear to be fused (Figure 23B-B''). The ventro-medial domain seems less affected, but appears thinner. Some ORN classes are no longer restricted to one of the domains and send their axon on different routes to their target glomeruli, as exemplary shown for the Or22a class in Figure 26A and B.

The presence of projection domains in *Drosophila* does not necessarily points to a functional relevance like it has been shown in the mice olfactory system. In the mouse ORNs from different zones in the olfactory epithelium project their axons to corresponding areas of the olfactory bulb in zone-exclusive fascicles, indicating positional information is maintained and used to project to the correct target (Mori, von Campenhouse & Yoshihara 2000).

3.4.2 Projection domain specificity of Or 47a axons

On the example of Or47a neurons it was tried to determine whether a similar mechanism as in the mouse is also present in *Drosophila*. To investigate how stereotypic these domains are and how frequent variations to this pattern appear, the ORNs axons were labeled with a membrane bound CD8 GFP under the control of Or47aGal4 (Figure 24) and their projection analyzed.

In most of the cases observed Or47a neurons project along the central domain to the DM3 glomerulus. From there an additional branch is sent to the other hemisphere to innervate the same glomerulus on the contra-lateral side.

The exclusive projection of Or47a axons along this central domain is found in 84% of the AL examined (n=94). In the remaining 16% not all axons project along the central domain, a small amount grows more dorsally, but still manages to reach the DM3 glomerulus. In these cases almost never more than two axons sheer out from the central projection domain, only in 3% of all ALs investigated this number is exceeded (Figure 24D). In this experiment no ectopic targeting at unspecific locations could be observed.

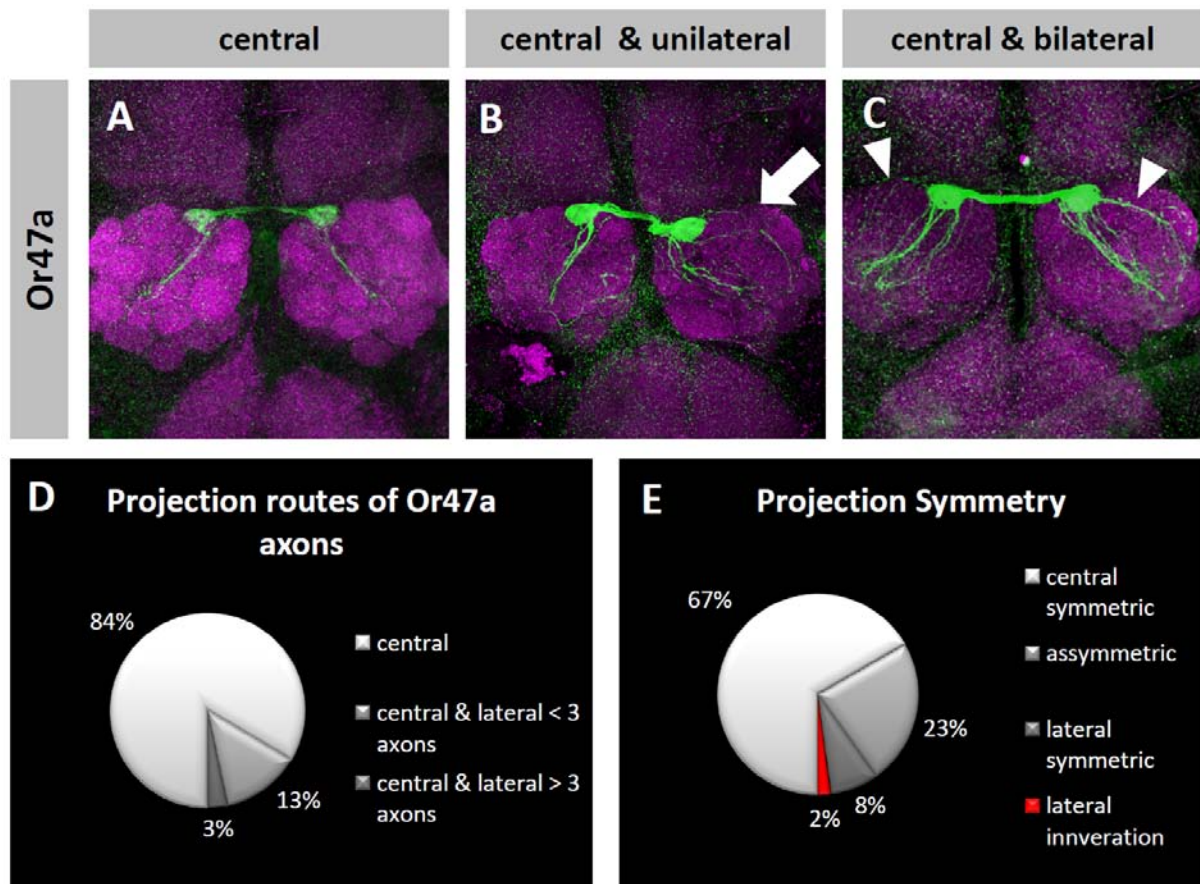


Figure 24 – Or47a axons project preferentially along the central domain to their target glomerulus

(A-C) Projections of Or47a axons. (A) Or47a neurons projecting along the central domain. (B) Most Or47a axons project along the central domain, single axons shear out dorso laterally, only on one hemisphere of the AL (arrow). (C) The majority of Or 47a axons projects along the central projection domain, some on more dorso-lateral routes, on both halves of the AL. (D) Quantifications of the central and lateral projecting Or47a axons, (E) Quantification of the degree of symmetry found in Or47a projections. Genotype: (A-C) eyFLP UAS-mCD8; FRT42/FRT42; Or47aGAL4 UASmCD8. Or47a expression is labeled with α -GFP (green), neuropil with α -ncad (magenta).

3.4.2.1 Contra-lateral projections are not affected in *dark^{verpeilt}* mutants

A hall mark of the Or47a mis-targeting phenotype in *dark^{verpeilt}* mutants is the symmetry of the lateral ectopic glomerulus. Therefore it was tested whether dorso-lateral sheering out in the wild type is also symmetrically. To answer this question the projections of Or47a axons in both hemispheres was analyzed. In total, 67% of the brains observed exclusively showed a projection only along the central route in both hemispheres of the AL (n=51, Figure 24A). 23% of the brains showed some axons projecting dorso-laterally, but only on

one hemisphere of the AL (Figure 24 B). 10% showed a more or less symmetric use of the dorso-lateral domain, in most of the cases the number of axons differed between both sides of the AL (Figure 24C). In 2% of all investigated brains showed ectopic termini in the dorso-lateral region of the AL, in all of these examples these structures were only found in one hemisphere (Figure 24 E, data not shown).

The results indicate a strong preference of OR47a axons to use the central projection domain, but even when shifting dorso-laterally they still manage to innervate the correct target in the vast majority of these cases. In the wild type the rare ectopic targeting of single ORNs in the dorso-lateral AL does not lead to mis-targeting of the contra-lateral branch. It remains unclear whether the lateral innervating axons also innervate the medial DM3 glomerulus. However, since no lateral innervation was found to be symmetric and no axons were found that extend to the dorso-lateral AL on the contra-lateral AL these results indicate that the target specificity of the contra-lateral branch is determined by the innervation in the wild type glomerulus.

Next the projections of Or47a axons in *dark^{V8}* mutants were analyzed. Mitotic clones were induced using eyFLP in wild type and heterozygous *dark^{V8}* mutant flies, the ORN axons were again labeled with a membrane bound CD8 GFP under the control of Or47aGal4.

The projection of Or47a axons in the wild type clones does not differ from the pattern described in the previous experiment; the axons are mostly restricted to the central projection domain (Figure 25A). In *dark^{V8}* mutant clones the projection pattern is more diverse. Axons innervating the DM3 glomerulus mostly still project within the central domain, but often less tight associated with each other compared to the wild type. ORNs innervating the ectopic glomerulus separate from the central domain shortly after entering the AL and project more along the dorso-lateral domain. Like the centrally projecting axons they do not show a tight association among each other (Figure 25 B, C).

In the wild type the contra-lateral branches of the axons form a dense fascicle, even if the ipsi-lateral projections spread widely over the central domain. In *dark^{V8}* mutant clones, the central projecting axons show the same pattern as in the wild type and project across the commissure in one tight fascicle. Occasionally some axons form a little loop but return to the main fascicle before entering the contra-lateral glomerulus. The contra-lateral projecting axons also form a commissural branch and associate tightly with each other

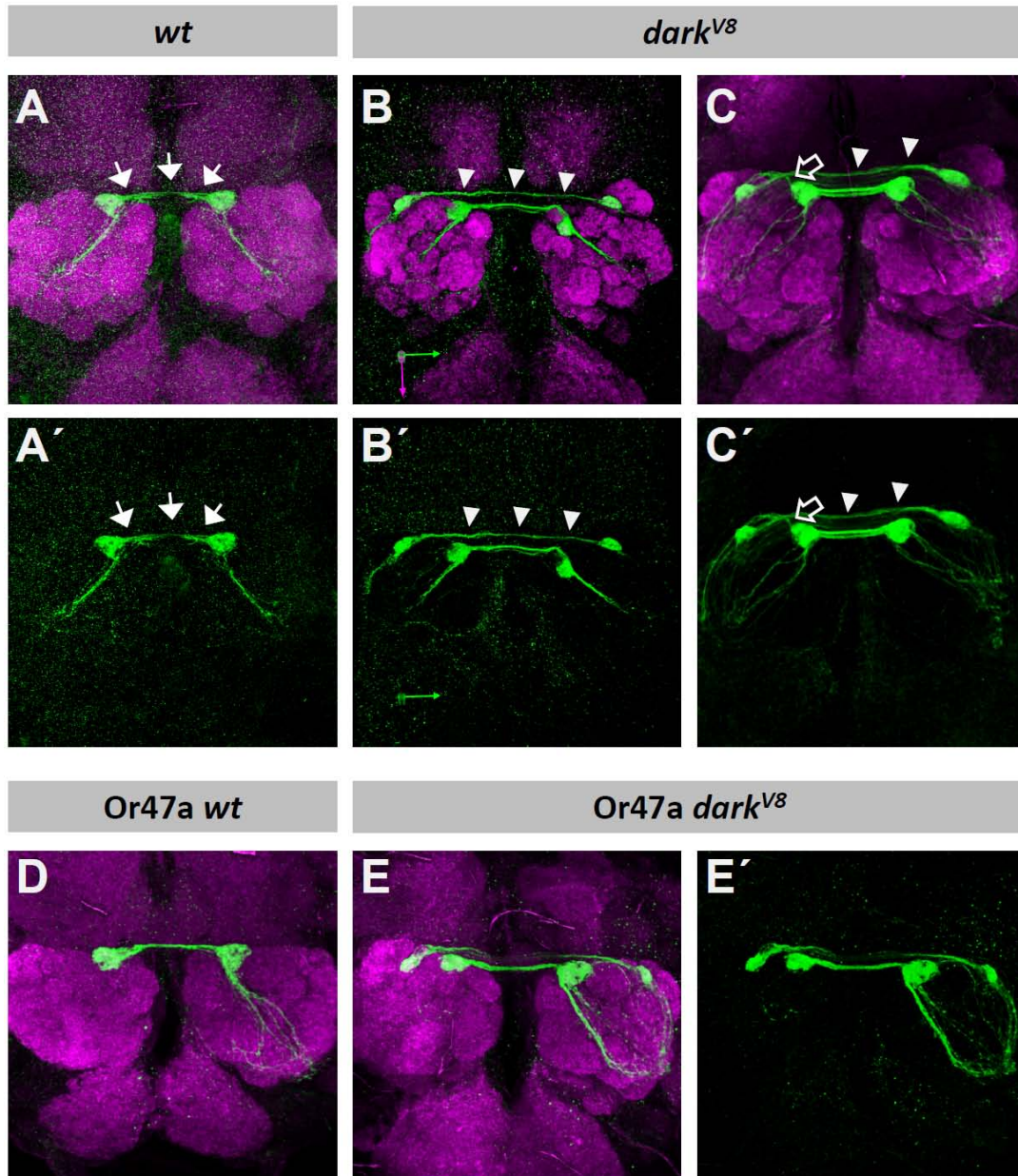


Figure 25 – Commissural projection of Or47a axons

(A-C) Bi-lateral innervations of Or47a axons and commissural projections. (A,A') In the wild-type control the axons project along the central domain, innervate the glomerulus and form a dense contra-lateral fascicle to the second hemisphere (arrows). (B-C') In *dark^{V8}* mutants some axons project more dorso-laterally, forming an ectopic glomerulus. They also send a commissural branch but do not intermingle with DM3 innervating axons (arrowheads). Dorso-lateral projecting ORNs that do not innervate the lateral glomerulus but DM3 do this from the ipsi-lateral side (open arrow in C, C'). (D-E) Ipsi-lateral innervations after ablation of the right antennal. (D) Or47a neurons innervate both hemispheres of the AL after removal of the 3rd antennal segment. (E) In *dark^{V8}* mutants both, the DM3 and the ectopic glomerulus receive contra-lateral innervations. Genotypes: (A,D) *eyFLP UAS-mCD8; FRT42/FRT42; Or47aGAL4 UASmCD8*, (B,C,E) *eyFLP UAS-mCD8; FRT42dark^{V8}/FRT42; Or47aGAL4 UASmCD8*. Or47a expression is labeled with α -GFP (green), neuropil with α -ncad (magenta).

while crossing over to the other hemisphere of the AL. Interestingly, this additional commissural branch does not intermingle with the one formed by the axons innervating the DM3 glomerulus (arrowheads in Figure 25 B, C).

This experiment was repeated with flies in which the right antenna was ablated to investigate whether the contra-lateral projection of mis-targeting axons also innervate the equivalent lateral target on the other hemisphere. Or47a neurons in unilaterally de-antennized flies show the same projection pattern as in unaffected flies, again the stereotypic, symmetric innervations of the dorso-lateral AL is present for both the DM3 and the lateral glomerulus (Figure 25 E). These results illustrate that the mis-projecting ORNs still form a contra-lateral branch that grows independently from the normal projecting ORNs across the commissure and they are able to recognize and innervate the equivalent structure on the contra-lateral lobe.

Taken together these experiments show that Or47a axons do not strictly follow projection routes, but in the wild type this has almost no effect on targeting and also contra-lateral projections. This suggests that the formation of the ectopic glomerulus in *dark^{verpeilt}* is therefore not induced by simply shifting Or47a axons to the dorso-lateral projection domain.

3.5 Characterization of the ORN targeting phenotype in *dark^{verpeilt}*

To elucidate the characteristics of the ectopic glomerulus formed by Or47a neurons in *dark^{verpeilt}* mutant clones a detailed phenotypic analysis was performed. Also the requirement of *dark* in the targeting of other classes was analyzed. Most of these experiments were done with the *dark^{V8}* allele.

3.5.1 Not all ORN classes are affected in *dark^{verpeilt}*

As a general disorganization of the projection domain organization in *dark^{verpeilt}* mutants was detected it was tested whether also other classes show defects in their projection and targeting. Therefore several ORN classes were labeled using a membrane or synaptic localized GFP expressed under the control OR-specific Gal4 drivers. The innervations of the different classes were analyzed in eyFLP induced mitotic clones.

In total 25 ORN classes were tested for changes in the projection and innervation pattern compared to the wild type. Most of the classes do not exhibit any changes in their targeting (Figure 26; Table 04). A few classes show a wild type glomerular innervation, but some of the in-growing axons use alternative projection domains on the way to their target (compare Figure 26; Table 04). In the wild type, axons of Or22a neurons project towards the DM2 glomerulus in a loose array along the ventro-lateral projection route. In *dark* mutants the projection of these axons is more widely spread across the anterior surface of the AL, some growing even more ventrally, others more dorsally, and some even surround the AL and approach the DM2 glomerulus from the posterior side (Figure 26 A, B). Such a change in the projection route taken can be found in roughly on quarter of the examined ORN classes. In most of these cases the axons are shifted to more dorsal projection routes.

In addition, three of these classes also show a specific targeting phenotype, Or47a, Or43a and Or67a. The mis-targeting varies in each class, while Or47a forms a strong glomerular structure (Figure 1), Or43a axons only show weak, less converged ectopic targeting in the lateral AL, close to the entry point of the antennal nerve (Figure 26E, F). In contrast, the mis-innervation of Or67a axons is not clearly distinguishable from the innervated DM6 glomerulus; the axons appear to “spill out” laterally, forming a elongated structure connected to the wild type target of this class (Figure 26K, L). The results of the single class are summarized in Table 04.

All classes showing ectopic ORN innervations also exhibit alterations in the projection routes taken by their axons. The formation of ectopic structures does not affect the innervations of ORNs targeting to neighboring glomeruli.

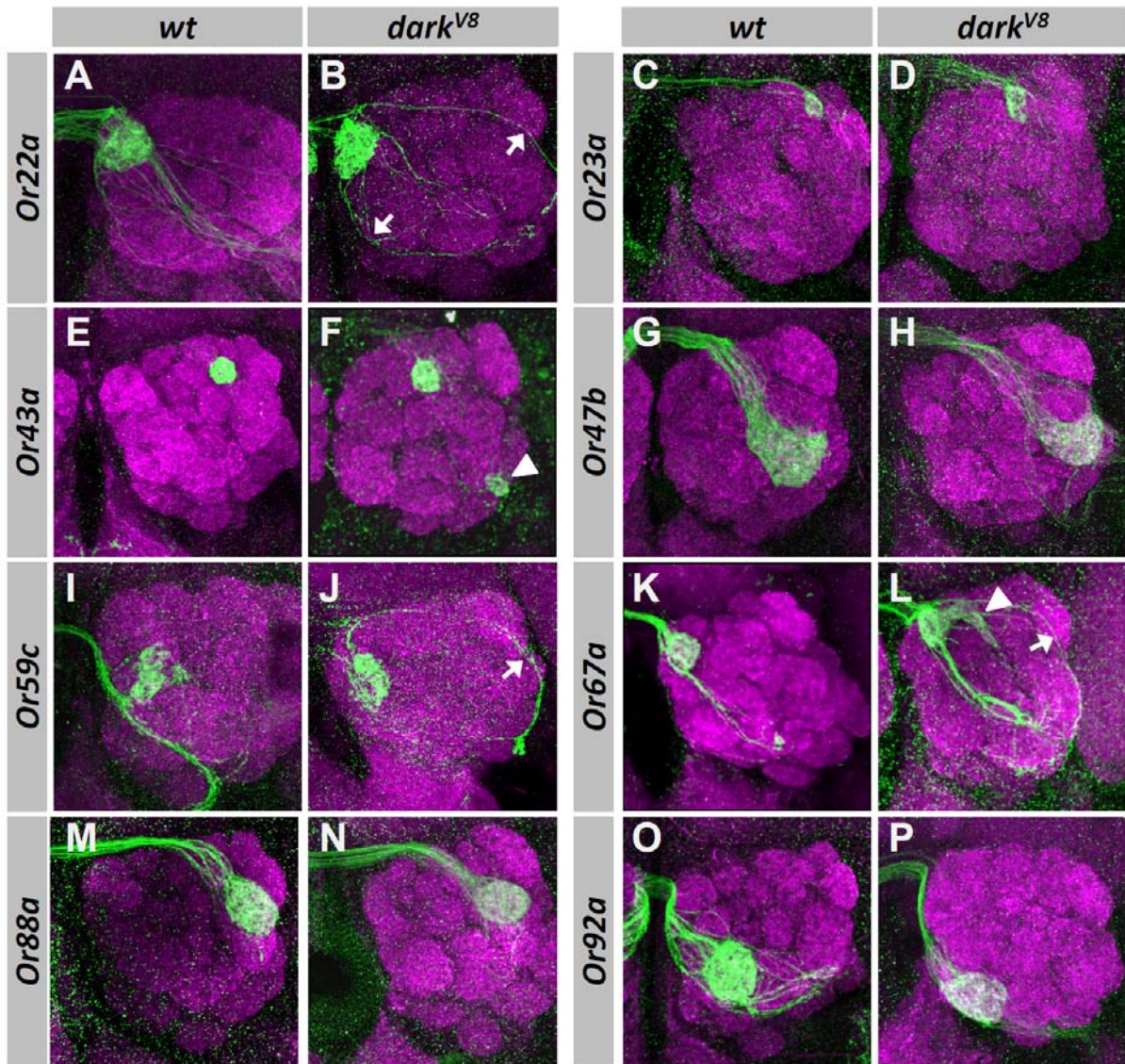


Figure 26 – *Dark^{V8}* causes mis-targeting in several ORN classes

Not all ORN classes show projection or innervations defects. In some ORN classes the axons take alternative projection domains (arrows in B, J) compared to the wild type, but innervate the correct glomerulus. The Or43a class exhibits an ectopic glomerulus in the lateral AL, at the entry point of the antennal nerve (arrowhead in F). Or67a axons grow more dorsally (arrow in L) and the glomerulus is mis-shaped and elongated to the lateral side (arrowhead in L). Genotypes: (A, C, G, I, K, M, O) *eyFLP UAS-mCD8GFP; FRT42/FRT42 PCNA; Or(XX)Gal4 UAS-mCD8GFP*, (B, D, H, J, L, N, P) *eyFLP UAS-mCD8GFP; FRT42 dark^{V8}/FRT42 PCNA; Or(XX)Gal4 UAS-mCD8GFP*, (E) *eyFLP; FRT42/FRT42 PCNA; Or43aGal4 UAS-sytGFP*, (F) *eyFLP; FRT42 dark^{V8}/FRT42 PCNA; Or43aGal4 UAS-sytGFP*. OR expression is labeled with α -GFP (green), neuropil with α -ncad (magenta).

Table 04 – Summary of ORN phenotypes in *dark*^{V8} clones. The glomeruli are named after Couto et al. The projection domains are indicated d = dorso-lateral, c = central, v = ventro-medial

ORN class	glomerulus	Projection route	Targeting phenotype	Projection phenotype	ORN class	glomerulus	Projection route	Targeting phenotype	Projection phenotype
19a	DC1	c	-	-	59c	1	v	-	+
22a	DM2	v	-	+	65a	DL3	d	-	-
23a	DA3	d	-	-	67a	DM6	c	+	+
42a	VM7	v	-	+	67b	VA3	c	-	-
42b	DM1	d?	-	-	67c	VC4	?	-	-
43a	DA4l	d	+	+	69a	D	?	-	-
43b	VM2	v	-	-	71a	VC2	c	-	-
46a	VA7l	c	-	-	82a	VA6	c	-	-
47a	DM3	c	+	+	83c	DC3	d	-	-
47b	VA1V	c	-	-	88a	VA1d	c	-	-
49a	DL4	d	-	-	92a	VA2	c	-	-
49b	VA2	c?	-	-	98a	VM5v	v	-	-
					Gr21d	V	v	-	-

3.5.2 The mis-targeting phenotype in *dark*^{verpeilt} is Cell autonomous

The most striking phenotype of *dark*^{verpeilt} mutants is the mis-targeting of Or47a neurons to the dorso-lateral region of the AL. To further analyze this structure a MARCM analysis was performed in eyFLP induced clones combined with a membrane bound CD8GFP to visualize axons (Figure 27).

In wild type MARCM clones the projection and innervation is not different from the pattern described previously.

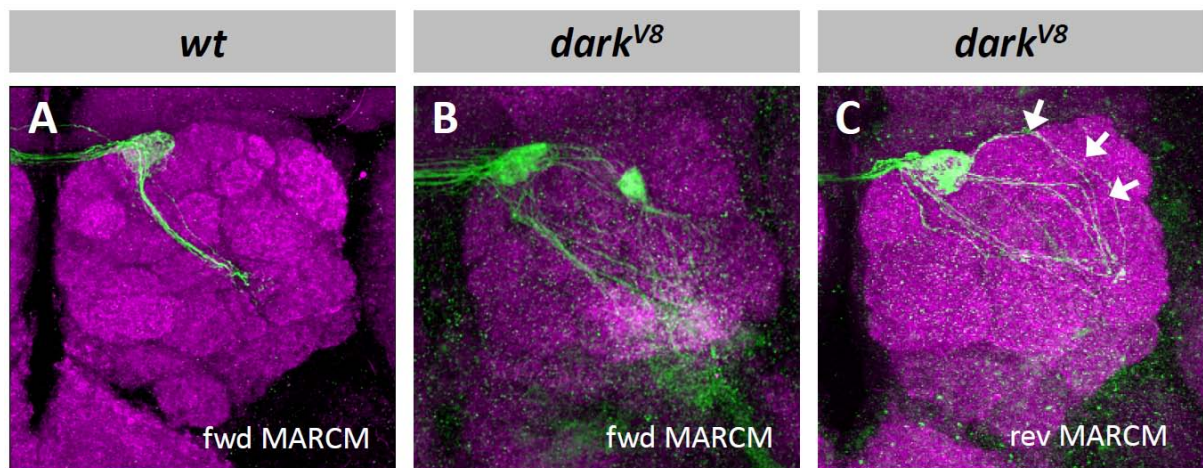


Figure 27 – Mis-targeting of Or47a neurons is cell autonomous

In MARCM clones only homozygous cells are labeled. (A) In the wild type Or47a grow along the central domain and converge onto the DM3 glomerulus. (B) In $dark^{V8}$ some Or47a axons do not innervate the DM3, but an additional glomerulus in the dorso-lateral AL. (C) In a reverse MARCM approach only homozygous wild type axons are labeled in a $dark^{V8}$ clonal background. Here not all Or47a axons grow along the central domain, but also more dorso-laterally (arrows). Genotypes: (A) eyFLP; FRT42/FRT42 Gal80; Or47aGal4 UAS-mCD8GFP, (B) eyFLP; FRT42 $dark^{V8}$ /FRT42 Gal80; Or47aGal4 UAS-mCD8GFP, (C) eyFLP; FRT42/FRT42 $dark^{V8}$ Gal80; Or47aGal4 UAS-mCD8GFP. OR expression is labeled with α -GFP (green), neuropil with α -ncad (magenta).

Interestingly, homozygous $dark^{V8}$ mutant Or47a axons innervate both the wild type target and the ectopic structure close to the DA3 glomerulus. Axons of the mis-projecting ORNs separate from the central projection domain and shift dorso-laterally, eventually ending up innervating the dorso-lateral glomerulus. Also the axons targeting the DM3 glomerulus appear to grow less ordered and spread out widely, but mainly within the central domain (Figure 27B) in $dark^{V8}$ mutant clones.

In a “reverse MARCM” approach homozygous wild type axons were labeled in a $dark^{V8}$ mutant clonal background. In this experiment also wild type axons are found that also shift towards the dorso-lateral route. These axons project close the dorso-lateral region of the ectopic glomerulus but do not form synapses in the area (Figure 27C). Instead they continue growing along the dorso-lateral projection domain and eventually innervate DM3, similarly to the lateral projecting axons found in 23% of the analyzed wild type ALs (see 1.4.2). In contrast, here the amount of lateral axons is increased, and lateral projections are found in all analyzed brains.

These data support the separation of the phenotype of *dark^{verpeilt}* in two parts. The ectopic innervation of Or47a axons in the dorso-lateral AL appears to be mediated cell autonomously, although the wild type axons project into this region, they do not form synapses. On the other hand, a shift of the projection route taken by the axons can also be observed in homozygous wild type ORN axons; therefore the choice of the projection route is regulated non-cell autonomously.

3.5.2.1 The ectopic structure is exclusively formed by mutant axons

Though the MARCM analysis suggests a cell autonomous function for *dark* in ORN targeting, these data do not allow excluding a contribution of heterozygous ORNs to the lateral glomerulus. To analyze the targeting behavior of the different subsets in *dark^{verpeilt}* mutant clones the MARCM analysis was repeated, this time labeling homozygous mutant axons with the membrane marker CD2 and the synapses of all Or47a neurons with a Gal4 independent Or47a:sytGFP promoter fusion (Figure 28).

In a analysis for co-localization of CD2 and GFP signal in the DM3 glomerulus and the ectopic structure it can be distinguished between homozygous mutant axons (co-labeling of both signals) and wild type and heterozygous synapses (GFP only) to elucidate the contribution of each fraction to the innervations found in *dark^{verpeilt}* mutant clones.

In both glomerular structures CD2 signal from the homozygous mutant ORNs is found, as expected from the previous experiment (Figure 28A). Taking a close look on the distribution of the CD2 versus the synaptic GFP reveals a strong co-labeling of both signals at both the DM3 and the ectopic positions, but in contrast to the latter, in the wild type target also some areas appear to remain CD2 negative, indicating that this space is exclusively innervated by wild type Or47a axons (Figure 28 B, C-C'). Artificial labeling of areas containing both signals (yellow) and GFP alone (magenta) in Figure 28 B shows this more clearly. Also the scatter plot of the co-localization clearly indicates voxels that are only labeled in green, representing GFP signal only.

In the ectopic glomerulus no areas are found that display only GFP labeling, the visualization of co-localization only shows yellow signal indicating the presence of both CD2

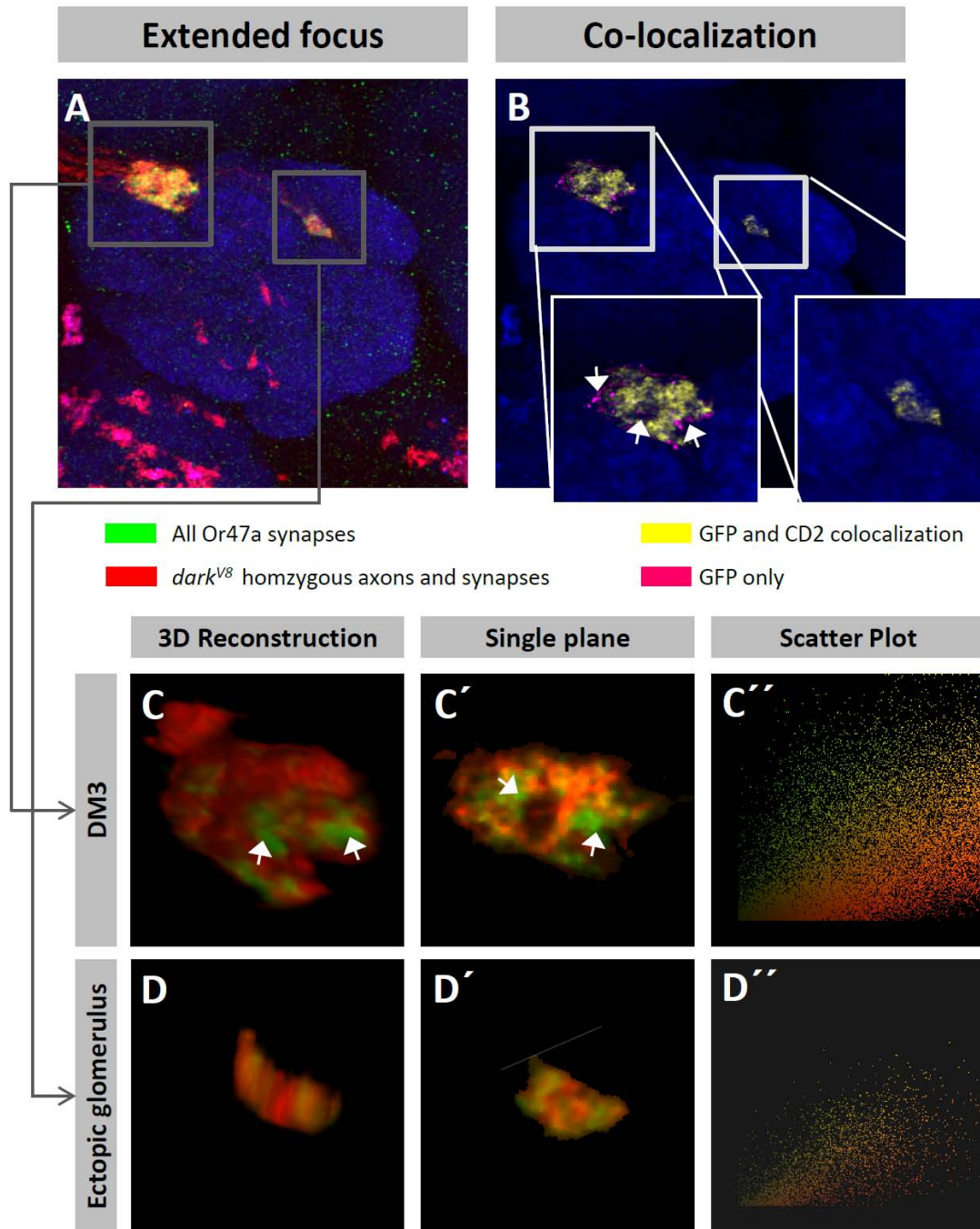


Figure 28 – The ectopic glomerulus is exclusively formed by $dark^{V8}$ mutant ORNs

(A) Labeling of wild type and homozygous mutant ORNs in a $dark^{V8}$ MARCM clone (B) Co-localization of wildtype and homozygous mutants. Areas containing both subpopulations are yellow, areas with only wildtype neurons magenta (arrows). (C-C') Co-localization in the DM3 glomerulus. Green areas contain only wildtype neurons (arrows), red areas contain mutant and wildtype. (C'') Scatter plot of the co-localization assay. Yellow dots represent co-localization. (D-D') Co-localization in the lateral glomerulus. Only areas containing both signals are present, indicating only homozygous mutant ORNs. (D'') Scatter plot of the co-localization assay of the lateral glomerulus. Yellow dots represent co-localization. Genotype: $eyFLP\ UAS-CD2; FRT42\ dark^{V8}\ Or47a:sytGFP/FRT42\ Gal80; Or47aGal4\ UAS-CD2$. All Or47a synapses are labeled with α -GFP (green), $dark^{V8}$ homozygous ORNs with α -CD2 (red) and neuropil with α -ncad (blue).

and GFP signal. Also in the scatter plot of the co-labeling in the lateral position no GFP-only voxels appear (Figure 28 D).

The presence of voxels only labeled with CD2 is probably caused by the axons of *dark*^{V8} homozygous mutant axons.

This experiment confirms the findings of the previous experiment; the lateral glomerulus is exclusively formed by *dark*^{V8} homozygous mutant axons, pointing to a cell autonomous function of *dark* in target decision of ORNs. Interestingly, homozygous mutant axons innervating the DM3 do not separate from their wild type counterparts and seem to integrate normal in this glomerulus.

3.5.3 The ectopic glomerulus needs a certain amount of axons to be stabilized

In order to determine a requirement of a critical amount of mis-projecting axons to induce ectopic targeting in the dorso-lateral AL, small homozygous mutant clones were induced using hsFLP MARCM clones. With this method it is theoretically possible to label individual axons, in practice the timing of setting the heatshock is a critical issue, so frequently more than one neuron is marked. Three different phenotypes could be distinguished, central projecting axons, central and lateral projecting axons and central and lateral projecting axons which formed ectopic axon termini in the dorso-lateral AL (Figure 29 A-C).

In total 22 clones were examined, ranging from single labeled neurons up to 14 (Figure 21 D). Nine of these clones only contain ORNs projecting along the central route to the DM3 glomerulus, and except one clone with eight axons labeled, only clones with up to three axons marked show no laterally growing axons. On contrary, clones that exhibit lateral projecting axons contained at least for labeled cells, only two clones each with two axons labeled exhibited one axon growing along the dorso-lateral domain. In more than half of the brains that showed lateral projections only single axons were found. In five cases more than one axon projecting laterally were observed, and in three of these examples these axons formed ectopic termini in the dorso-lateral region of the AL. More than one lateral axon were only labeled when the total clone size was larger than five cells, lateral axon termini only appeared in clones containing eight or more cells. In two of the three brains that showed this phenotype, in addition a single axon not innervating the lateral position

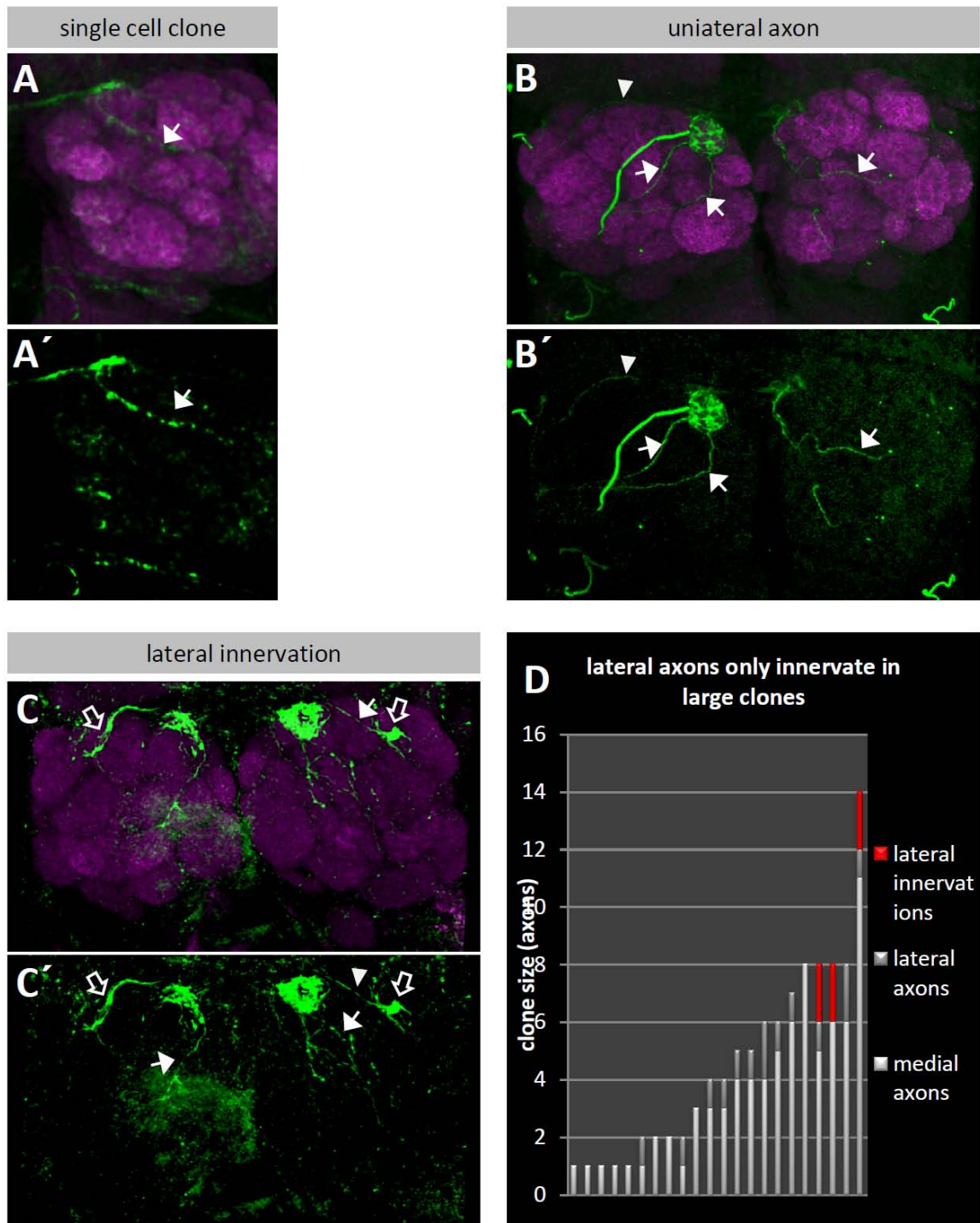


Figure 29 – The formation of the lateral glomerulus requires a critical amount of lateral projecting axons

(A-C) *dark^{V8}* mutant heatshock induced clones with different numbers of Or47a neurons labeled. (A,A') Single Or47a axon projecting centrally (arrow). (B, B') 4-cell clone with three centrally projecting (arrows) and one lateral projecting axon (arrowhead). (C, C') Larger clone with central (arrows) and lateral (arrowheads) projecting ORNs. Also lateral innervation is present (empty arrow). (D) Quantification of this experiment. Genotype: *hsFLP UAS-CD2; FRT42 dark^{V8}/FRT42 Gal80; Or47aGal4 UAS CD2*. Or47a axons are labeled with α -CD2 (green) and neuropil with α -ncad (magenta).

was found. The presence of lateral axon termini was symmetric in all three examples; in contrast, laterally projecting axons usually were only present on one half of the AL.

Lateral projecting ORN axons only stop close to the DA3 glomerulus in larger clones, and in contrast to the previous MARCM experiment (see 1.5.2), not all lateral projecting homozygous *dark*^{V8} ORNs stop at the lateral position, indicating a requirement of certain amount of ORNs to stabilize the ectopic innervation in the dorso-lateral AL.

3.5.4 Mis-projecting Or47a axons sort out from other classes

The convergence of ORN axons onto a single glomerulus and the separation of neighboring classes is one of the key characteristics of the olfactory system. To test whether the mis-projecting Or47a axons still retain this ability Or47a neurons were labeled together with a second ORN class that projects to a glomerulus adjacent to the ectopic structure in *dark*^{V8}. The ORN classes 49a and 23a were analyzed respectively in combination with OR47a in mitotic clones. By using two different membrane associated markers, CD2 and CD8GFP, it is not only possible to examine the innervations of the two classes, but also to detect putative interactions of the in-growing axons. Both Or23a and Or49a neurons show no phenotype in *dark*^{verpeilt} (Figure 26, Table 04).

Or49a neurons project their axons to the DL4 glomerulus in the dorso-lateral AL, rather distant from DM3, the wild type target of the Or47a class. As expected, in the control clones no interaction between these two classes can be observed (Figure 30 A). In *dark*^{V8} mutant clones the ectopic glomerulus of mutant Or47a axons is right above of the DL4 glomerulus and in a frontal view in the AL they appear to overlap at least partly with the Or49a innervation. However, in the orthogonal view from dorsal, the two structures appear to touch each other, but a clear separation between the Or47a and the Or49a labeling becomes obvious (Figure 30 B, B').

The wild type target of the Or23a class, the DA3 glomerulus is positioned on the anterior surface of the AL on top of the DL4 glomerulus, in a comparable distance of the DM3 glomerulus as DL4. Therefore, in the wild type again no interaction between Or47a and Or23a axons occurs (Figure 30C). In *dark*^{V8} mutant clones the area directly adjacent to the DA3 is occupied by the ectopic Or47a glomerulus, but no intermingling of the Or23a and

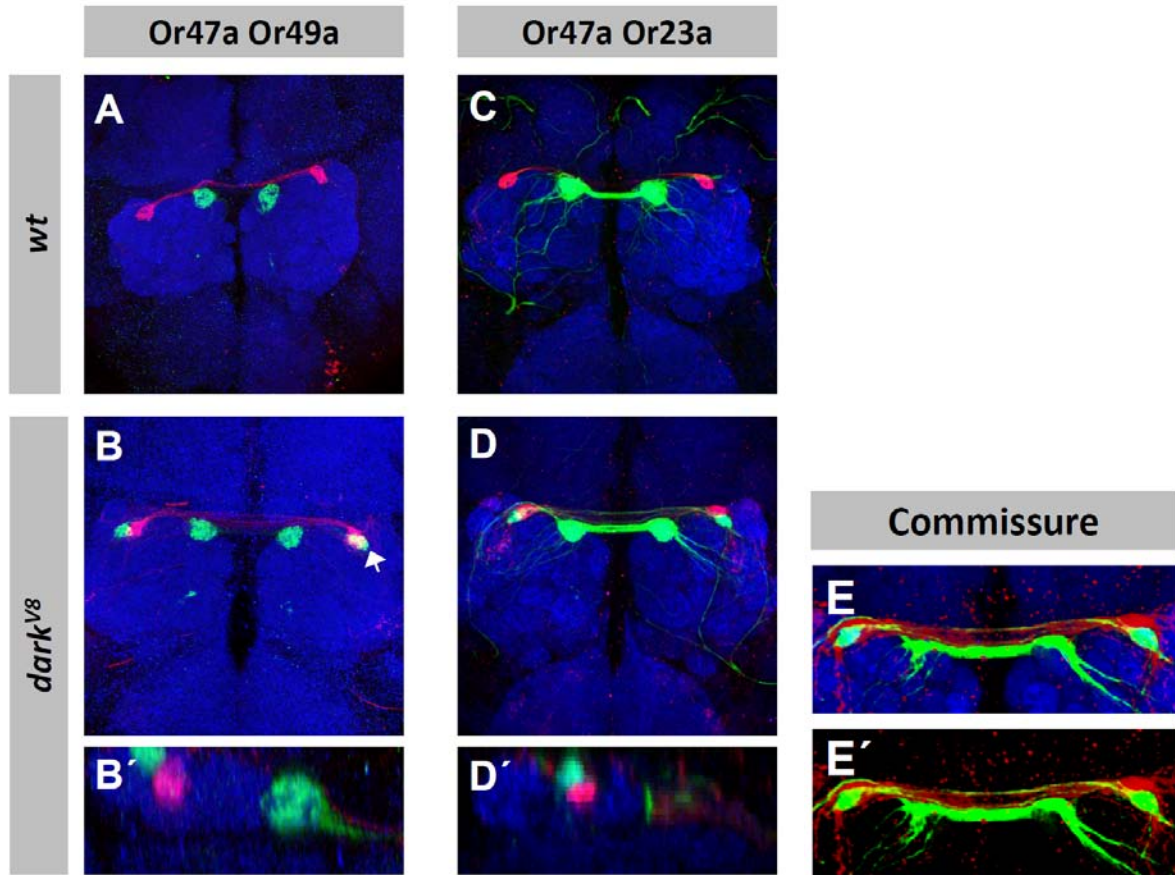


Figure 30 – *dark^{V8}* mutant ORNs sort out from neighboring ORN classes

(A-B) Co-labeling of Or47a and Or49a neurons. (A) In the wild type the two classes do not interact at all. (B) In *dark^{V8}* clones Or47a and Or49a axons project to adjacent glomeruli, but seem not to interact. The yellow labeling (arrow) is an artifact from merging the confocal stack. (B') dorsal view on the two glomeruli, no overlap is detectable. (C-E) Co-labeling of Or47a and Or23a neurons. (C) In the wild type no interaction can be detected between Or47a and Or23a. (D) In *dark^{V8}* the axons terminate directly adjacent to each other but do not intermingle, as also shown in a dorsal view (D'). (E, E') A close look on the commissure shows that Or23a axons grow between the two commissural branches of the Or47a axons in *dark^{V8}* clones. Genotypes: (A) eyFLP UAS-CD2; FRT42 Or47a::syGFP/FRT42; Or49aGal4 UAS-CD2, (B) eyFLP UAS-CD2; FRT42 *dark^{V8}* Or47a::syGFP/FRT42; Or49aGal4 UAS-CD2, (C) eyFLP UAS-CD2; FRT42 Or23a::CD8GFP/FRT42; Or47aGal4 UAS-CD2, (D,E) eyFLP UAS-CD2; FRT42 *dark^{V8}* Or23a::CD8GFP/FRT42; Or47aGal4 UAS-CD2. In (A, B) Or 47a is labeled with α -GFP (green), Or49a with α -CD2 (red) and the neuropil with α -ncad (blue). In (D,E) Or47a is labeled with α -CD2 (green) Or23a with α -GFP (red) and the neuropil with α -ncad (blue).

the Or47a axon population is detectable (Figure 30 D, D'). Interestingly, the commissural projections of Or23a neurons are right between the branches of the two fractions of Or47a axons. Though the Or23a axons do not fasciculate as much as the Or47a axons, it appears as if at least some branches of the Or23a neurons associate with the Or47a axons projecting dorsally across the commissure (Figure 30 E).

These results show that mis-projecting Or47a neurons sort out precisely from the neighboring classes. The partial association of Or47a and Or23a axons indicates a relation between these two classes in respect to their projection behavior.

3.5.5 Misprojecting Or47a axons interact with projection neurons

To get an idea if the ectopic structure in *dark*^{V8} actually forms a functional glomerulus it was analyzed whether the mis-targeting axons interact with PN dendrites. One approach was to label about 2/3 of all PNs using the GH146Gal4 driver and independently mark Or47a-synapses with a synaptic GFP.

The Co-labeling of the Or47a synapses together with all PN dendrites reveals a tight intermingling within the DM3 glomerulus. In single confocal slices small holes are detectable in the GFP signal of the ORNs synapses which are densely filled with PN dendrites. The boundaries of the DM3 glomerulus are also clearly detectable when looking at the dendrite staining alone (Figure 31 A, A'). In wild type the area occupied by lateral projecting Or47a neurons in *dark*^{verpeilt} remains free of PN dendrites (Figure 31 A'', compare Figure 1).

A comparable situation is also found in the DM3 glomerulus of *dark* mutant ALs. The ORN dendrite pattern is virtually undistinguishable from the wild type (Figure 31B, B'). Examination of the lateral glomerulus shows a similar mixing of PNs and ORNs, though the signal strength of the dendrites is weaker than in the DM3. However, the intensity matches with the neighboring glomeruli. In addition, the dendrite pattern in the dorso-lateral AL does not allow identifying the ectopic glomerulus as an individual structure (Figure 31 C, C').

Further, it was analyzed which class of PNs that gets innervated by the mis-projecting axons. It has been described that PN dendrites are flexible to changes in the ORN pattern

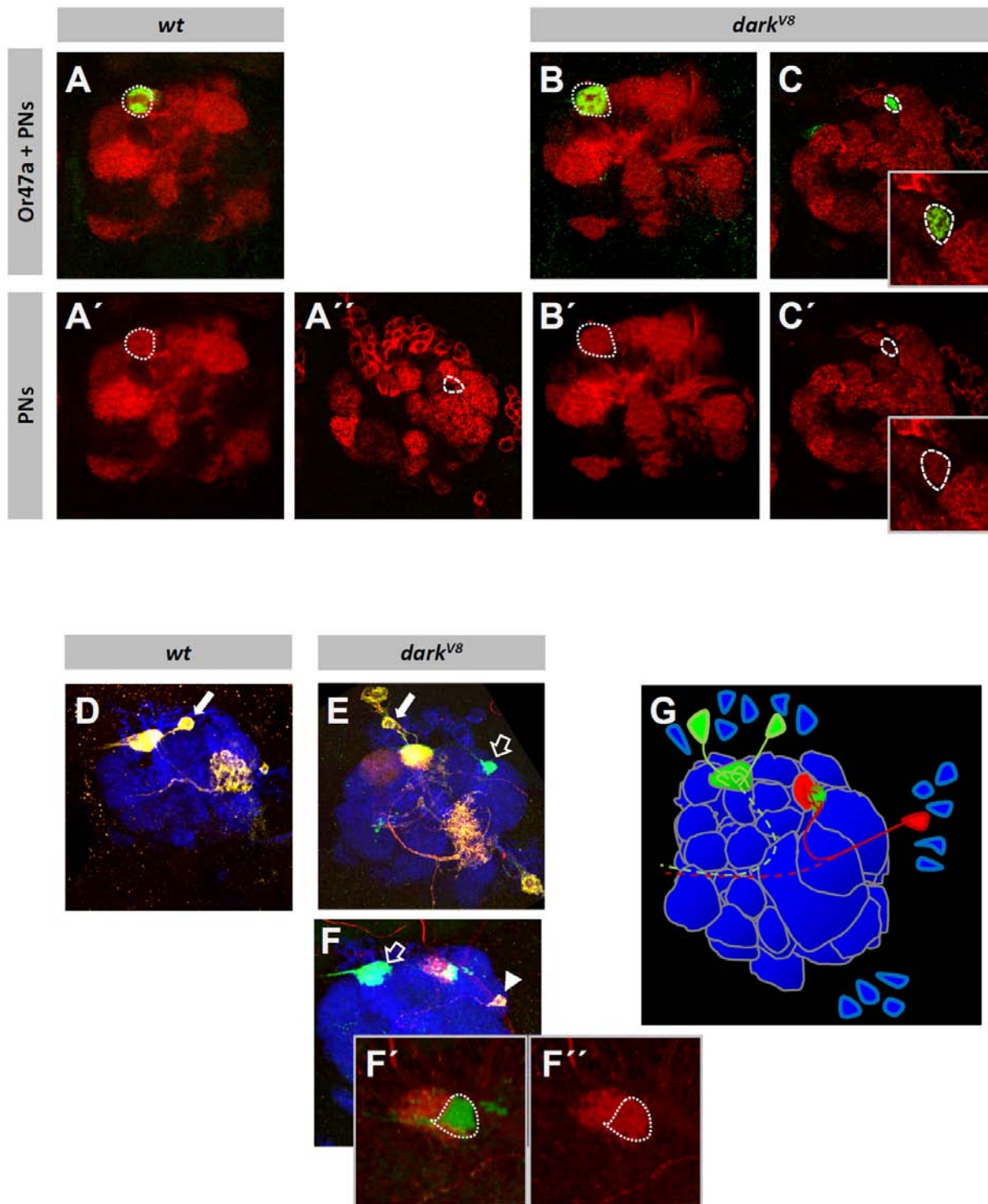


Figure 31 – Lateral innervating ORNs specifically interact with target neurons
See Figure legend on next page

Figure 31 – Lateral innervating ORNs specifically interact with target neurons

(A-C') PNs interact with Or47a axons. (A, A') In wild type PN dendrites invade the area of the DM3 glomerulus and fill the gaps between the OR47a synapses. (A'') The space occupied by lateral projecting ORNs in *dark^{V8}* mutants remains empty in wild type. (B) In *dark^{V8}* mutants the PN dendrites in DM3 show the same pattern as in wild type. (C) PN dendrites are also found in the ectopic glomerulus innervated by lateral projecting Or47a neurons in *dark^{V8}*. (D) A single PN from the dorsal cluster is identifiable that sends its dendrites to the DM3 glomerulus. (E) In *dark^{V8}* a single PN sends its dendrites to the DM3, but does not extend to the lateral glomerulus. The labeling of the lateral Or47a innervation shows no signs of PN dendrites from this PN. (F) A lateral PN extends its dendrites to the dorso-lateral AL and receives input from mis-projecting Or47a axons. (F', F'') The lateral glomerulus is not completely innervated by Or47a neurons. (G) Scheme of the PNs interacting with Or47a axons in *dark^{V8}*. Genotypes: (A) eyFLP; FRT42 Or47a:sytGFP/FRT42; GH146Gal4 UAS-CD2, (B,C) eyFLP; FRT42 *dark^{V8}* Or47a:sytGFP/FRT42; GH146Gal4 UAS-CD2, (D) eyFLP UAS>CD2>CD8; FRT42 Or47a:sytGFP/FRT42; GH146Gal4, (E,F) eyFLP UAS>CD2>CD8; FRT42 *dark^{V8}* Or47a:sytGFP/FRT42; GH146Gal4. Stainings: (A-C) Or47a synapses are labeled with α -GFP (green), PNs with α -CD2 (red). (D-F) Or47a synapses are labeled with α -GFP (green), single labeled PNs are stained with α -GFP and α -CD8 (red + green = yellow) and the remaining PNs with α -CD2 (blue).

and can extend their dendrites, within a certain radius, to receive innervation of the respective ORN axons even at atypical positions (Zierau, personal communication). To analyze whether the specific ORN-PN matching is also maintained in *dark^{verpeilt}* mutant clones a hsFLP based approach was used to label individual PNs. Using a hsFLP with a flip-out CD2>CD8 reporter it is possible to label single PNs and identify their class according to the position of the cell body and the pattern of their dendrites. By inducing recombination, applying a short heat shock between 25 and 40 h APF, individual PNs could be attributed to the DM3 glomerulus. Co-labeling of the ORN innervations of Or47a neurons allows detecting the position and presumable identity of the PNs receiving input from this class in wild type and *dark^{V8}* mutant clones. The dendrites innervated by Or47a neurons in the DM3 glomerulus belong to PNs that are located in the dorsal cluster. In the wild type control, single neurons can be identified with dendrites restricted to the DM3 glomerulus that are innervated by OR47a axons (Figure 31 D).

In *dark^{V8}* mutants the Or47a innervations in DM3 glomerulus are also filled with dendrites belonging to a neuron located in the dorsal PN cluster, the lateral Or47a innervation in this situation shows no dendrite signal from this PN (Figure 31E). In a different clone a single PN is labeled which sends its dendrites to the lateral region of the AL and appears to get innervated by the lateral projecting Or47a axons. In this example, the DM3 innervations of

Or47a axons do not co-localize with PN dendrites of this lateral neuron (Figure 31F). Interestingly, the glomerular structure at the lateral position marked by the dendrites of this PN is not completely overlapping with the signal from the lateral innervating Or47a synapses (Figure 31 F', F''). The position of the dendrites and the location of the cell body in the lateral cluster of this PN indicate that it presumably belongs to the DA3 glomerulus, which is innervated by Or23a neurons in the wild type.

From these results it can be concluded that the mis-projecting ORN axons lose their target specificity and form contact with PNs regularly innervated by ORNs of a different ORN class. However, these connections appear to be specific to the dendrites of DA3 specific PNs that presumably also receive input from Or23a axons. This is supported by the finding that the ectopic glomerulus in *dark^{verpeilt}* mutant clones is always located directly adjacent to the DA3 glomerulus.

3.6 LRR Cell adhesion molecules are predominantly restricted to one projection domain

In chapter 3.4 it was shown that the axons in the olfactory system of *Drosophila*, similar to the situation in vertebrates, are organized in projection domains. How these domains are established and whether they have any impact on the ORN targeting remains elusive.

Thought a simple shift of Or47a neurons to the dorso-lateral projection domain does not lead to mis-innervation in the lateral AL, a strong preference to this domain by the *dark^{verpeilt}* mutant axons forming the ectopic glomerulus can be observed, suggesting altered properties in these neurons according to the choice of the projection route.

To gain further insights in the properties of the projection domains molecules were analyzed that have an expression pattern restricted more or less exclusively to one of the domains. Analysis of the expression patterns of two cell adhesion molecules belonging to the Leucin-rich-repeat family, Capricious (Caps) and Connectin (Con) in the peripheral olfactory system showed that these molecules are mainly expressed by neurons projecting in the ventral and medial or the dorso-lateral domain, respectively (Sieglitz, 2007).

Caps is expressed in about one third of all ORNs. Labeling of Caps expressing ORNs by expressing a membrane bound CD8GFP has been shown that its expression is predominantly found in ORN classes that project to ventro-medial glomeruli, therefore

projecting along the ventro-medial projection route (Figure 32A). In *dark*^{V8} mutant clones the pattern is less ordered showing a slight preference of the ORN axons to project along more dorsal routes (Figure 32B), comparable to the effect found for the entirety of ORNs upon labeling with Or83b (see 1.4.1).

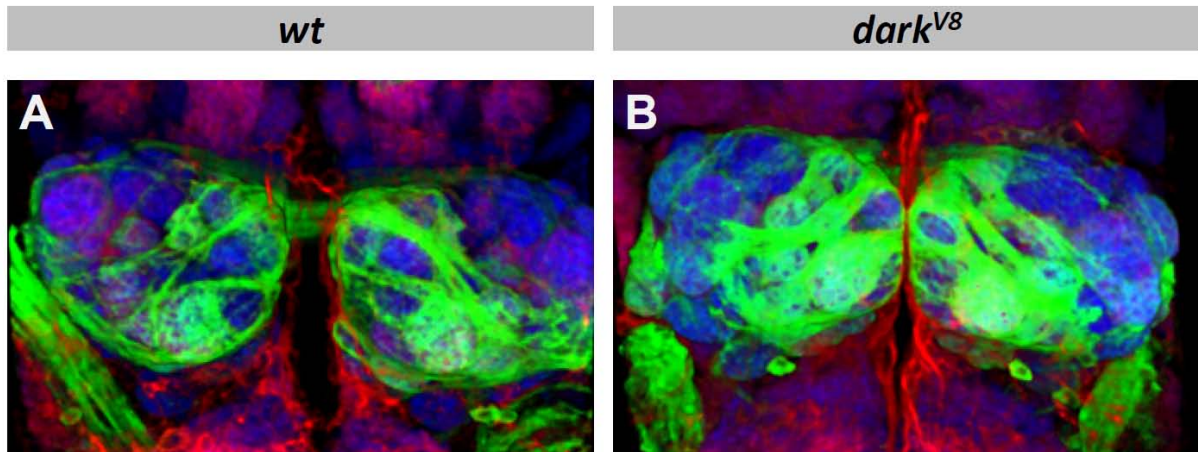


Figure 32 – Capricious predominantly labels ORNs projecting along the ventro-medial domain (A,B) Connectin is expressed by ORNs mainly innervating targets in the ventro-medial AL. In *dark*^{V8} mutants the projections of these neurons are less restricted to the ventro-medial projection domain and appear shifted in a dorsal direction (B). Genotypes: (A) *eyFLP UAS>CD2>CD8, FRT42/FRT42 Gal80; CapsGal4*, (B) *eyFLP UAS>CD2>CD8, FRT42 dark^{V8}/FRT42Gal80; CapsGal4*. Caps expressing ORNs are labeled with α -GFP (green), Caps expressing PNs with α -CD2 (red) and the neuropil with α -ncad (blue).

Con is expressed in about one third of the ORN classes and is also found in some PNs. In some glomeruli Con is expressed in both, the pre- and postsynaptic neurons. Other glomeruli only show Con in the ORNs or the PNs (Sieglitz, 2007) In contrast to Caps, Con expressing ORNs mainly project to glomeruli in the dorsal and lateral area of the AL with few exceptions innervating targets more ventral and medial (Figure 33). The expression of Caps and Con in the ORNs is summarized in Table 05.

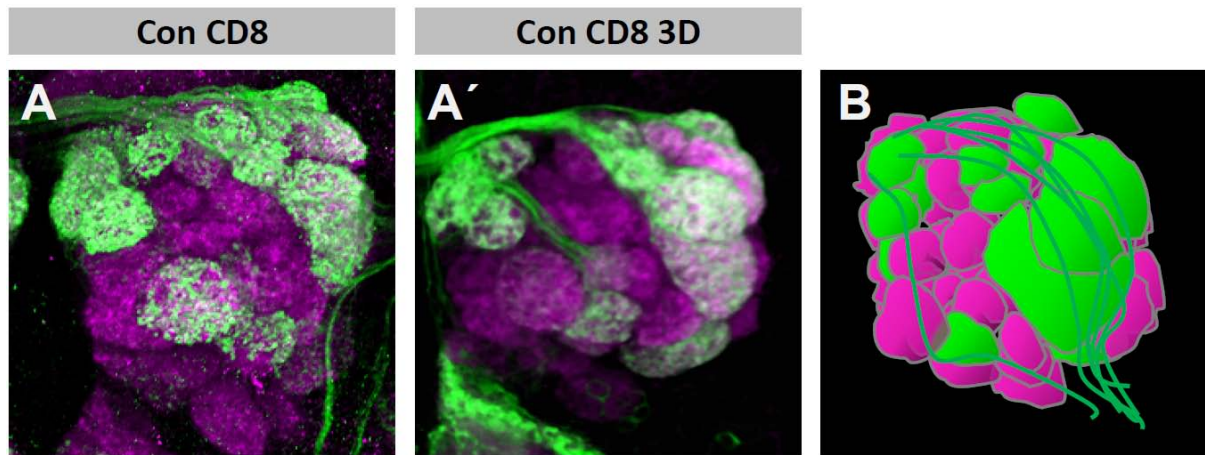


Figure 33 – Connectin predominantly labels ORNs projecting along the dorso-lateral domain

Connectin expressing ORNs mainly innervate glomeruli in the dorsal AL (A) and project along the dorso-lateral projection domain (A'). The main projection routes are schematically shown in (B). Genotype: ConGal4 UAS-mCD8GFP. Con expression is labeled with α -GFP (green), neuropil with α -ncad (magenta).

Both Caps and Con are not expressed by Or47a neurons in wild type. Since the single class analysis revealed that the shift of ORN projections in *dark*^{V8} mutants is predominantly in a dorso-lateral direction, and also the ectopic target of the Or47a axons is in this area, it was decided to have a closer look on the Con-positive projection domain. Also the Or23a class that shows some association with the ectopic glomerulus in *dark*^{V8} mutants is expressing Con.

Table 05 – Expression pattern of Capricious and Connectin in ORNs

ORN class	glomerulus	Con expression	Caps expression	ORN class	glomerulus	Con expression	Caps expression
Or2a	DA4l	+		Or56a	DA2		
Or7a	DL5			Or59b	DM4		
Or9a	VM3			Or59c	1		
Or10a	DL1			Or65a	DL3	+	
Or19a	DC1			Or67a	DM6	+	+
Or22a	DM2	+	+	Or67b	VA3	+	+
Or23a	DA3	+		Or67c	VC4		
Or33c	VC1			Or67d	DA1	+	
Or35a	VC3			Or69a	D		
Or42a	VM7	+	+	Or71a	VC2		+
Or42b	DM1		+	Or82a	VA6		+
Or43a	DA4l	+		Or83c	DC3		+
Or43b	VM2			Or85a	DM5	+	+
Or46a	VA7l		+	Or85b	VM5d	+	
Or47a	DM3			Or85d	VA4	+	
Or47b	VA1V	+	weak	Or88a	VA1d	+	weak
Or49a	DL4	+		Or92a	VA2	+	+
Or49b	VA2			Or98a	VM5v		
				Gr21a	V		

3.6.1 Connectin is mainly expressed in the trichoid sensilla

First the distribution of Con expressing ORNs in the antenna was examined. Since it is very difficult to perform an immune staining in here because the antibodies do not penetrate the cuticle, a UAS-CD8cherry construct under the control of ConGal4 was expressed and the fluorescence imaged directly with a confocal microscope. The highest density of Con

expressing neurons is found in the distal part of the antenna, decreasing in a dorsal direction (Figure 34). This area has been described to be mainly populated with trichoid sensilla (Couto, Alenius & Dickson 2005). ORNs in trichoid sensilla mainly project to the glomeruli in the dorso-lateral AL.

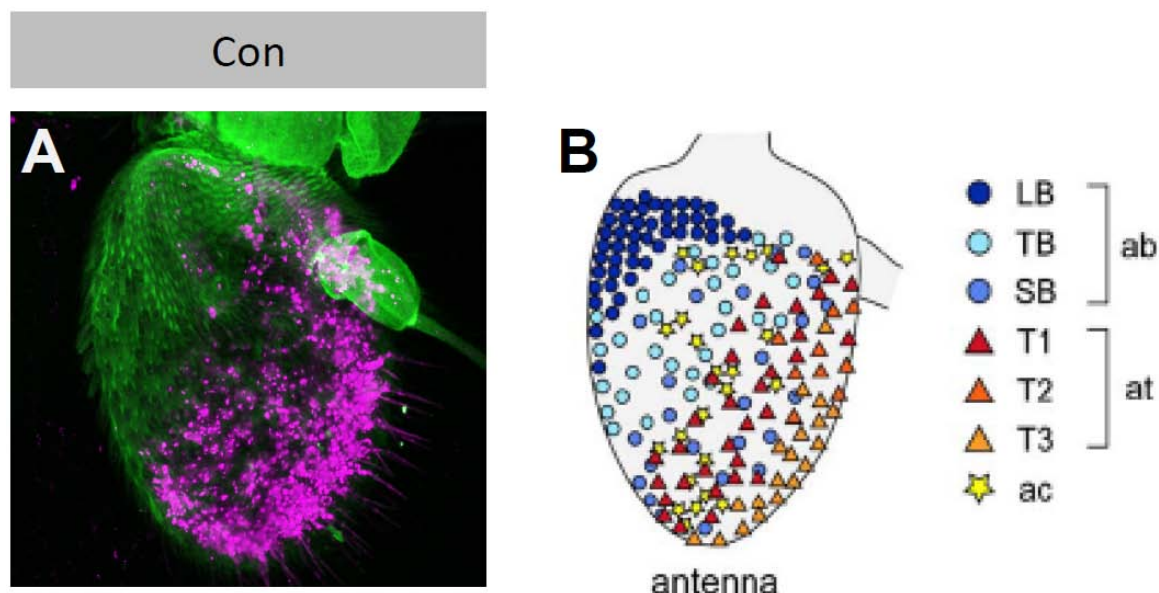


Figure 34 – Connectin is expressed in a continuous patch in the distal part of the 3rd antennal segment

The ORNs that express Con are arranged in a continuous patch in the distal part of the antenna (A). This area mainly contains trichoid sensilla (T1, T2, T3, triangles in (B)) (B taken from Couto et al., 2005.) Genotype: ConGal4 UAS-mCD8cherry. Con expressing ORNs are labeled with the endogenous cherry fluorescence (magenta), the outline of the antenna is shown by endogenous fluorescence of the cuticle (green).

3.6.2 Con expression during development

Con expression can be detected early in development of the olfactory system even before proto-glomeruli are formed, the exact time point has not been determined. At about 30h after puparium formation (APF) two Con positive fascicles can be detected, one presumably representing the ventro-medial, the other one the dorso-lateral projection domain (Figure 35 A). At late stages around 80h APF the AL has almost developed to its adult shape and still the ORNs in the dorso-lateral domain retain Con expression (Figure 35 B). The expression level appears to be elevated in the dorso-lateral glomeruli DL3 and DA3.

This appears even more obvious at 90h APF when the expression of Or47a starts (Figure 35 C).

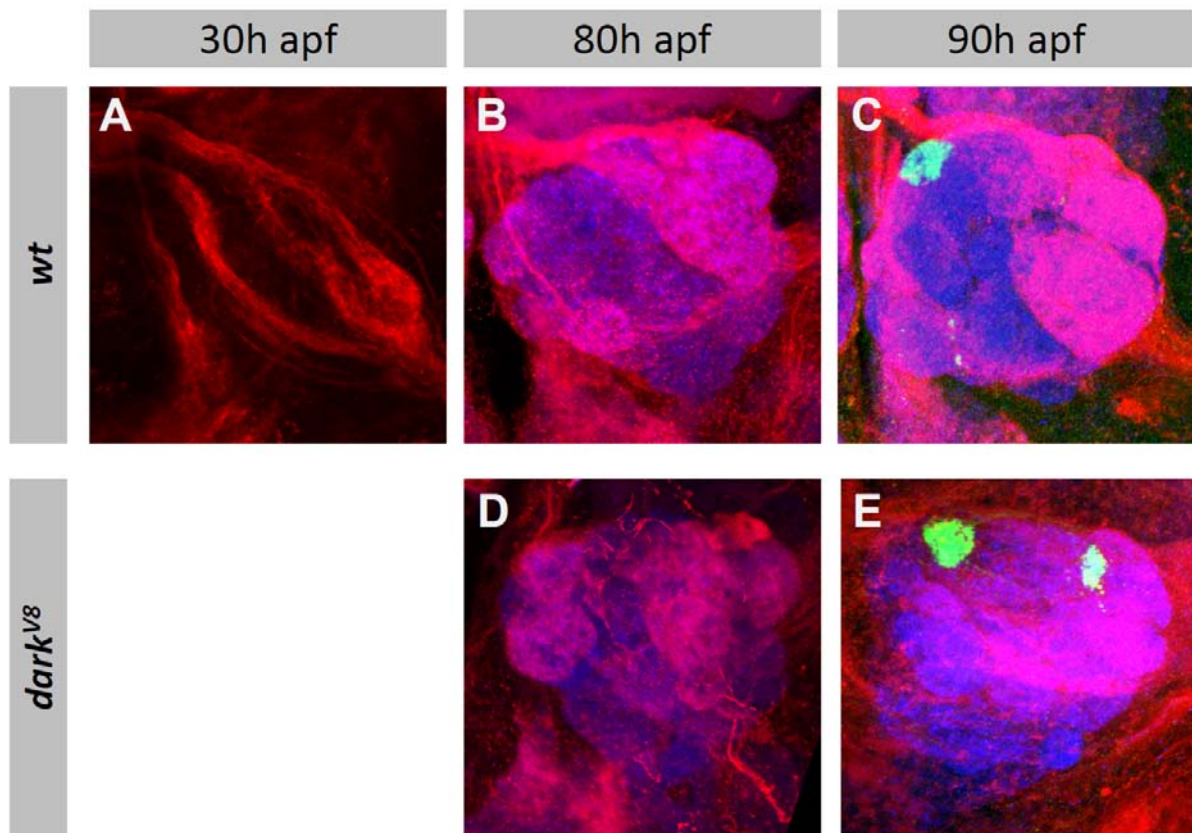


Figure 35 – Connectin expression during ORN development

(A-C) Con expression at different stages during pupal development. (A) At 30h APF two Con positive fascicles are visible, presumably representing axons projecting along the dorso-lateral and the ventro-medial projection domain. (B) At 80h APF Cn expression appears enriched in the dorso-lateral AL. (C) At 90h APF, the Con levels in the dorso-lateral AL look even higher than at 80h APF. Or47a neurons do not express Con. (D-E) Con expression at late pupal stages in homozygous *dark^{v8}* pupae. (D) The Con expression pattern at 80h APF in *dark^{v8}* mutants looks less distinct than in the wildtype. Like in wild-type, an enrichment of Con is detected in the dorso-lateral AL. (E) At 90h APF the Con expression looks less ordered, the whole AL structure seems affected, presumably caused by degeneration effects. Genotypes: FRT 42 Or47a:sytGFP, (B) FRT42 *dark^{v8}* Or47a:sytGFP. OR47a expression is visualized with α -GFP (green), Con expression with α -Con (red), neuropil is stained with α -ncad (blue).

In homozygous *dark^{v8}* mutants the Con expression at 80h AFP appears less ordered, though like in the wild type, the levels in the dorso-lateral AL appears to be higher (Figure 35 D). Later, at 90hAPF the Con is found all over the dorsal half of the AL. Also, the whole structure of the AL is not as clear as in the wild type and at this stage individual glomeruli are hard to distinguish in the N-Cad staining to visualize the neuropil. The expression of

Or47a however is still restricted to glomerular structures. Interestingly, the lateral glomerulus is in the middle of the Con expressing domain and no decrease in the Con levels in this structure can be observed (Figure 35 E).

Since the *dark*^{V8} mutants are lethal as pupae and the exact stage has not been determined. The morphological changes might be caused by degeneration processes and not be directly related to changes in Con expression due to the mutation in *dark*.

Con expression is turned off shortly after hatching, in one week old flies almost no Con can be detected by the antibody (data not shown).

3.6.3 The ectopic Or47a glomerulus in *dark*^{V8} mutants is Con positive

The fact that Con is down regulated at the end of pupal development makes it tough to analyze changes in Con expression in *dark*^{verpeilt} mutants compared to the wild type. To circumvent this problem a UAS-CD2 construct under the control of ConGal4 was expressed and brains of young adult flies in wild type and *dark*^{V8} mutant clones analyzed.

The general pattern of Con is not changed in *dark*^{V8} mutants. The commissural fascicle of dorso-lateral projecting axons appears slightly thicker and the ventro-medial domain somehow thinner, but the glomerular pattern, except for the lateral glomerulus formed by the mis-innervating Or47a axons, remains unchanged (Figure 36 A, B).

As mentioned before, Or47a neurons do not express Con. This is true for both wild type and *dark*^{V8} mutants for Or47a neurons innervating the DM3 glomerulus (Figure 36 C-D'). In contrast, the lateral glomerulus in *dark*^{V8} clones appears Con positive (Figure 36 E, E').

The dorso-lateral projection domain shows little changes in *dark*^{V8} clones compared to the wild type, indicating that in contrast to the ventro-medial domain visualized by Caps expression, axons in this domain do not get shifted even more dorsally.

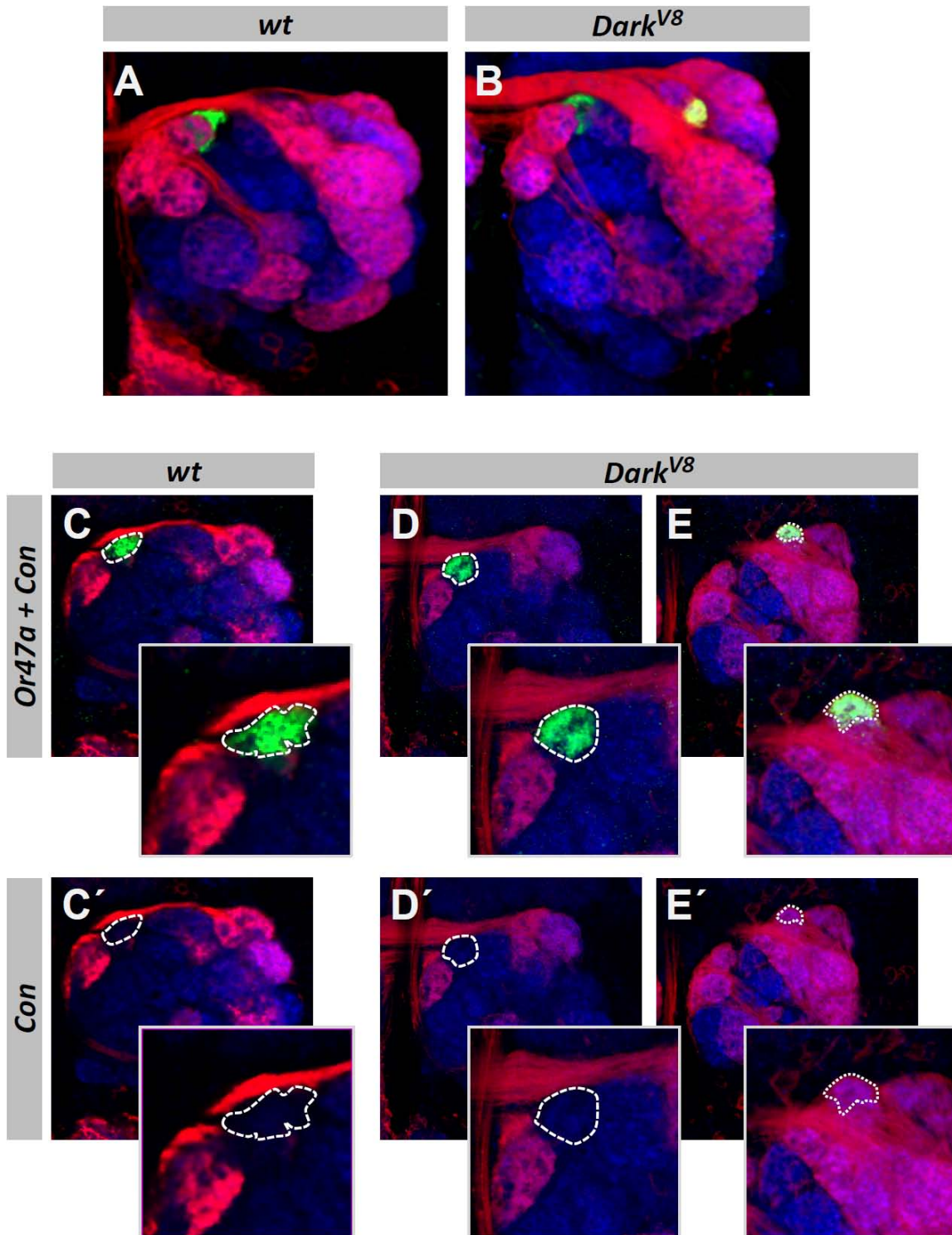


Figure 36 - Lateral projecting Or47a neurons in *dark^{V8}* ectopically express Connectin

(A,B) The overall expression pattern of Con does not change in *dark^{V8}* mutants. (C, C') In the wild type, Or47a neurons innervating the DM3 glomerulus (dotted line) do not express Connectin. (D,D'). The DM3 glomerulus remains Con negative in *dark^{V8}* mutants (dotted line in (D, D')). In contrast, the lateral glomerulus innervated by Or47a neurons is Con positive (dotted lines in (E, E')). Genotypes: (A, C) *eyFLP, FRT42 Or47a:sytGFP/FTR42; ConGal4 UAS-CD2*, (B, D, E) *eyFLP, FRT42 dark^{V8} Or47a:sytGFP/FTR42; ConGal4 UAS-CD2*. Or47a expression is labeled with α-GFP (green), Con expression with α-CD2 (red), neuropil is stained with α-ncad (blue).

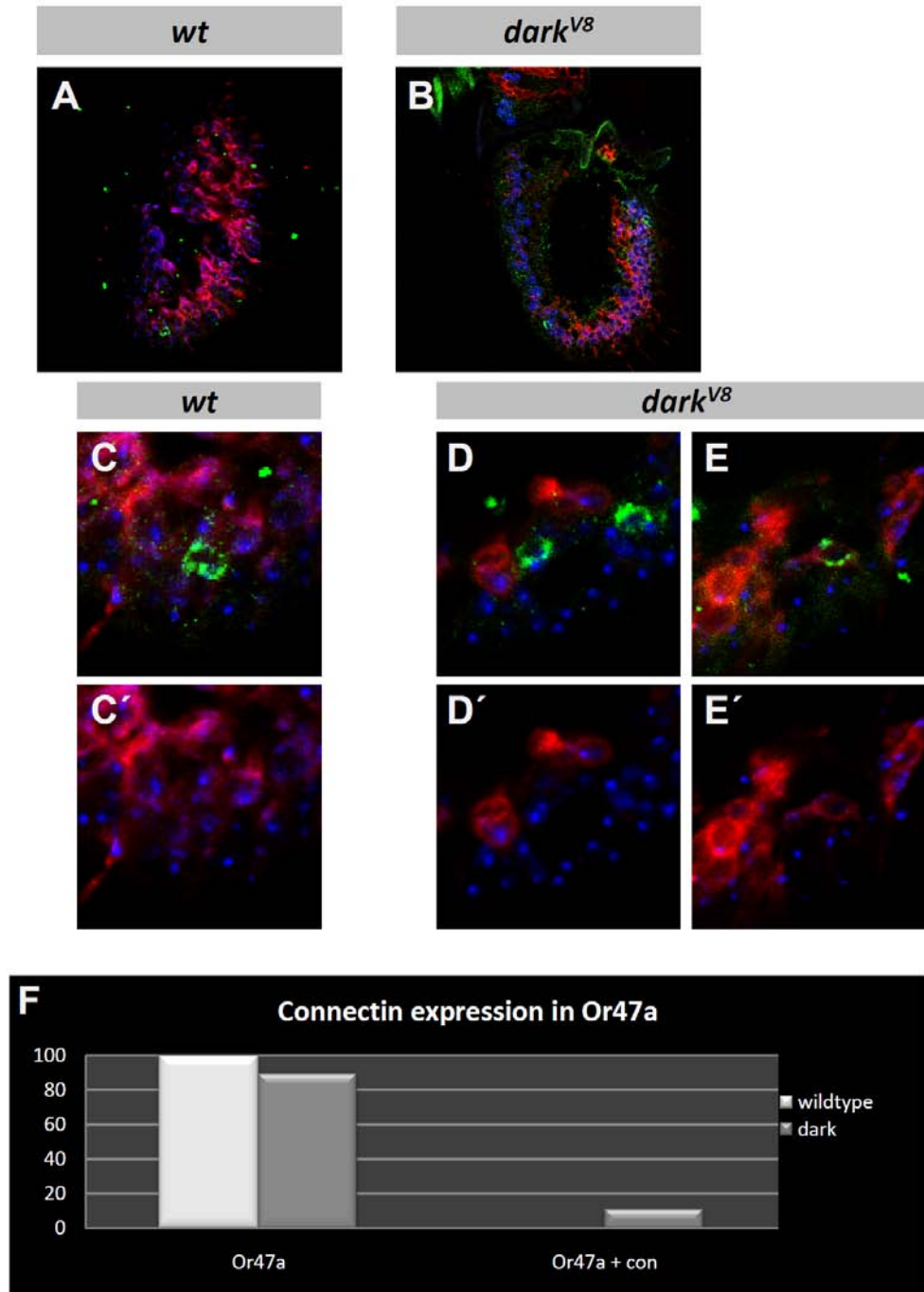


Figure 37 – Connectin is mis-expressed in Or47a neurons

(A,B) Cryosections of adult wild type and *dark^{V8}* antennae. Con expression is predominantly found in the lower distal part of the antenna. (C-E) Magnifications of Con expressing ORNs of wildtype (C) and *dark^{V8}* antennae (D, E). In wild type, Con expressing ORNs do not express Or47a (C, C'). In *dark^{V8}* mutant antennae, most of the Or47a neurons do not express Con (D, D'), in some cases Co expression of Or47a and Con can be observed (E, E'). Genotypes: (A, C) eyFLP, FRT42 Or47a:sytGFP/FTR42; ConGal4 UAS-CD2, (B, D, E) eyFLP, FRT42 *dark^{V8}* Or47a:sytGFP/FTR42; ConGal4 UAS-CD2. Or47a expression is labeled with α -GFP (green), Con expression with α -CD2 (red), nuclei are stained with toto3 (blue).

3.6.4 *Dark* mutant Or47a neurons express Con

To confirm the ectopic Con expression found in the dorso-lateral glomerulus in *dark^{verpeilt}* clones Or47a neurons were tested for co-expression of Con and Or47a. As mentioned above it is not possible to stain whole mount antenna, therefore cryosections were performed and the expression of Con and Or47a subsequently labeled in an antibody staining.

In the wild type no Con expressing Or47a neurons could be detected (n=12) (Figure 37A, C-C'). In *dark^{V8}* mutant clones the majority of Or47a neurons do not express Con, presumably representing the fraction that innervates the DM3 glomerulus which is still Con negative also in the mutant (Figure 37 B, D-D'). However, about 10% of the Or47a neurons in *dark^{V8}* mutants express both Con and Or47a. (n=16) (Figure 37 E, E').

3.6.5 Con mutants do not affect OR47a targeting

Connectin itself has been described to control targeting of motor axons in the embryonic nervous system (Nose, Mahajan & Goodman 1992). To test whether Connectin also has a function in the targeting of Or47a ORNs, the hypomorph allele *con^{Fvex238}* and a UAS-conRNAi construct were tested for defects in the olfactory system. The innervation of Or47a was visualized via a synaptic localized GFP under the control of Or47a Gal4.

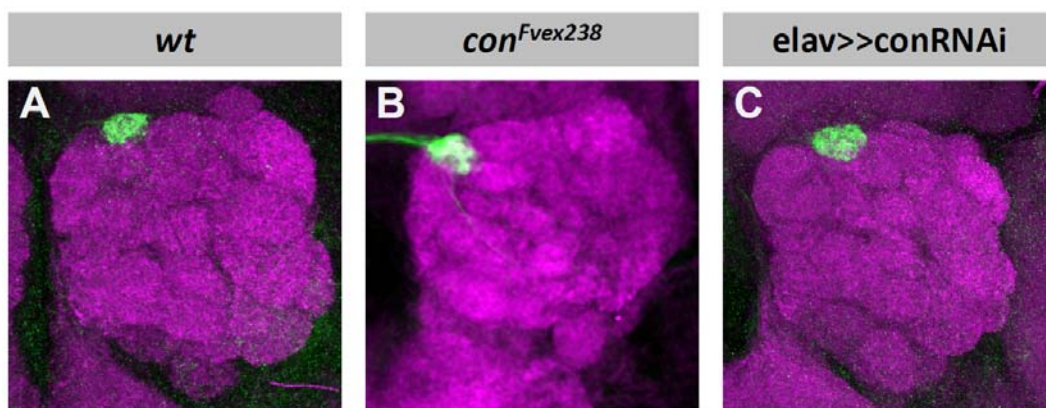


Figure 38– Loss of Con function does not affect ORN targeting

(A) In the wildtype the innervation of Or47a neurons is restricted to the DM3 glomerulus. (B) Flies homozygous for the allele *Con^{Fvex238}* do not show changes in the Or47a innervation pattern. (C) Knock-down of Con via RNAi in the nervous system does not affect OR47a targeting. Genotypes: (A) FRT42 Or47a:sytGFP, (B) FRT42 Or47a:sytGFP; *Con^{Fvex238}*^{-/-}, (C) *elavGal4*; FRT42 Or47a:syt UAS-conRNAi. Or47a expression is labeled with α -GFP (green), neuropil with α -ncad (magenta).

The Con^{Fvex238} allele is viable and fertile; therefore the analysis was performed in homozygous animals. No effect on Or47a targeting can be observed, but the overall glomerular structure seems less sharp than in the wild type (Figure 38 B).

Elav driven knock down of Con via RNAi also does not affect the innervation of Or47a axons, in this experiment also the glomerular boundaries are not affected (Figure 38 C).

Since Con is not expressed in Or47a neurons this results are not unexpected. However, previous experiments had shown that the loss of Con function in other ORN classes also does not lead to alterations of the connection pattern in other classes that endogenously express Con (Or47b and Or88a) (Sieglitz, 2007), indicating that Con is not essential for pathfinding in the olfactory system.

3.6.6 Knock down in *dark* mutant ORNs rescues the mis-targeting phenotype

The ectopic expression of Con in the mis-projecting Or47a neurons in *dark*^{verpeilt} raises the question whether this has an influence on the targeting of these neurons. To answer this question Con was knocked down only in homozygous mutant *dark*^{V8} ORNs via RNAi.

Similar to the previous experiment, knock down of Con in MARCM clones had no effect on the targeting of Or47a axons in the wild type control (Figure 39 A). Expression of the RNAi construct in *dark*^{V8} homozygous mutant ORNs is able to suppress the ORN mis-targeting in about 50% of the observed cases (Figure 39 C). Even when the mis-targeting is not completely abolished the morphology of the ectopic glomerulus is affected in half of the brains showing this phenotype. Often the lateral innervation is smaller, split into two structures or elongated in a medial direction (Figure 39 D).

These data indicate an influence of Con in the mis-targeting of Or47a neurons in *dark*^{V8} mutants.

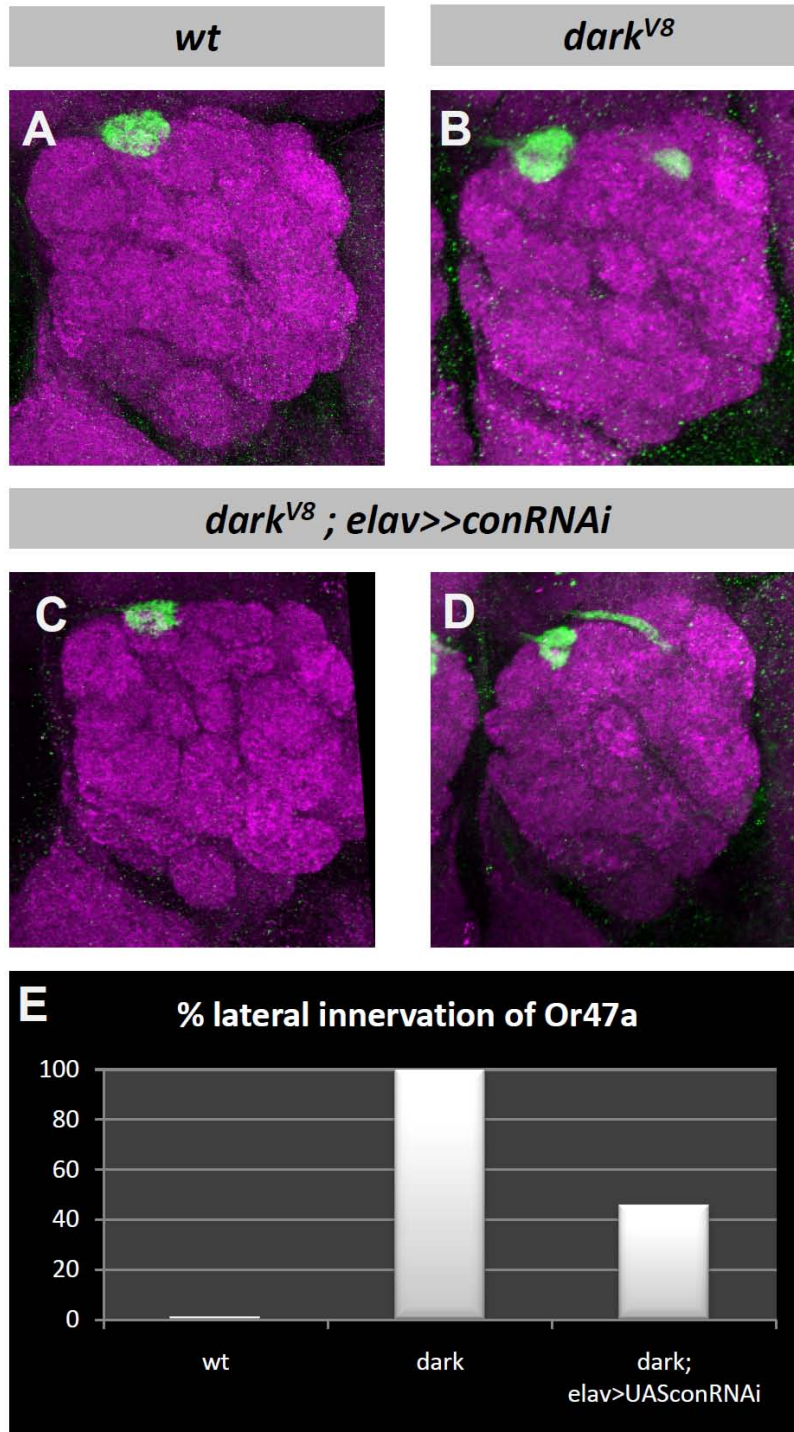


Figure 39 – Knock down of *Con* in *dark^{V8}* homozygous ORNs represses mis-targeting

(A, B) Projections of Or47a neurons in wildtype and *dark^{V8}* MARCM clones. (C, D) Knock down of *Con* via *elavGal4* driven RNAi in *dark^{V8}* MARCM clones. In some cases this leads to a complete suppression of ORN mis-targeting (C), in other cases only to morphological changes of the ectopic glomerulus (D). The percentage of complete rescues is quantified in (E). Genotypes: (A) *eyFLP*; *FRT42 Or47a:sytGFP /FRT42 Gal80*; (B) *eyFLP*; *FRT42 dark^{V8} Or47a:sytGFP /FRT42 Gal80*, (C,D) *eyFLP elavGal4*; *FRT42 Or47a:syt UAS-conRNAi/FRT42 Gal80*. Or47a expression is labeled with α -GFP (green), neuropil with α -ncad (magenta).

3.6.7 Con over-expression in 47aORNs does not affect OR47a targeting

To analyze a putative instructive role for Con in directing *dark*^{V8} mutant ORNs to a lateral target Con was over-expressed in wild type and *dark*^{V8} mutants to test whether this is sufficient to redirect the axons to the lateral AL.

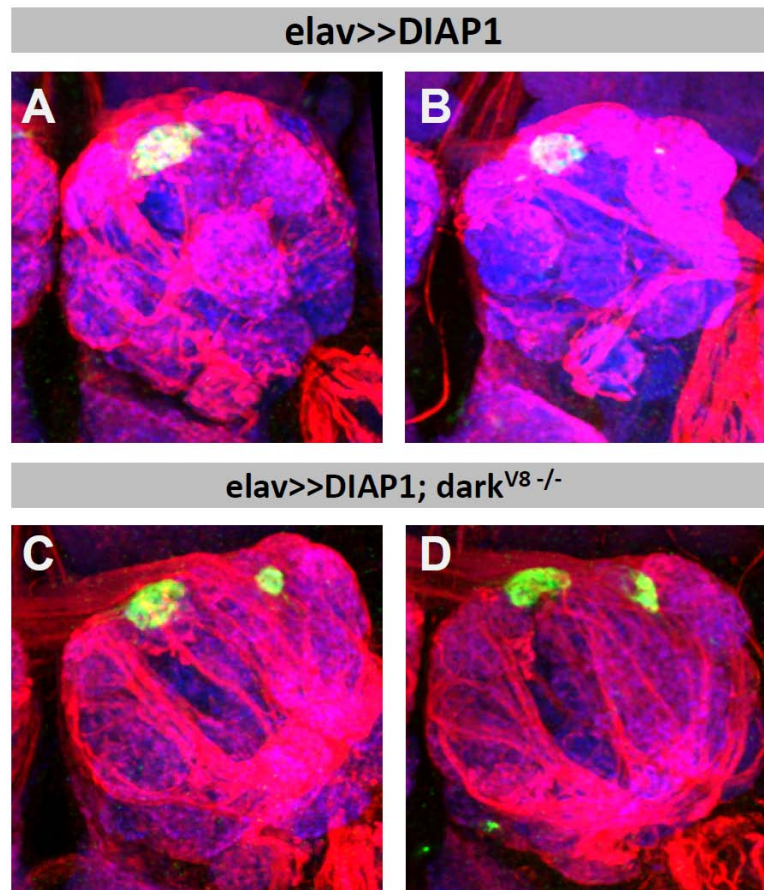


Figure 40 – Over-expression of Con in MARCM clones does not affect OR47a target specificity

(A, B) Over-expression of Con in wild type MARCM clones. The innervation of Or47a axons is restricted to the DM3 glomerulus, though the pattern of the in-growing ORN axons does not correlate to projection domains. (C, D) Over-expression of Con in *dark*^{V8} MARCM clones does not change the number of neurons projecting to the ectopic glomerulus. The pattern of in-growing ORNs is similarly disturbed as in *dark*^{V8} clones without over-expression of Con. Genotypes: (A,B) eyFLP elav Gal4; FRT42 Or47a:sytGFP /FRT42 Gal80; UAS-Con, (C,D) eyFLP elav Gal4; FRT42 *dark*^{V8} Or47a:sytGFP /FRT42 Gal80; UAS-Con. OR47a expression is visualized with α -GFP (green), Con expression with α -Con (red), neuropil is stained with α -ncad (blue).

Con mis-expression in eyFLP induced MARCM clones has no effect on the targeting of the Or47a neurons. However, the domain organization of ORN axons is disturbed and less ordered in neurons mis-expressing con compared to the wild type (Figure 40A, B; compare Figure 23)

Over-expression of Con in *dark*^{V8} homozygous ORNs does not lead to the projection of more Or47a axons to a lateral target. Both the innervations of the DM3 and the lateral glomerulus are unchanged compared to the wild type (Figure 40C, D).

These results suggest that Con alone is not sufficient to alter Or47a targeting, though it appears to have an effect on the general domain organization in the olfactory system.

3.6.8 Over expression of Con in PNs leads to changes in ectopic Or47a target specificity

Most of the Con expressing ORN classes, projecting to the dorso-lateral AL, innervate glomeruli of which the PNs also express Con. The only exceptions in this area of the antennal lobe are the glomeruli innervated by the ORN classes Or49a and Or23a, in which Con is only found in the pre-synaptic neurons. Since Or47a does not express Con at all it was analyzed whether the absence of Con in PN dendrites provides a crucial targeting clue that allows the integration of Or47a synapses in the DA3 glomerulus.

When over-expressed in PNs, again using the GH146Gal4 driver in eyFLP induced clones, no changes in the innervation of the DM3 glomerulus can be observed in the wild type (Figure 42 A). In contrast, over-expression in PNs causes *dark*^{V8} mutant ORNs to avoid the lateral target (Figure 41 B). This effect is not always equally strong. In some rare cases the lateral glomerulus disappears almost completely, in the majority of the brains observed some Or47a axons still target the dorso-lateral AL, but the innervation is reduced. Sometimes a split of the ectopic glomerulus can be observed, leading to two unconnected structures. Frequently the morphology of the lateral glomerulus is altered, exhibiting a medial elongation that sometimes reaches the DM3 glomerulus, resulting in a continuous Or47a innervation spanning across the dorsal AL (Figure 41 C, D).

From this it can be concluded that the Con expression in the PNs is involved in the target specificity of mis-projecting Or47a axons in *dark*^{V8} mutants.

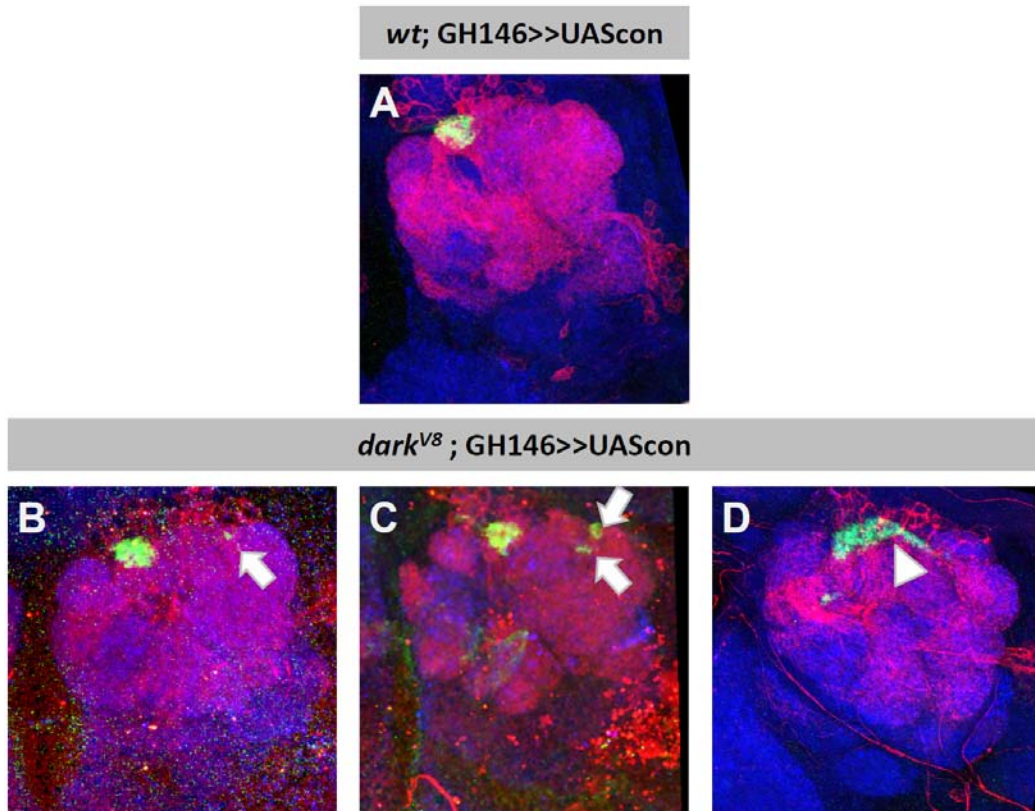


Figure 41 – Mis-expression of Con in PNs changes target specificity of lateral projecting Or47a neurons in *dark^{V8}*

(A) Mis-expression of Con in PNs via GH146Gal4 does not affect Or47a axon targeting in wild type clones. The innervation remains restricted to the DM3 glomerulus. (B-D) In a mutant *dark^{V8}* clonal background overexpression of Con in PNs reduces lateral targeting of Or47a neurons. In some cases the lateral glomerulus is severely reduced (B, arrow), in others split in two parts (C, arrows), or it loses its glomerular shape and extends towards the DM3 region (D, arrowhead). Genotypes: (A) eyFLP, FRT42 Or47a:sytGFP/FRT42, GH146Gal4 UAS-Con, (B-D) eyFLP, FRT42 *dark^{V8}* Or47a:sytGFP/FRT42, GH146Gal4 UAS-Con. OR47a expression is visualized with α -GFP (green), PNs are stained with α -CD2 (red), neuropil is stained with α -ncad (blue).

4 Discussion

The scope of this project was the molecular mechanism underlying the specific targeting of olfactory receptor neurons in *Drosophila*. The study was based on the mutant *verpeilt* that causes a stereotypic mis-targeting phenotype of olfactory sensory neurons. Using different approaches, the *verpeilt* mutant could be mapped to the gene *dark* (*Drosophila apaf1-related-killer*), an apoptosis promoting factor. In the subsequent analysis, the role of *dark* in axon targeting was determined.

4.1 Mapping of the *verpeilt* mutations to the *dark* gene

The first approach to narrow down the genomic region containing the *verpeilt* mutations was a complementation analysis against a set of deficiencies covering almost the whole right arm of the second chromosome. This method allows a rough mapping of the *verpeilt* lethality to the cytological region 53D14 to 53F8. Within this region of interest, several lethal P-element insertions for complementation of the *verpeilt* lethality were tested.

Since none of the pre-existing P-elements seems to affect the *verpeilt* locus new insertions that disrupt the *verpeilt* gene affected were created by P-element remobilization. In total three new P-element insertions were generated that failed to complement the *verpeilt* lethality. Mapping via inverse PCR revealed that all three insertions were located at different cytological positions, two of which are even outside the region determined by the previous complementation analysis against the deficiencies. These *verpeilt* alleles caused an additional lethality uncovered by adjacent deficiencies that are able to complement the *verpeilt* alleles. Therefore it is unlikely that the new insertions of the P-element all affect the same gene, but induce a second lethality at the integration site additional to the *verpeilt* lethality within the pre-defined region. There are several explanations for this finding. The P-elements could have inserted in a regulatory region that affects the transcription of the gene affected in *verpeilt*. These regions can be rather distant from the actual coding sequence, therefore not giving a direct hint which gene is disrupted by the *verpeilt* mutations. In addition the excision process during the mobilization of a P-element is not always precise, frequently certain parts of the insertion remain at the previous insertion site or neighboring genomic sequences are disrupted in this process (Gray, Tanaka & Sved 2006). Also, during

the mobilization event P-elements sometimes get duplicated or get integrated in the genome but remobilized immediately and then insert somewhere else (Hiesinger & Bellen 2004).

Analysis of the initial P-element insertion sites could not detect any deletion or additional bases in the previous location of the P-element, indicating no imprecise excision was induced during the mobilization.

In case the new insertions affect a regulatory precise removal of the insertion should reverse the lethality. To test this, the P-elements in their new locations were mobilized again and analyzed for their ability to rescue lethality. For both insertions locating next to the deficiency that uncovers the *verpeilt* locus, the additional lethality could be reversed, but these alleles still failed to complement *verpeilt*.

This indicates a “hit and run” event (Hiesinger & Bellen 2004; Salzberg et al. 1997). The P-element might have inserted in the *verpeilt* gene, but then got translocated to its final position. These results prevent to determine the location of the *verpeilt* gene. Even more puzzling, a phenotypic analysis of the created P-elements revealed no defect in Or47a-targeting, indicating that the lethality and the phenotype might not be correlated. At this point this approach failed to identify the location of the *verpeilt* locus.

The region pre-determined during the complementation against the deficiencies still spans over 110 kb and contains about 40 annotated genes. To restrict the number of candidate genes further small, defined deficiencies were created using FRT containing piggyBac insertions (Parks et al. 2004). Three independent deletions were established, combinatorial complementation analysis led to a set of eleven candidate genes.

To confirm these data a meiotic recombination approach was performed. According to the recombination frequency of a dominant marker, (*white*⁺ P-element in a *white* background) the meiotic position of the *verpeilt* lethality can be determined (Zhai et al. 2003). The results of this experiment put the locus of the mutation close to the cytologic region 53E4. Though this method allows restricting the location of a given lethality to a small region, it is not sufficient to identify the gene affected directly.

The eleven candidate genes were then sequenced, leading to the identification of independent base-pair exchanges in the *dark* gene in all *verpeilt* alleles (Niehues 2008).

4.2 Phenotypic implications

The phenotype of the *verpeilt* mutant is characterized by two defects in olfactory targeting. The ORN axons lose their global segregation in the AL while projecting to their target glomeruli. Instead they grow all over the AL surface, but most ORN classes eventually reach their designated target and form regular glomeruli. The more prominent phenotype in *verpeilt* mutant is the ectopic targeting of ORN classes to ectopic glomeruli. In contrast to other ORN targeting mutants (Hummel et al. 2003), in *verpeilt* the newly formed glomeruli are localized at stereotype positions and show little variations among different individuals.

4.3 Projection domains

Olfactory sensory neurons in insects and vertebrates have been described to segregate in distinct projection domains when entering their CNS target area (Vassar, Ngai & Axel 1993; Satoda et al. 1995; Tolbert et al. 2004). In the mouse olfactory system it has been shown that the olfactory epithelium is subdivided in four major zones defined by the type of ORs expressed. More homologue ORs tend to be expressed by neurons located in the same zone. This zonal organization is also maintained in the olfactory bulb (Yoshihara et al. 1997; Mori 1999). The mechanisms of the determination of the zonal projection domains have not been identified yet. It has been suggested that different expression levels of the olfactory cell adhesion molecule (OCAM), which is a homologue of N-Cad, could serve this function (Mori 1999; Chehrehasa et al. 2005). Intriguingly, a knock-out of OCAM does not affect the zonal projection but rather disrupts the inter-glomerular organization (Walz et al. 2006a; Mombaerts, 2006). Whether there are similar molecules that are able to compensate for a loss of OCAM remains elusive.

4.3.1 In-growing ORN axons sort out in projection domains in *Drosophila*

These investigations showed a similar zonal organization of the ingrowing ORN axons in *Drosophila*. Four major axonal projection domains could be distinguished, a dorso-lateral, a central, a ventro-medial and a posterior domain. ORNs of a given class usually project their axons mainly within one of these projection domains, though frequently single axons were

observed that sheered out and used an alternative route to the target glomerulus. In the antennal sensory epithelium, trichoid sensilla are mainly found in continuous area at the distal part of the antenna (Couto, Alenius & Dickson 2005). The ORNs housed in these sensilla type have been implicated to be involved in pheromone detection (Benton, Vannice & Vosshall 2007). Most ORNs from these sensilla project their axons along the dorso-lateral domain and innervate glomeruli in the dorsal part of the AL that form a continuous cluster. Similarly, glomeruli innervated by ORNs basiconic sensilla agglomerate in the medial and ventral area of the AL (Couto, Alenius & Dickson 2005).

In *dark^{verpeilt}* mutants these projection domains are disturbed, especially the dorso-ventral and the central domain appear to be fused. Changes of the projection routes are detectable in multiple ORN classes e.g. Or22a neurons leave their preferred ventro medial projection domain and approach their target glomerulus DM2 from more dorsal and even posterior directions. Except for the classes Or43a, Or47a and Or67a this does not cause an innervation at ectopic positions of these axons.

4.3.2 Domain organization is not sufficient for precise ORN targeting

A hypothesis for the formation of the ectopic Or47a glomerulus in *dark^{verpeilt}* was that the mis-guidance of Or47a axons to the dorso-lateral domain could lead them to an alternative target at which they terminate and form synapses. Bhalerao et al. reported that some ORN classes in *Drosophila* have secondary targets besides their primary glomerulus (Bhalerao et al. 2003). They described two alternative targets Or47a neurons, one in the ventro-medial region and the other in the dorso-lateral AL, at a corresponding region as the ectopic glomerulus found in *dark^{verpeilt}* mutants. A hypothesis to explain the phenotypes in *dark^{verpeilt}* could be that by the disruption of the wild type axonal projection domains some axons get guided to a secondary target, thus explaining the spatial specificity of the ectopic innervations found in this mutant. However, this appears not to be the only reason for the phenotype because of two findings. First, single lateral projecting OR47a axons are also found in 16% of the wild type ALs examined, without showing ectopic innervations. This might be due to a requirement of a certain amount of axons required to stabilize this ectopic innervations. However, the second evidence rules out this possibility: in a *dark^{verpeilt}* mutant background a significant amount of wild type ORN axons projects along the dorso-lateral

domain, but they do not innervate the ectopic glomerulus though enough mutant ORNs are present to exceed a putative critical amount. In addition, the secondary targets described by Bhalerao et al., 2003, never appeared in the control brains.

These results indicate that the domain organization is not sufficient to prevent axons from mis-targeting and has only a supportive function in ORN targeting.

Another hypothesis for the formation of the ectopic glomerulus was a defect in contra-lateral projection. The mechanisms that guide a secondary axonal branch across the commissure are unknown. A defect of target recognition on the contralateral side could cause a mis-targeting only in the opposite hemisphere of the AL. To investigate this possibility unilateral antennal ablations were performed and the contra-lateral projection behavior of the remaining ORNs analyzed. Not only is the ectopic glomerulus present in the contra-lateral AL, it also gets innervated on the ipsi-lateral side. The ingrowing ORNs completely ignore the DM3 glomerulus and form a separate branch across the commissure, ruling out the idea of defective contra-lateral projections.

4.4 ORN targeting requires *dark* function only in some ORN classes

To better understand the defects in the olfactory system caused by the *dark*^{*verpeilt*} mutations a detailed phenotypic analysis was performed. It could be shown that 6 of the 25 analyzed classes are affected in their choice of the projection domain. Compared to the rather disturbed appearance of the innervation pattern of all neurons when labeled with an Or83b driven axonal marker this number seems a little low. This might be due to the fact that only half of the 50 ORN classes were tested in the single class analysis; the remaining ones might also show defects in projection route choice.

In addition three ORN classes mis-target in *dark*^{*verpeilt*} mutants. All affected classes target to glomeruli in the dorsal half of the AL. In Or67d neurons the glomerular boundaries of the DM6 are extended to the lateral AL, reaching almost to the area of the ectopic glomerulus innervated by OR47a neurons. Or43a neurons innervate an additional position close to the entry point of the antennal nerve, Or47a neurons project to an additional target in the dorso-lateral AL close to the DA3 glomerulus.

The affected ORNs are all housed in different sensilla, Or43a in the trichoid sensillum at3, Or47a in the basiconic ab5 and Or67a in the basiconic ab10 sensillum. In none of the cases the other neurons housed in the same sensillum showed either projection or targeting defects. Interestingly the Or43a uses the dorso-lateral projection domain on the way to their target, again supporting the idea that a shift of projection is not the only reason for mistargeting of ORNs in *dark^{verpeilt}* mutants.

These results also indicate a specific requirement of *dark* only in few ORN classes.

4.4.1 The *dark^{verpeilt}* induced targeting phenotype is cell autonomous

In eyFLP induced *dark* mutant MARCM clones still innervate in both glomeruli of Or47a axons is observed. A defective *dark* function is thus not instructive for mis-targeting. Axonal intra-class communication could account for this effect. Homozygous mutant ORNs might communicate with their wild type counterparts which compensate for the lack of innate target information.

In a “reverse MARCM” experiment no innervation of the lateral glomerulus by wild type Or47a neurons occurs. Interestingly, the axons are widely spread over the AL and no longer restricted to the central projection domain. This suggests that there indeed is an axonal intra-class interaction between the different Or47a populations. Homozygous mutant axons might recruit wild type axons to project in the dorso-lateral domain, though this is not sufficient to induce ectopic targeting of wild type axons. Therefore the phenotype can be divided in a cell autonomous component responsible for the ectopic targeting and a non autonomous part that via axon-axon interactions lead to an altered choice of the projection domain.

The subgroup of homozygous mutant ORNs that innervates the DM3 glomerulus integrates normally in the DM3 glomerulus and intermingles with wild type ORNs. Within the glomerulus no sub-fractionation takes place. Apart from the unordered projection pattern these homozygous mutant neurons behave like the wild type which indicates a differential effect of *dark^{verpeilt}* on subpopulations of Or47a neurons.

To determine whether a critical amount is needed for a stabilization of the ectopic glomerulus small *dark^{verpeilt}* clones were induced and analyzed for the number of axons that

innervate in the dorso-lateral AL. Axon termini could only be observed in clones containing at least eight cells, in all these cases at least two axons contributed to the ectopic structure. However, the results are not conclusive. Since the number of the mutant ORNs that innervate the ectopic glomerulus in eyFLP induced clones could not be determined due to resolution limitations of confocal microscopy, and homozygous mutant ORNs also innervate the DM3 glomerulus the obtained results might not be representative. In addition, dependent on the time of the heatshock different sub populations of OR47a neurons might be affected that respond differently to the change in *dark* function.

4.4.2 *Dark^{verpeilt}* affects ORN projection identity

An important characteristic of glomerular innervations is the segregation from other classes and the restriction to one glomerulus. The ability to sort out from other classes is not defective in the ectopic projecting *dark^{verpeilt}* mutant neurons. The analysis of the neuronal interactions within the glomerulus reveals that the ectopic projecting ORNs in *dark^{verpeilt}* mutants do interact with PN dendrites. Furthermore this innervation is specific to PNs that also appear to get innervated by Or23a neurons in the wild type.

Taken together the results of the phenotypic analysis of the ectopic glomerulus show that the mis-targeting axons maintain the main glomerular features, they are able to converge to a dense glomerulus, sort out from other classes, innervate the equivalent glomerulus on the contra-lateral hemisphere of the AL and interact with PNs. Only the projection towards the target is changed and the mutants lose their synaptic specificity and build synapses with class unspecific dendrites.

This implicates a change in the neuronal projection identity. It has been shown in the mouse olfactory system, that subtle changes in the OR gene could affect targeting choice (Feinstein & Mombaerts 2004). The smaller the changes are the lesser changes in target choice were observed. ORs that differed only in a few amino acids actually innervated the same glomerulus, but within its borders, the different subpopulations sorted out from each other. A very similar phenotype is found for the DA3 glomerulus, except that the two ORN classes are not very close related (Couto, Alenius & Dickson 2005). However, *dark^{verpeilt}* could cause a shift of the neuronal identity from Or47a to Or23a. A hint for this is present in the fact that the mis-projecting ORNs ectopically express Connectin (see below).

4.5 Impacts of apoptosis on ORN targeting

The *dark* gene encodes a pro-apoptotic factor and required for most, but not all programmed cell death in *Drosophila* (Mills et al. 2006). Apoptosis is a conserved mechanism involved in many developmental processes for the selective removal of cells. A sophisticated mechanism is needed to kill just the right cells and not affect neighboring tissues. The actual execution is performed by a specific set of cysteinyl aspartate specific proteases, called caspases, which cleave specific substrates, and induce activation of a nuclease that cuts DNA. This process has to be tightly regulated to avoid killing cells by accident. Therefore, the activation of caspases is of crucial importance and needs to be controlled precisely to avoid collateral damage. The basic mechanism of apoptosis is evolutionary conserved though and found in all higher animals from *C. elegans* to vertebrates (Feinstein-Rotkopf & Arama 2009).

In *C. elegans*, the process of programmed cell death rather simple with only four key components involved (Vaux & Korsmeyer, 1999). An external stimulus activates the EGL1 protein which antagonizes the inhibitory factor CED-9. CED-9 forms a complex with the pro-apoptotic factor CED-4, upon binding of EGL1 CED-4 is released from this complex. Free CED-4 oligomerizes and serves as a scaffold for the auto-activation of CED-3, the only caspase in *C. elegans* (Peden, Killian & Xue 2008).

In vertebrates this process is more diverse (Kumar, 2007). The apoptosis machinery involves at least nine different initiator caspases and four effector caspases. Four activation complexes have been identified, the apoptosome, containing the CED-4 homologue Apaf-1, the death inducing signaling complex (DISC), the inflammasomes and the PIDDosome, each is activating a specific effector caspase (Duan & Dixit 1997). The regulation and function of the complexes is highly specific, depending on different death inducing stimuli. The apoptosome for example is activated upon release of mitochondrial cytochrome C, while the DISC complex is sensitive to the activation of death receptors (reviewed by Yi & Yuan, 2009).

The mechanism of apoptosis in *Drosophila* is shown in Figure 42. *Drosophila* has three major caspases, the initiator caspase DRONC, a homologue of the vertebrate caspase9, the effector caspase DrICE, a homologue of caspase3 and another effector caspase called Dcp-1. DRONC and DrICE, similar to the vertebrate system, initially are expressed as a pro-caspase that needs additional processing to get activated. The inactive DRONC monomer has been

described to homodimerize and subsequently auto-activate itself. However, this auto-activation is enhanced by binding to the pro-apoptotic factor *Dark*, the homologue of CED-4/Apaf-1 (Snipas et al. 2008). The *Dark*-DRONC complex is also called the apoptosome and can also interact with the pro-

caspace3 and lead to its activation, thereby promoting apoptosis. But in contrast to the vertebrate system, *Dark* and DRONC are expressed constantly in *Drosophila*, together with the *Drosophila* inhibitor of apoptosis protein 1 (DIAP1, Adams & Cory, 2002). DIAP1 binds to the apoptosome after the *dark* mediated auto-activation of *dark*. This leads to a cleavage of the C-terminus of *dark* by DRONC, followed by a degradation of the apoptosome-complex and finally leading to a degradation of the active DRONC

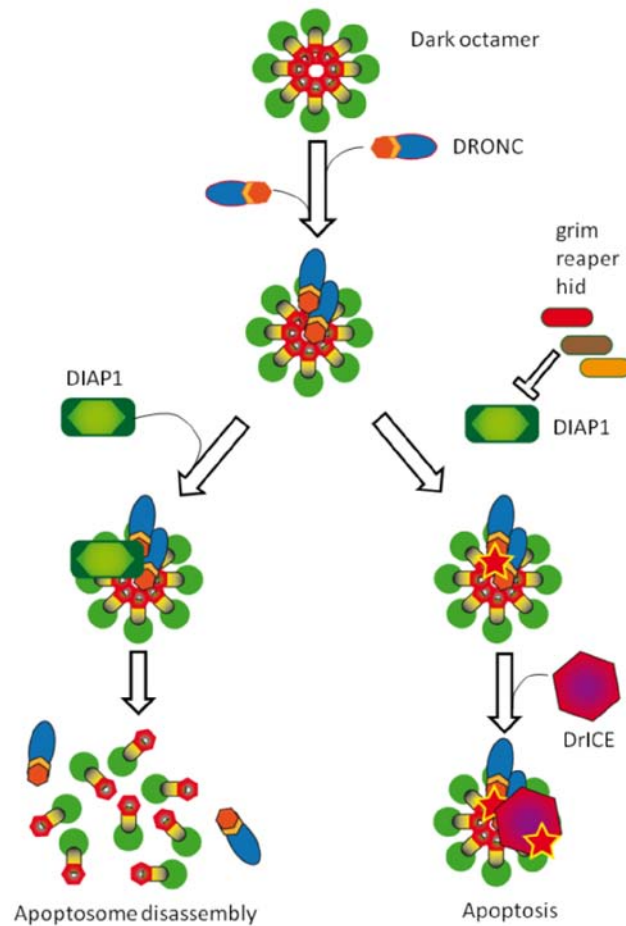


Figure 42 – The *Drosophila* apoptosis pathway

The *Drosophila* apoptosome is build of a *dark* octamer that can bind DRONC, supporting ist dimerization and auto activation. After binding of DRONC DIAP1 is recruited to the apoptosome, leading to its degeneration. If the pro-apoptotic factors grim reaper and hid are also expressed, they block DIAP1 function, the apoptosome can bind DrICE which in turn gets activated by DRONC leading to apoptosis. accumulation of active DRONC and subsequent activation of the effector caspase DrICE. In contrast to the vertebrate system, the role of cytochrome c in apoptosome activation remains elusive (Arama et al. 2005; Yu et al. 2006).

In order to promote activation of the pro-caspase DRONC the *Dark* protein forms an octameric ring with the CARD domain pointing inwards. In vitro the formation of this structure can be induced by addition of dATP to a pool of monomeric *Dark*. However, a large excess was required, indicating the requirement of a second activator that promotes *Dark* octamer formation. In contrast to the vertebrate apoptosome formed by Apaf-1 cytochrome-c appears not to be required for this process in *Drosophila*. The WD repeats assemble in the outer ring of the apoptosome and regulate the activity of the complex. A deletion of the WD domain is described to stimulate the promotion of cell death (Rodriguez et al., 1999; Yu et al. 2006).

The *dark*^{verpeilt} alleles found in the ORN targeting screen affect apoptosis similar to the alleles previously described (Mills et al. 2006; Srivastava et al. 2006). In a GheF assay, the rescue of hid induced apoptosis in *dark*^{verpeilt} alleles looked even slightly better than in a defined null allele of *dark*. In this experiment the eyes of *dark* null mutants are restored almost to their full size, but the typical honeycomb-like structure is lost resulting in a slightly rough appearance. This is probably caused by a lack of apoptosis in interommatidial cells which in the wild type are removed via programmed cell death during pupal development (Brachmann & Cagan, 2003). In *dark*^{verpeilt} mutants the ommatidial pattern appears less affected, the structure of the eye is more regular. This indicates a differential influence of this allele in regulating apoptosis. To further investigate this effect it would be necessary to perform an ultra-structural analysis of the eye to determine the difference in cell types and comparison of these with the wild type and *dark* null situation.

The effect on apoptosis could explain the phenotype in the olfactory system. One could imagine that due to the lack of apoptosis more ORNs are generated in the developing antenna. These neurons might then target to an ectopic position in the AL, resulting in an extra glomerulus as found in *verpeilt* mutants.

4.5.1 Lack of apoptosis does not cause ORN mis-targeting

To test this hypothesis the number of two ORN classes in the antenna was quantified. Neither for the Or 47a class nor for the Or23a class significant changes could be observed. Therefore the ectopic targeting observed in *dark*^{V8} clones is not caused by additional neurons due to less apoptosis.

A second possibility would be that another population of cells is affected in *dark* mutants, which has a guiding function to direct the ORN axons to their target glomeruli. To test this hypothesis apoptosis was artificially blocked in a *dark* independent manner by over-expression of downstream components of the cell death pathway. None of the tested components was able to induce ORN mis-targeting. Loss of apoptosis is therefore unlikely to cause the phenotype in the *dark^{verpeilt}* alleles, although, effects of the driver cannot be excluded. The defective targeting of Or47a is therefore most likely independent of programmed cell death.

However, caspase activation does not always lead to cell death and several non-apoptotic processes have been described in which local Caspase activity is required. This involves, among others processes, border cell migration, sperm individualization, arista development and dendrite pruning (Kuranaga & Miura 2007). The pruning process in refining dendrites requires the local activation of the caspase pathway. General over-expression of hid, a pro-apoptotic factor lead to cell death, while suppression of caspase function strongly suppresses pruning. This indicates that caspase activity is restricted locally only to branches that need to be removed, which is also confirmed by staining sensitive to a cleaved caspase substrate (Williams et al. 2006).

A similar mechanism could be imagined to be required in ORNs to remove temporary axon branches that target to atypical glomeruli in the AL during development. It has been described that ORN targeting is refined in the olfactory system of the mouse, after initially targeting to multiple glomeruli the innervation of a given class gets later restricted to one target (Zou et al. 2004). A comparable mechanism has not been described in *Drosophila* so far. Also, the suppression of caspase function via expression of DIAP1 or p35 should affect also local processes. This points to not only to an apoptosis- but also caspase-independent mechanism of *dark* in governing ORN targeting.

4.5.2 The ORN-mis-targeting phenotype is allele specific

To investigate the requirement of the different domains within the *Dark* protein in total 20 independent alleles were tested for their influence on the size or morphology of the ectopic glomerulus formed by OR47a axons. In about half of the alleles tested no axon targeting phenotype occurs, including the defined null allele *dark⁸²*. The induction of ORN mis-targeting does not correlate with a specific domain affected in the mutants. Mutations in the

CED4/Nod domain, the WD40 repeats and in the C-terminal domain, for each in about 50% an ectopic glomerulus is induced while the other half of the alleles shows no or only a mild phenotype in the olfactory system. For the Card domain and the HD2 domain only one allele was available respectively, therefore no conclusion can be made. The ORN mistargeting phenotype is also not dependent on nature of the allele since ORN mistargeting is found in alleles carrying a premature stop codon and mis-sense mutations.

Furthermore, the ability of the *verpeilt* alleles to suppress *hid* induced apoptosis in a Ghf assay is not related to the induction of ORN mis-targeting. Alleles that have a strong effect on apoptosis, like the null allele *dark*⁸² do not cause ectopic innervations in the olfactory system. Conversely, alleles that have little impact on apoptosis suppression, like the alleles *dark*^{M20} or *dark*^{N10}, also do not cause ORN mis-targeting, with the exception of the allele *dark*^{B2}. Weak *dark* alleles having only minor effects on apoptosis and no effect on ORN targeting contain mutations in different domains, therefore no correlation between domain requirement and allele strength can be made.

Interestingly, comparison of the degree of suppression of *hid* induced apoptosis revealed that in the *dark*^{V8} allele the overall arrangement resembled more or less the wildtype phenotype, while in *dark*⁸² allele only the size of the eye is restored, but the eye itself looks less regular than the wildtype. Since the regular pattern of the ommatidia is dependent on the apoptosis mediated removal of interommatidial cells (Cordero et al. 2004), these results indicate a altered function of *dark*^{V8} in suppression of *hid* induced apoptosis.

Again these results confirm that the ORN mis-targeting defects is independent of apoptosis in *dark*^{verpeilt} mutants. Also, this could explain why no phenocopy of the ORN mis-targeting defect was observed for the P-insertions created during the “local hop” mapping approach.

Most *dark* trans-combinations lead to lethality. However, three alleles, *dark*^{M20}, *dark*^{N10} and *dark*^{N5} are sufficient to rescue to viability in trans to other *dark* alleles. None of these alleles shows an ORN mis-targeting phenotype in eyFLP induced mitotic clones, suggesting these are rather weak alleles. However, in trans to the *dark*^{V8} allele *dark*^{M20} and *dark*^{N10} display an ectopic Or47a glomerulus as seen in mitotic clones of *dark*^{verpeilt}.

The trans combination *dark*^{N5}/*dark*^{V8} is viable and does not lead to mis-targeting in the olfactory system. *Dark*^{N5} contains an amino acid exchange at position 977 within the WD

repeats. The WD repeats are thought to regulate the apoptosis promoting activity of *dark*. Changes of the structure of this domain might lead to a decrease in apoptosome formation, but lead to an increase in DRONC activation, sufficient to rescue of the lethality in *dark*^{V8}/*dark*^{N5} trans-animals.

Both alleles, *dark*^{M20} and *dark*^{N10}, affect the CED4/NOD domain indicating a requirement of this domain for ORN targeting. The CED4/NOD domain has been implicated in *dark* oligomerization. Defects in this domain may affect the formation of the apoptosome but not its function. In case of the trans situation, the intact CED4/NOD domain of the *dark*^{V8} allele might be sufficient to induce a heteromeric octamer consisting of the mutant isoforms. This could be sufficient to induce apoptosis thus rescuing the lethality. Such a heteromeric apoptosome might lack the ability to process a certain component required for correct ORN targeting.

This raises the question by which mechanism the *dark*^{verpeilt} mutations induce the formation of the ectopic glomerulus. Since the absence of *dark* in the null allele *dark*⁸² is not affecting ORN targeting it is unlikely that the mis-targeting is dependent on the function of *dark* itself. This suggests a novel, apoptosis independent function of *dark* in ORN targeting.

The different mutations in the *dark* gene analyzed in this thesis may have different effects on the formation of the apoptosome. Mutations that do not affect ORN targeting might abolish the oligomerization at all due to conformational changes, therefore leading to a loss of function phenotype concerning apoptosis, but do not affect ORN targeting, as observed for *dark*⁸². In *dark*^{verpeilt} alleles oligomerization might still take place, but affect the function of the apoptosome, impairing binding or processing of complex components, thus leading to defects in ORN targeting.

4.5.3 The *dark*^{verpeilt} mutations show dominant negative properties

Over-expression of wild type *dark* is not sufficient to rescue the lethality of the *dark*^{verpeilt} alleles. This could point to a dominant negative function of the *dark*^{verpeilt} mutations. One scenario would be that the mutant apoptosome cannot be cleaved at its C-terminal domain due to truncations or misfolding of the *Dark* protein. This could lead to an impaired disassembly of the apoptosome. In case this hypothetical complex would still retain its ability to bind to DRONC, this could lead to a decrease of free DRONC that can be processed by the

apoptosome built of wild type *dark*. Another possibility would be a hetero-oligomerization of wild type and mutant *dark* protein that has a decreased apoptotic activity.

Wild type *dark* is also not able to rescue the mis-targeting phenotype when expressed in eyFLP induced *dark*^{V8} mutant clones. Since the function of *dark* in ORN targeting appears to be apoptosis independent this finding supports the hypothesis of a hetero-oligomerisation of wild type and *dark*^{V8} proteins.

Interestingly the over-expression of a hypermorphic mutation of *dark*, *dark*^V is able to suppress both the lethality and the formation of the ectopic glomerulus in *dark*^{verpeilt}. In *dark*^V the DRONC cleavage site in the C-terminal domain is mutated from Aspartate to Alanin thereby preventing processing of *dark* by DRONC. In combination with *dark*^{V8} the *dark*^V isoform might be able to stabilize the defective hetero-octamer thus regaining its properties in activating DRONC and other substrates.

Another unsolved issue is the mechanism by which *dark*^{verpeilt} induces lateral targeting of Or47a neurons. This is especially puzzling since no ectopic glomerulus is found in *dark* null mutants, arguing against a simple loss of function phenotype. One hypothesis, based on the assumption of a defective apoptosome, that this complex titrates out a factor required for the prevention of lateral targeting of Or47a neurons. A candidate was DIAP1, since it is known that it is involved in non-apoptotic processes including actin cytoskeleton organization (Kuranaga et al. 2006). DIAP1 could be required for the degradation of a guidance cue directing Or47a to the dorso-lateral AL via its ubiquitin ligase domain. This process could be apoptosome independent. In *dark*^{verpeilt} mutants, DIAP1 could be recruited to the apoptosome but not be released, therefore not be available to regulate ORN targeting. This hypothesis could not be verified; a loss of DIAP1 should have the same effect, but does not lead to ectopic glomerulus formation. Another prediction would be that over-expression of DIAP1 in *dark*^{verpeilt} mutants should be able to compensate for the lack of free DIAP1 caused by defective apoptosome regulation. However, over-expression has no effect on the lateral glomerulus in *dark*^{verpeilt} mutant clones. A similar mechanism could still be true, though the molecules involved have yet to be determined.

4.6 Connectin is required but not sufficient for lateral OR47a targeting in *dark^{verpeilt}* mutants

The phenotypic description of the projection domains provides no insights of how this pattern is established. The analysis of the LRR cell adhesion molecules Capricious and Connectin, which are expressed mainly in the ventro-medial or dorso-lateral projection domain respectively, was thought to allow the investigation of the involvement of axonal pre-sorting in projection domains in ORN mis-targeting observed in *dark^{verpeilt}* mutants. Both domains are affected in *dark^{verpeilt}* mutants, which is in contrast to the rather specific requirement of *dark* function found in the single class analysis.

4.6.1 Con is not expressed in all *dark^{verpeilt}* mutant Or47a neurons

The finding of ectopically expressed Con only in ectopic projecting *dark^{verpeilt}* mutant ORNs provides a first link between the projection domain organization and the mis-targeting. In contrast to the wildtype, in *dark^{verpeilt}* homozygous mutants a sub-fraction of Or47a neurons ectopically express Connectin. Interestingly it is not expressed in all mutant Or47a neurons, but only by those that form the lateral glomerulus. An RNAi mediated knock down of Con only in homozygous mutant ORNs is able to suppress the lateral targeting phenotype. This indicates an instructive role for Con in this process. However, loss of Con does not affect ORN targeting and over-expression in a wild type background does not induce the formation of an ectopic glomerulus or increases the number of ORNs targeting to the lateral glomerulus in *dark^{verpeilt}*. Con therefore is required but not sufficient for sensory neuron targeting to the lateral glomerulus.

The question remains why ectopic Con expression is restricted only to a small subpopulation of Or47a neurons in *dark^{verpeilt}*. A comparison of the spatial distribution of Con positive and Or47a neurons suggests a partial overlap in the antenna at the edges of the con expressing patch in the distal part of the antenna (Figure 43 A-C). An explanation for the differential expression of Con in *dark^{verpeilt}* mutants could be that the Con expression is induced in the whole distal part of the antenna, including the Or47a neurons located in this area. *Dark* function might be required to suppress the instructive signal, preventing Con expression in these cells thus circumventing entering of the dorso-lateral domain and formation of the ectopic glomerulus. Or47a neurons outside of that region do not receive this signal, therefore they remain Con negative (Figure 43 D).

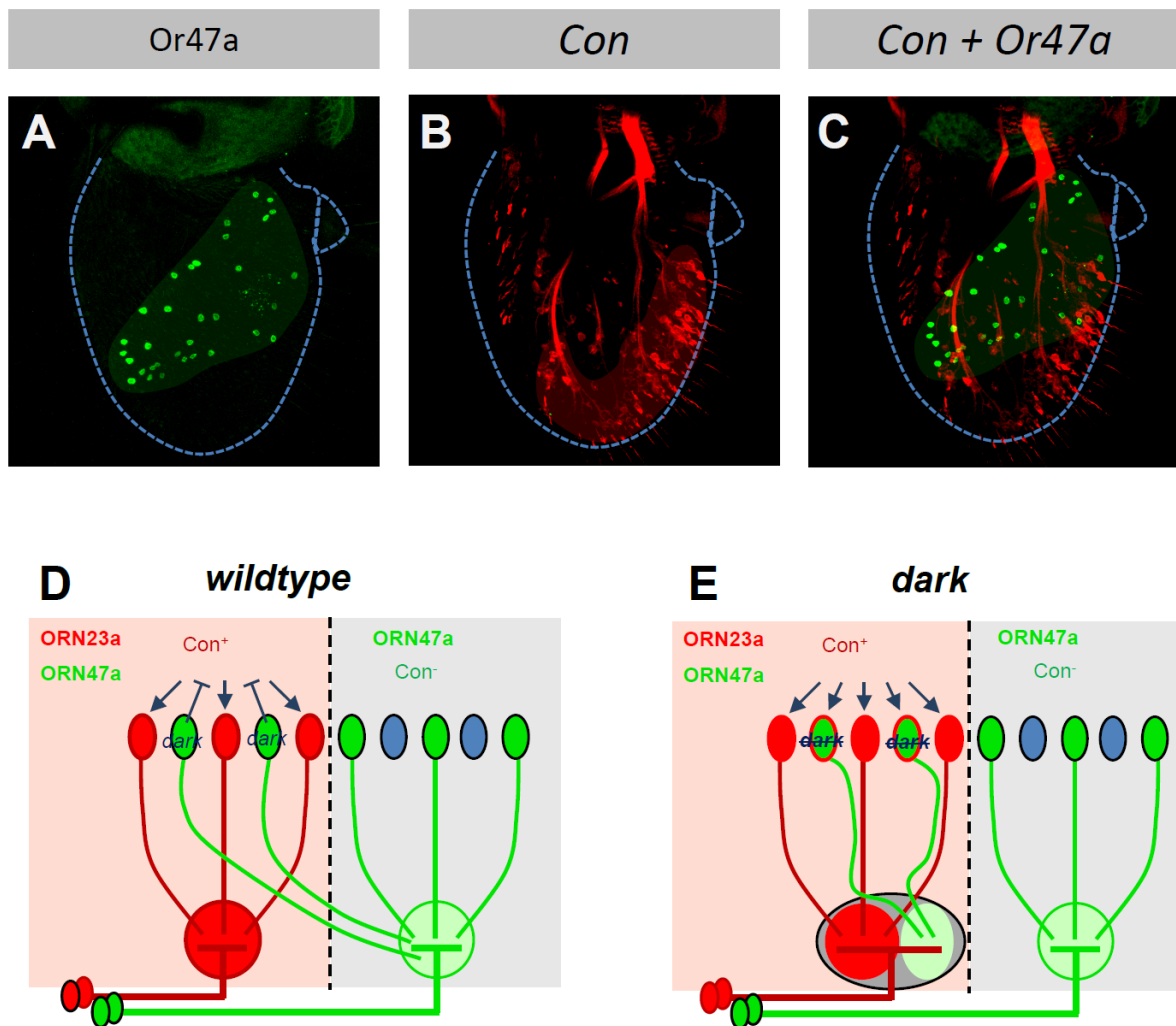


Figure 43 – Local *Dark* activity is required for Connectin regulation

(A-C) Comparison of the spatial expression of *Con* and *Or47a* reveals that most *Or47a* neurons are located outside the *Con* expressing domain in the distal part of the 3rd antennal segment. Few ORNs of this class however, are found within this domain (white circles in C). Suggesting a instructive signal that induces *Con* expression in the distal 3rd antennal segment, *dark* would be required in the *Or47a* neurons within this region, but dispensable for *Or47a* neurons located more basal in the antenna (D). Defective *dark* function within the radius of the instructive signal for *con* expression would lead to ectopic expression in *OR47a* neurons and thus formation of an ectopic glomerulus (E).

4.6.2 Ectopic Con expression in *dark^{verpeilt}* is due to transcriptional up-regulation

The notion that Con mis-expressing Or47a neurons can not only be detected by antibody staining, but also a ConGal4 driver suggests that the regulation of Con by *dark* is mediated on a transcriptional level.

Besides its requirement in lateral targeting, Con appears also have an impact on target recognition. The finding that only the PNs of DA3 and DL4 are Con negative in the dorso-lateral area of the AL suggests that the mis-projecting ORNs in *dark^{verpeilt}* choose these dendrites to form connections, presumably because they are most similar to the PN dendrites in DM3, which also do not express Con. This hypothesis is supported by the fact that over-expression of Con in PNs does affect the morphology and size of the lateral glomerulus. Interestingly the innervation of DM3 target remains unchanged, indicating that other recognition molecules in the wild type target neurons stabilize correct targeting of Or47a axons to these dendrites.

Though no mis-expression of Caps could be detected, the fact that both Con and Caps expression is more or less restricted in to ORNs projecting preferentially only along one projection domain lead to the hypothesis of a functional relevance of these proteins in establishing the domain organization of ingrowing ORNs. Disturbance of this pattern and changes in the expression of these molecules, as observed for Con in *dark^{verpeilt}* mutants suggest a function in ORN targeting to specific domains. Over-expression of Connectin does not affect ORN targeting, indicating a mechanism dependent on differential expression of these molecules in different ORN classes, suggesting a combinatorial code of cell adhesion molecules that grants an individual projection identity for every ORN class. However, this sorting process is not instructive to guide ORNs to their specific glomeruli, as frequently axons can be observed taking alternative routes to their target. This indicates a rather supportive role of the domain organization in the formation of the olfactory map.

4.7 Precise regulation of *dark* is required for olfactory targeting

It could be shown that distinct truncations and amino acid changes in *dark^{verpeilt}* mutants cause axon mis-targeting, although the complete loss of function does not interfere with ORN connectivity. These alterations affect multiple domains of the *Dark* protein, while other mutations in the same domains resemble a loss-of-function situation as observed for the

defined null allele *dark*⁸². However, only these *dark*^{verpeilt} mutations lead to ectopic expression of Con in a subset of Or47a neurons.

These two classes of *dark* mutations allow the functional separation of its role in apoptosis and olfactory system development. The fact that neither the defects in apoptosis nor the ORN mis-targeting of the *dark*^{verpeilt} mutations can be rescued by a wild type version of *dark* suggests a dominant negative effect of the *dark*^{verpeilt} mutations. This is most likely due to the requirement of *Dark* to assemble into a high-order apoptosome protein complex, which is an essential prerequisite for *Dark*-dependent DRONC activation. In contrast to the artificial expression of wild type *Dark*, the expression of a constitutive-active form of *Dark* (*dark*^V) fully rescues the *dark*^{verpeilt} defects indicating that the apoptosome build by *Dark*^{verpeilt} class monomers is able to assemble with monomeric DRONC but prevents its dimerization of activation. Alternatively, the dominant negative effect of the *dark*^{verpeilt} apoptosome could also be caused by a defective turnover of the *Dark*/DRONC complex, therefore sequestering out so far unknown effectors of neuronal differentiation. Incorporation of *Dark*^V could stabilize the apoptosome, therefore re-gaining at least parts of its function.

One critical target of *dark*-mediated *Dark* regulation during neuronal differentiation is the cell adhesion molecule Connectin. This failure of target choice is at least to some extent dependent on the ectopic expression of Connectin, suggesting that it is one of the determinants of the projection identity. Since the ectopic expression of Connectin is induced on a transcriptional level in *dark*^{verpeilt}, one hypothesis could be that the actual regulator of Connectin expression in a subset of ORN47a is controlled by the apoptosome. Changes in the apoptosome due to *dark*^{verpeilt} mutations might lead to a defective release of this putative factor thus leading to ectopic expression of Con. Alternatively a defective apoptosome could change the binding properties of the complex leading to a neomorph function that might activate con transcription.

Another hypothesis based on the assumption of a defective apoptosome could be that this complex titrates out a factor that is required to prevent Connectin expression. A candidate is DIAP1. It has been described that it is involved in non-apoptotic processes including actin cytoskeleton organization (Kuranaga et al. 2006). DIAP1 could be required for the degradation of a guidance cue directing Or47a to the dorso-lateral AL via its ubiquitin ligase domain in an apoptosome independent fashion. In *dark*^{verpeilt} mutants, DIAP1 could be

recruited to the apoptosome but not be released, therefore not be available to regulate ORN targeting. However, the loss of DIAP1 did not lead to ectopic glomerulus formation. Another prediction would be that over-expression of DIAP1 in *dark^{verpeilt}* mutants should be able to compensate for the lack of free DIAP1 caused by defective apoptosome regulation. However, over-expression has no effect on the lateral glomerulus in *dark^{verpeilt}* mutant clones. A similar mechanism could be mediated via DIAP2, which is described to be dispensable for apoptosis but to have certain features in common with DIAP1, like its ubiquitin ligase domain. DIAP2 might also compensate for a defective DAIP1 function in *dark^{verpeilt}* mutants.

The fact, that *dark^v* is able to rescue the lethality and the ORN phenotype of *dark^{v8}*, leads to the suggestion that the stability of the apoptosome is crucial for the processing of DRONC. Since DRONC has been shown to have some potential for *dark*-independent auto-activation (Rodriguez et al. 2002); Snipas et al. 2008), this basal activity might be sufficient to suppress Connectin expression due to DRONC mediated regulation of a Connectin activator. In *dark^{v8}* mutants DRONC binds to a defective apoptosome, thus preventing it from auto-activation, therefore the expression of Con cannot be suppressed. Re-expression of *dark^v* in this background could lead to the formation of a functional apoptosome, and since it cannot be cleaved by DRONC, it could compensate for the lack of activation by the defective *dark^{verpeilt}* apoptosome. This would leave enough active DRONC to suppress Con expression and even rescue the lethality.

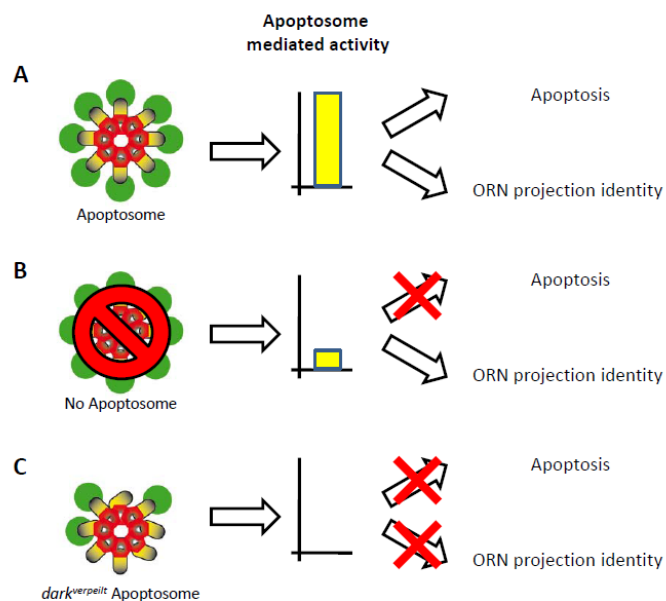


Figure 44 – Apoptosome activity mediated functions

(A) The wild type apoptosome results in high activity of the processed substrates (B) Without a functioning apoptosome high activity required for apoptosis is blocked, but a basal level is maintained by alternative mechanisms, e.g. autoactivation, sufficient for proper ORN targeting. (C) A *dark^{verpeilt}* apoptosome acts as a dominant negative, not only blocking apoptosis but also other apoptosome associated mechanisms by titrating out potential substrates.

Some results from this work contradict this model. A total lack of DRONC does not explain the slightly different rescue of the GMR hind induced eye reduction obtained with the *dark*^{V8} allele in the Ghf assay, but this effect could be explained by compensatory mechanisms if no apoptosis mediated cell death takes place at all. Another contra point would be that the over-expression of *dark*^V has been described to decrease DRONC levels (Shapiro et al. 2008), arguing against a re-gain of DRONC function. In the background of a *dark*^{verpeilt} mutant and a therefore presumed total loss of DRONC function the feedback mechanism down regulating DRONC might not result in strong DRONC repression. However, a similar mechanism could still apply for another yet unknown substrate of the apoptosome. A theoretical mechanism is shown in Figure 44.

All these models have one thing in common: they all depend on the correct formation and regulation of *dark* activity. Shapiro et al. have shown that *Dark* and DRONC are constantly expressed in the cells but regulate each other over a mutual feedback inhibition, also reliant on DIAP1 function. The levels of *Dark* and DRONC are low, and because of the constant turnover it is hard to detect. Only if apoptosis is induced *Dark* and DRONC expression increases to a detectable level (Shapiro et al. 2008). Therefore functions of the apoptosome in non-apoptotic cells are poorly understood. However, the results presented here findings suggest that basic activity of the apoptosome is sufficient to ensure proper wiring in the olfactory system.

In any of these models *dark* acts as a mediator of the process that actually leads to the change in the expression of *Con* and putative other determinants of ORN projection identity. Further research is required to uncover the link between the apoptosome and regulation ORN targeting.

5 Abstract

The olfactory system of *Drosophila* consists of about 1500 olfactory receptor neurons, subdivided in roughly 50 classes, each of which connects to a class specific set of target neurons, forming synaptic glomeruli in the antennal lobe. The in-growing axons sort out into one of four major projection domains which guide them to their target, reducing the complexity of target choice and supporting each ORN class to form only one synaptic glomerulus.

To unravel the mechanisms that allow the ORN axons to form these connections we performed a mosaic screen. One of the complementation groups identified, initially called *verpeilt* (*vpt*), affects the sorting into the projection domains, eventually causing axons of the Or47a class to form two glomeruli instead of one.

The gene affected in the *vpt* mutant is called *Apaf1-related killer* (*dark*) and is a known activator of apoptosis. However, several experiments could show that the extra glomerulus in *dark* mutants is not caused by additional neurons due to less apoptosis. Neither could blockage of apoptosis induce the phenotype nor could activation of apoptosis rescue it.

Surprisingly, not all *dark* alleles exhibit the mis-targeting phenotype, though all have an effect on apoptosis regulation. Also, the ability of the different alleles examined to induce the mis-targeting phenotype does not correlate with a specific domain. Since *dark* is involved in apoptosome formation and builds an octamer, we suggest that some alleles cause a mis-regulation of apoptosome stability, thereby causing ORN mis-targeting, rather than displaying a total loss of function.

In addition, mis-projecting Or47a-axons ectopically express the cell adhesion molecule Connectin, and a RNAi mediated knock-down of Con is able to suppress the phenotype in *dark* mutant clones.

From these results, we suggest a model in which the different ORN classes sort out according to a combinatorial code of cell adhesion molecules defining a projection identity, which is dependent on a proper function of the apoptosome, but is not affected by the lack of apoptosis itself.

6 Literature

- Adams, J.M. & Cory, S., 2002. Apoptosomes: engines for caspase activation. *Current Opinion in Cell Biology* pp. 715-720.
- Akdemir, F. et al., 2006. Autophagy occurs upstream or parallel to the apoptosome during histolytic cell death. *Development*, 133(8) pp. 1457-1465.
- Ang, L., 2003. Dock and Pak regulate olfactory axon pathfinding in *Drosophila*. *Development*, 130(7) pp. 1307-1316.
- Arama, E. et al., 2005. The two *Drosophila* cytochrome C proteins can function in both respiration and caspase activation. *The EMBO Journal*, 25(1) pp. 232-243.
- Asahina, K. et al., 2009. A circuit supporting concentration-invariant odor perception in *Drosophila*. *Journal of biology*, 8(1) p. 9.
- Benton, R. et al., 2009. Variant ionotropic glutamate receptors as chemosensory receptors in *drosophila*. *Cell*, 136(1) pp. 149-162.
- Benton, R., Vannice, K.S. & Vosshall, L.B., 2007. An essential role for a CD36-related receptor in pheromone detection in *Drosophila*. *Nature*, 450(7167) pp. 289-93.
- Berdnik, D. et al., 2008. MicroRNA Processing Pathway Regulates Olfactory Neuron Morphogenesis. *Current Biology*, 18(22) pp. 1754-1759.
- Berdnik, D. et al., 2006. Wiring stability of the adult *Drosophila* olfactory circuit after lesion. *The Journal of neuroscience : the official journal of the Society for Neuroscience*, 26(13) pp. 3367-76.
- Bhalerao, S. et al., 2003. Olfactory neurons expressing identified receptor genes project to subsets of glomeruli within the antennal lobe of *Drosophila melanogaster*. *Journal of neurobiology*, 54(4) pp. 577-92.
- Brachmann, C.B. & Cagan, R.L., 2003. Patterning the fly eye: the role of apoptosis. *Trends in genetics*, 19(2) pp. 91-96.
- Brand, a.H. & Perrimon, N., 1993. Targeted gene expression as a means of altering cell fates and generating dominant phenotypes. *Development (Cambridge, England)*, 118(2) pp. 401-15.
- Brown, a. et al., 2000. Topographic mapping from the retina to the midbrain is controlled by relative but not absolute levels of EphA receptor signaling. *Cell*, 102(1) pp. 77-88.

- Buck, L. & Axel, R., 1991. A novel multigene family may encode odorant receptors: a molecular basis for odor recognition. *Cell*, 65(1) pp. 175-87.
- Calof, a.L. et al., 1998. The neuronal stem cell of the olfactory epithelium. *Journal of neurobiology*, 36(2) pp. 190-205.
- Chehrehasa, F., St John, J. & Key, B., 2005. The sorting behaviour of olfactory and vomeronasal axons during regeneration. *Journal of molecular histology*, 36(6-7) pp. 427-36.
- Clandinin, T.R. et al., 2001. N-Cadherin Regulates Target Specificity in the . , 30 pp. 437-450.
- Cooper, D.M., Granville, D.J. & Lowenberger, C., 2009. The insect caspases. *Apoptosis*.
- Cordero, J. et al., 2004. A role for wingless in an early pupal cell death event that contributes to patterning the Drosophila eye. *Mechanisms of development*, 121(12) pp. 1523-30.
- Couto, A., Alenius, M. & Dickson, B., 2005. *Molecular, Anatomical, and Functional Organization of the Olfactory System*,
- Cutforth, T. et al., 2003. Axonal ephrin-As and odorant receptors: coordinate determination of the olfactory sensory map. *Cell*, 114(3) pp. 311-22.
- DasGupta, S. & Waddell, S., 2008. Learned odor discrimination in Drosophila without combinatorial odor maps in the antennal lobe. *Current biology : CB*, 18(21) pp. 1668-74.
- Dickson, B.J., 2002. Molecular mechanisms of axon guidance. *Science (New York, N.Y.)*, 298(5600) pp. 1959-64.
- Dobritsa, A.A. et al., 2003. Integrating the Molecular and Cellular Basis of Odor Coding in the Drosophila antenna. *Response*, 37 pp. 827-841.
- Duan, H. & Dixit, V.M., 1997. RAIDD is a new 'death' adaptor molecule. *Group*, 385 pp. 86-89.
- Endo, K. et al., 2007. Notch signal organizes the Drosophila olfactory circuitry by diversifying the sensory neuronal lineages. *Nature Neuroscience*, 10(2) pp. 153-160.
- Feinstein, P. & Mombaerts, P., 2004. A contextual model for axonal sorting into glomeruli in the mouse olfactory system. *Cell*, 117(6) pp. 817-31.
- Feinstein-Rotkopf, Y. & Arama, E., 2009. Can't live without them, can live with them: roles of caspases during vital cellular processes. *Apoptosis : an international journal on programmed cell death*.
- Flanagan, J.G. & Vanderhaeghen, P., 1998. The ephrins and Eph receptors in neural development. *Annual review of neuroscience*, 21 pp. 309-45.

- Gao, F. et al., 2000. Control of Dendritic Field Formation in *Drosophila*: The Roles of Flamingo and Competition between Homologous Neurons. , 28 pp. 91-101.
- Godzik, A., 2003. The apoptosis database. *Cell Death and Differentiation* pp. 621-633.
- Golic, K.G. & Lindquist, S., 1989. The FLP recombinase of yeast catalyzes site-specific recombination in the *Drosophila* genome. *Cell*, 59(3) pp. 499-509.
- Gray, Y.H., Tanaka, M.M. & Sved, J.A., 2006. P-Element-Induced Recombination. *Elements*, 1610 pp. 1601-1610.
- Gupta, B.P. & Rodrigues, V., 1997. atonal is a proneural gene for a subset of olfactory sense organs in *Drosophila*. *Genes to Cells*, (Simpson 1990) pp. 225-233.
- Hawkins, C.J. et al., 2000. The *Drosophila* caspase DRONC cleaves following glutamate or aspartate and is regulated by DIAP1, HID, and GRIM. *The Journal of biological chemistry*, 275(35) pp. 27084-93.
- Hay, B.A., Wolff, T. & Rubin, G.M., 1994. Expression of baculovirus P35 prevents cell death in *Drosophila*. *Scanning*, 2129 pp. 2121-2129.
- Hiesinger, P.R. & Bellen, H.J., 2004. News and views - Flying in the face of total disruption. *Nature Genetics*, 36(3) pp. 211-212.
- Huber, A.B. et al., 2003. Signaling at the growth cone: ligand-Receptor complexes and the control of axon growth and guidance. *Annual Review of Neuroscience*, 26(1) pp. 509-563.
- Hummel, T. & Zipursky, S.L., 2004. Afferent induction of olfactory glomeruli requires N-cadherin. *Neuron*, 42(1) pp. 77-88.
- Hummel, T. et al., 2003. Axonal Targeting of Olfactory Receptor Neurons is controlled by Dscam. *Neuron*, 37 pp. 221-231.
- Imai, T. et al., 2009. Pre-Target Axon Sorting Establishes the Neural Map Topography. *Science*, (July).
- Imai, T., Suzuki, M. & Sakano, H., 2006. Odorant receptor-derived cAMP signals direct axonal targeting. *Science (New York, N.Y.)*, 314(5799) pp. 657-61.
- Jefferis, G.S. & Hummel, T., 2006. Wiring specificity in the olfactory system. *Seminars in Cell & Developmental Biology*, 17(1) pp. 50-65.
- Jefferis, G.S. et al., 2004. Developmental origin of wiring specificity in the olfactory system of *Drosophila*. *Development (Cambridge, England)*, 131(1) pp. 117-30.

- Jefferis, G.S. et al., 2001. Target neuron prespecification in the olfactory map of *Drosophila*. *Nature*, 414(November) pp. 204-208.
- Kanuka, H. et al., 1999. Control of the Cell Death Pathway by Dapaf-1, a *Drosophila* Apaf-1/CED-4-Related Caspase Activator. *Molecular Cell*, 4 pp. 757-769.
- Keleman, K. & Dickson, B.J., 2001. Short- and Long-Range Repulsion by the . , 32 pp. 605-617.
- Kidd, T., Bland, K.S. & Goodman, C.S., 1999. Slit is the midline repellent for the robo receptor in *Drosophila*. *Cell*, 96(6) pp. 785-94.
- Kolodziej, P.a. et al., 1996. frazzled encodes a *Drosophila* member of the DCC immunoglobulin subfamily and is required for CNS and motor axon guidance. *Cell*, 87(2) pp. 197-204.
- Kumar, S., 2007. Caspase function in programmed cell death. *Cell death and differentiation*, 14(1) pp. 32-43.
- Kuranaga, E. & Miura, M., 2007. Nonapoptotic functions of caspases: caspases as regulatory molecules for immunity and cell-fate determination. *Trends in Cell Biology*, 17(3) pp. 135-144.
- Kuranaga, E. et al., 2006. *Drosophila* IKK-Related Kinase Regulates Nonapoptotic Function of Caspases via Degradation of IAPs. *Cell*, 126(3) pp. 583-596.
- Laissue, P.P. et al., 1999. Three-Dimensional Reconstruction of the Antennal Lobe in. *Journal of Comparative Neurology*, 552(May 1998) pp. 543-552.
- Larsson, M.C. et al., 2004. Or83b Encodes a Broadly Expressed Odorant Receptor Essential for *Drosophila* Olfaction. *Neuron*, 43 pp. 703-714.
- Lattemann, M. et al., 2007. Semaphorin-1a controls receptor neuron-specific axonal convergence in the primary olfactory center of *Drosophila*. *Neuron*, 53(2) pp. 169-84.
- Lee, T. & Luo, L., 1999. Mosaic analysis with a repressible cell marker for studies of gene function in neuronal morphogenesis. *Neuron*, 22(3) pp. 451-61.
- Li, H. et al., 1999. Vertebrate Slit, a Secreted Ligand for the Transmembrane Protein Roundabout, Is a Repellent for Olfactory Bulb Axons. *October*, 96(6) pp. 807-818.
- Lienhard, M.C. & Stocker, R.F., 1991. The development of the sensory neuron pattern in the antennal disc of wild-type and mutant (*lz3, ssa*) *Drosophila melanogaster*. *Development (Cambridge, England)*, 112(4) pp. 1063-75.
- Lledo, P., Merkle, F.T. & Alvarez-Buylla, A., 2008. Origin and function of olfactory bulb interneuron diversity. *Trends in neurosciences*, 31(8) pp. 392-400.

- Meier, P. et al., 2000. caspase DRONC is regulated by DIAP1. , 19(4) pp. 598-611.
- Mills, K. et al., 2006. The *Drosophila melanogaster* Apaf-1 homologue ARK is required for most, but not all, programmed cell death. *The Journal of Cell Biology*, 172(6) pp. 809-815.
- Mombaerts, P., 2006. Axonal Wiring in the Mouse Olfactory System. *Annual Review of Cell and Developmental Biology*, 22(1) pp. 713-737.
- Mori, K., von Campenhouse, H. & Yoshihara, Y., 2000. Zonal organization of the mammalian main and accessory olfactory systems. *Philosophical transactions of the Royal Society of London. Series B, Biological sciences*, 355(1404) pp. 1801-12.
- Mori, K., 1999. The Olfactory Bulb: Coding and Processing of Odor Molecule Information. *Science*, 286(5440) pp. 711-715.
- Muro, I., 2005. Cleavage of the Apoptosis Inhibitor DIAP1 by the Apical Caspase DRONC in Both Normal and Apoptotic *Drosophila* Cells. *Journal of Biological Chemistry*, 280(19) pp. 18683-18688.
- Neuhaus, E.M. et al., 2005. Odorant receptor heterodimerization in the olfactory system of *Drosophila melanogaster*. *Nature neuroscience*, 8(1) pp. 15-7.
- Newsome, T.P., Asling, B. & Dickson, B.J., 2000. Analysis of *Drosophila* photoreceptor axon guidance in eye-specific mosaics. *Development (Cambridge, England)*, 127(4) pp. 851-60.
- Nose, A., Mahajan, V.B. & Goodman, C.S., 1992. Connectin: A homophilic cell adhesion molecule expressed on a subset of muscles and the motoneurons that innervate them in *Drosophila*. *Cell*, 70(4) pp. 553-567.
- Parks, A.L. et al., 2004. Systematic generation of high-resolution deletion coverage of the *Drosophila melanogaster* genome. *Nature Genetics*, 36(3) pp. 288-292.
- Pasquale, E.B., 2005. Eph receptor signalling casts a wide net on cell behaviour. *Nature reviews. Molecular cell biology*, 6(6) pp. 462-75.
- Pasquale, E.B., 1991. Identification of chicken embryo kinase 5, a developmentally regulated receptor-type tyrosine kinase of the Eph family. *Cell Regulation*, 2(July) pp. 523-534.
- Pasterkamp, R. & Kolodkin, A.L., 2003. Semaphorin junction: making tracks toward neural connectivity. *Current Opinion in Neurobiology*, 13(1) pp. 79-89.
- Peden, E., Killian, D.J. & Xue, D., 2008. Cell death specification in *C. elegans*. *Cell cycle*, 7(16) pp. 2479-2484.

-
- Petrovic, M. & Hummel, T., 2008. Temporal identity in axonal target layer recognition. *Nature*, 456(7223) pp. 800-803.
- Prakash, S. et al., 2005. Drosophila N-cadherin mediates an attractive interaction between photoreceptor axons and their targets. *Nature neuroscience*, 8(4) pp. 443-50.
- Reddy, G.V. et al., 1997. Development of the Drosophila olfactory sense organs utilizes cell-cell interactions as well as lineage. *Development (Cambridge, England)*, 124(3) pp. 703-12.
- Ressler, K.J., Sullivan, S.L. & Buck, L.B., 1993. A zonal organization of odorant receptor gene expression in the olfactory epithelium. *Cell*, 73(3) pp. 597-609.
- Rodriguez, A. et al., 1999. Dark is a Drosophila homologue of Apaf-1/CED-4 and functions in an evolutionarily conserved death pathway. *Nature*, 1(September).
- Rodriguez, A. et al., 2002. Unrestrained caspase-dependent cell death caused by loss of Diap1 function requires the Drosophila Apaf-1 homolog, Dark. *EMBO Journal*, 21(9) pp. 2189-2197.
- Salzberg, A. et al., 1997. P-Element Insertion Alleles of Essential Genes on the Third Chromosome of *Drosophila melanogaster*: Mutations Affecting Embryonic PNS Development. *Genetics*, 147 pp. 1723-41.
- Sato, K. et al., 2008. Insect olfactory receptors are heteromeric ligand-gated ion channels. *Nature*, 452(7190) pp. 1002-6.
- Satoda, M. et al., 1995. Differential Expression of Two Cell Surface Proteins, Neuropilin and Plexin, in *Xenopus* Olfactory Axon Subclasses. *Journal of Neuroscience*, 15(January) pp. 942-955.
- Schmucker, D. et al., 2000. Drosophila Dscam is an axon guidance receptor exhibiting extraordinary molecular diversity. *Cell*, 101(6) pp. 671-84.
- Schwartz, G.a. et al., 2000. Semaphorin 3A is required for guidance of olfactory axons in mice. *The Journal of neuroscience : the official journal of the Society for Neuroscience*, 20(20) pp. 7691-7.
- Scott, K. et al., 2001. A chemosensory gene family encoding candidate gustatory and olfactory receptors in *Drosophila*. *Cell*, 104(5) pp. 661-73.
- Serizawa, S., Miyamichi, K. & Sakano, H., 2005. Negative feedback regulation ensures the one neuron-one receptor rule in the mouse olfactory system. *Chemical senses*, 30 Suppl 1(suppl 1) pp. i99-100.

-
- Shapiro, P.J. et al., 2008. Regulation of the Drosophila apoptosome through feedback inhibition. *Nature Cell Biology*, 10(12) pp. 1440-1446.
- Simpson, J.H. et al., 2000. Short-range and long-range guidance by Slit and its Robo receptors: a combinatorial code of Robo receptors controls lateral position. *Cell*, 103(7) pp. 1019-32.
- Simpson, J.H. et al., 2000. Short-range and long-range guidance by slit and its Robo receptors. Robo and Robo2 play distinct roles in midline guidance. *Neuron*, 28(3) pp. 753-66.
- Snipas, S.J. et al., 2008. Activation mechanism and substrate specificity of the Drosophila initiator caspase DRONC. *Cell Death and Differentiation*, 15(5) pp. 938-945.
- Spletter, M.L. et al., 2007. Lola regulates Drosophila olfactory projection neuron identity and targeting specificity. *Neural development*, 2(July) p. 14.
- Srivastava, M. et al., 2006. ARK, the Apaf-1 related killer in Drosophila, requires diverse domains for its apoptotic activity. *Cell Death and Differentiation*, 14(1) pp. 92-102.
- Stocker, R.F., Heimbeck, G. & Belle, J.S., 1997. Neuroblast Ablation in. *Brand* pp. 443-456.
- Sweeney, N.T., Li, W. & Gao, F., 2002. Genetic manipulation of single neurons in vivo reveals specific roles of flamingo in neuronal morphogenesis. *Developmental biology*, 247(1) pp. 76-88.
- Tessier-Lavigne, M. & Goodman, C.S., 1996. The Molecular Biology of Axon Guidance. *Science*, 274(5290) pp. 1123-1133.
- Tichy, A.L., Ray, A. & Carlson, J.R., 2008. A new Drosophila POU gene, pdm3, acts in odor receptor expression and axon targeting of olfactory neurons. *The Journal of neuroscience : the official journal of the Society for Neuroscience*, 28(28) pp. 7121-9.
- Tolbert, L.P. et al., 2004. Bidirectional influences between neurons and glial cells in the developing olfactory system. *Progress in neurobiology*, 73(2) pp. 73-105.
- Tower, J. et al., 1993. Preferential Transposition of Drosophila. , 359 pp. 347-359.
- Vassar, R., Ngai, J. & Axel, R., 1993. Spatial segregation of odorant receptor expression in the mammalian olfactory epithelium. *Cell*, 74(2) pp. 309-18.
- Vaux, D.L. & Korsmeyer, S.J., 1999. Cell Death in Development Review. *Development*, 96 pp. 245-254.
- Wicher, D. et al., 2008. Drosophila odorant receptors are both ligand-gated and cyclic-nucleotide-activated cation channels. *Nature*, 452(7190) pp. 1007-11.

- Williams, D.W. et al., 2006. Local caspase activity directs engulfment of dendrites during pruning. *Nature Neuroscience*, 9(10) pp. 1234-1236.
- Xu, D. et al., 2005. The CARD-carrying caspase Dronc is essential for most, but not all, developmental cell death in *Drosophila*. *Development (Cambridge, England)*, 132(9) pp. 2125-34.
- Xu, T. & Rubin, G.M., 1993. Analysis of genetic mosaics in developing and adult *Drosophila* tissues. *Development (Cambridge, England)*, 117(4) pp. 1223-37.
- Yi, C.H. & Yuan, J., 2009. The Jekyll and Hyde functions of caspases. *Developmental cell*, 16(1) pp. 21-34.
- Yoshihara, Y. & Mori, K., 1997. Basic principles and molecular mechanisms of olfactory axon pathfinding. *Cell and tissue research*, 290(2) pp. 457-63.
- Yu, X. et al., 2006. Three-Dimensional structure of a double apoptosome formed by the *Drosophila* apaf-1 related killer. *Journal of Molecular Biology*, 355(3) pp. 577-589.
- Zhai, R.G. et al., 2003. Mapping *Drosophila* mutations with molecularly defined P element insertions. *Proceedings of the National Academy of Sciences of the United States of America*, 100(19) pp. 10860-5.
- Zhou, L. et al., 1999. HAC-1, a *Drosophila* Homolog of APAF-1 and CED-4, Functions in Developmental and Radiation-Induced Apoptosis. *Molecular Cell*, 4 pp. 745-755.
- Zhu, H. et al., 2006. Dendritic patterning by Dscam and synaptic partner matching in the *Drosophila* antennal lobe. *Nature neuroscience*, 9(3) pp. 349-55.
- Zou, D. et al., 2004. Postnatal refinement of peripheral olfactory projections. *Science (New York, N.Y.)*, 304(5679) pp. 1976-9.
- Shipman-Appasamy, P. M., Cohen, K. S. and Prystowsky, M. B. (1991). Nucleotide sequence of murine PCNA: interspecies comparison of the cDNA and the 5' flanking region of the gene. *DNA Seq* 2, 181-91.
- Niehues, S. (2008) Molekulare Charakterisierung der *vpt*-Mutante in *Drosophila*, Bachelor Thesis, Westfälische Wilhelms Univeristät, Münster
- Scheper, C.T. (2005) Genetische Untersuchung zur neuronalen Verschaltung des olfaktorischen Systems von *Drosophila melanogaster*, Westfälische Wilhelms Univeristät, Münster
- Sieglitz, F. (2007) Characterization of *engrailed* and *Connectin* in the olfactory system of *Drosophila*, Bachelor Thesis, Westfälische Wilhelms Univeristät, Münster

Steffes, G. (2007) Genetische Kontrolle axonaler Konvergenz und synaptischer Spezifität olfaktorischer Rezeptorneurone in *Drosophila melanogaster*, Dissertation, Westfälische Wilhelms Univeristät, Münster

Zierau, A. B. (2007) Analyse synaptischer Spezifität im olfaktorischen System von *Drosophila*, Dissertation, Westfälische Wilhelms Univeristät, Münster

7 Appendix

7.1 Abbreviations

AL	antenna lobe
APF	after puparium formation
CNS	central nervous system
FLP	Flippase
FRT	FLP-recombinase target
GR	gustatory receptor
Ig	immunoglobulin
MARCM	mosaic analysis with a repressible cell marker
LN	local interneuron
N-Cad	Neuronal Cadherin
OB	olfactory bulb
OE	olfactory epithelium
OR	olfactory receptor
ORN	olfactory receptor neuron
PN	projection neuron
PNS	peripheral nervous system
SOG	suboesophagial ganglion
SVZ	sub ventricular zone
UAS	upstream activation sequence

7.2 Figure Index

- Figure 01 – The vertebrate olfactory system
- Figure 02 – The *Drosophila* olfactory system
- Figure 03 – Zonal organization in the mouse olfactory system
- Figure 04 – Scheme of mitotic recombination technique
- Figure 05 – Dissection method for adult brains
- Figure 06 – *verpeilt* causes a stereotype ORN innervation in the dorso-lateral antennal lobe
- Figure 07 – Genomic region containing the *verpeilt* locus
- Figure 08 – Locations of the *verpeilt* P-element insertions
- Figure 09 – Creation of deficiencies by FRT containing piggyback insertions
- Figure 10 – Locations of the *dark^{verpeilt}* mutations.
- Figure 11 – Gene and protein structure of *dark*
- Figure 12 – *Dark^{verpeilt}* mutants show reduced cell death
- Figure 13 – *Dark^{vpt}* alleles suppress hid-induced apoptosis
- Figure 14 – *Dark^{V8}* does not affect ORN numbers
- Figure 15 – The *Drosophila* apoptosis pathway
- Figure 16 – Suppression of apoptosis does not affect Or47a targeting
- Figure 17 – Allele-specific effects of *dark* on ORN targeting
- Figure 18 – Or47a mis-targeting in viable dark trans-combinations
- Figure 19 – Over-expression of wild type dark in *dark^{V8}* ORNs
- Figure 20 – Loss of function of apoptosome components does not cause ORN mis-targeting
- Figure 21 – Over-expression of DAIP-1 does not affect Or47a-targeting in *dark^{V8}*
- Figure 22 – Or47a-axons project on alternative routes in *dark^{V8}*
- Figure 23 – Domain organization of ORN axons in *Drosophila*
- Figure 24 – Or47a axons project preferentially along the central domain to their target glomerulus
- Figure 25 – Commissural projection of Or47a axons
- Figure 26 – *Dark^{V8}* causes mis-targeting in several ORN classes
- Figure 27 – Mis-targeting of Or47a neurons is cell autonomous
- Figure 28 – The ectopic glomerulus is exclusively formed by *dark^{V8}* mutant ORNs

-
- Figure 29 – The formation of the lateral glomerulus requires a critical amount of lateral projecting axons
- Figure 30 – *dark*^{V8} mutant ORNs sort out from neighboring ORN classes
- Figure 31 – Lateral innervating ORNs specifically interact with target neurons
- Figure 32 – Capricious predominantly labels ORNs projecting along the ventro-medial domain
- Figure 33 – Connectin predominantly labels ORNs projecting along the dorso-lateral domain
- Figure 34 – Connectin is expressed in a continuous patch in the distal part of the 3rd antennal segment
- Figure 35 – Connectin expression during ORN development
- Figure 36 – Lateral projecting Or47a neurons in *dark*^{V8} ectopically express Connectin
- Figure 37 – Connectin is mis-expressed in Or47a neurons
- Figure 38 – Loss of Con function does not affect ORN targeting
- Figure 39 – Knock down of Con in *dark*^{V8} homozygous ORNs represses mis-targeting
- Figure 40 – Over-expression of Con in MARCM clones does not affect OR47a target specificity
- Figure 41 – Mis-expression of Con in PNs changes target specificity of lateral projecting Or47a neurons in *dark*^{V8}
- Figure 42 – The Drosophila apoptosis pathway
- Figure 43 – Local *Dark* activity is required for Connectin regulation
- Figure 44 – Apoptosome activity mediated functions

Lebenslauf

Christoph Tobias Scheper

Geburtsdatum 03. 04. 1980

Geburtsort Ankum

Familienstand ledig

Eltern: Gerd Scheper
Gertrud Scheper, geb. Meyer

Schulbildung 1986 – 1990 Grund- und Hauptschule mit Orientierungsstufe,
Badbergen
1992 – 1999 Artlandgymnasium Quakenbrück

Hochschulreife (Abitur): 01. 07. 1999 in Quakenbrück

Militärdienst 09/1999 - 10/1999 Grundausbildung 7./1
Luftwaffenausbildungsregiment, Goslar
11/1999 - 08/2000 4./ FlaRakGrp 25, Ahhorn

Studium: 10/ 2000 – 09/2005 Biologie (Dipl.)
an der Westfälischen Wilhelms
Universität Münster

Promotionsstudiengang: 11/2005 - Promotionsstudiengang an der WWU
Münster, Institut für Neuro- und
Verhaltensbiologie, Arbeitsgruppe
PD Dr. Thomas Hummel

Tätigkeiten: 10/2004 – 09/2005 Studentische Hilfskraft am Institut für
Neuro- und Entwicklungsbiologie, WWU
Münster
11/2005 - Beschäftigung als wissenschaftlicher
Mitarbeiter am Institut für Neuro- und
Entwicklungsbiologie, WWU Münster

Münster, den

Erklärung

Hiermit erkläre ich, dass ich die vorliegende Arbeit selbstständig verfasst und keine anderen als die angegebenen Hilfsmittel und Quellen benutzt habe. Alle Stellen der Arbeit, die dem Wortlaut oder dem Sinn nach anderen Werken entnommen sind, habe ich in jedem Fall unter Angabe der Quelle deutlich als Entlehnung kenntlich gemacht.

Münster, den.....

DANKSAGUNG

Diese Arbeit wurde unter der Betreuung von PD Dr. Thomas Hummel angefertigt.
Das Zweitgutachten wurde von Prof. Dr. Christian Klämbt angefertigt.

Bei Thomas möchte ich mich für die Vergabe des Themas, die ständige Unterstützung und für seine Geduld bedanken.

Bei Christian bedanke ich mich für die Übernahme des Zweitgutachtens, die gute Stimmung im Haus, und besonders für die neue Küche, die mich in den letzten fast ausschließlich ernährt hat.

Danke auch an meine Bachelor Florian und Sven, die viel zum Gelingen dieser Arbeit beigetragen haben.

Weiterhin großer Dank an alle aktuellen und ehemaligen Mitglieder der AG Hummel, Britta, Anna, Özzi, Junfeng, Milan, Lorin, Georg, Ariane, Marc, Katarina, Daniel, Bernd, Sascha, Claus, Christian, für ertragene Unordnung, laute Musik, nächtelange Scharmützel und Toleranz gegenüber einer bisweilen stinkende Ecke.

Ein großes Dankeschön auch an alle anderen aktuellen und ehemaligen Mitgliedern der AGs Klämbt, Bogdan und Aberle für die konstant gute Stimmung im Haus, weiterhin an alle (die ich hier absichtlich nicht alle aufzähle, aus Angst jemanden zu vergessen) für viele verschwendete Stunden vor dem Fernseher, auf dem Sonnendeck, in diversen Bars und Kneipen, Festivals, im Urlaub und im Schnee, auf Hochzeiten (special thanks to Yeliz and Özzi!) und bei vielen anderen Gelegenheiten. Außerdem Danke an Liane und Marion fürs Haarschneiden.

Ein besonderes Dankeschön an Evi für die konstante Fern-Unterstützung aus Dublin in frustigen Phasen an Evi.

Der größte Dank geht an meine Eltern und meine Familie für all die großartige Unterstützung in den letzten Jahren, auch wenn Ihr nie so genau verstanden habt was ich eigentlich die ganze Zeit gemacht habe.